Role of Smad2/3 linker serine phosphorylation in regulating TGF-β signalling

Manjari Trivedi

Thesis submitted towards fulfilment of the degree of
Doctor of Philosophy

Institute of Reproductive and Developmental Biology
Department of Metabolism, Digestion and Reproduction
Faculty of Medicine
Imperial College London

February 2022

Abstract

Transforming growth factor-β (TGF-β)/activin/nodal signalling play a critical role in many physiological and pathophysiological processes such as in embryogenesis, adult tissue homeostasis as well as in disease onset and progression. They signal via heteromeric complexes of type I and type II receptors, which phosphorylate and activate downstream signal effectors- Smad2 and Smad3 (Smad2/3). Phosphorylation of the C-terminal SxS motif of Smad2/3 by the receptors, induces them to form oligomeric complexes with Smad4 and accumulate in the nucleus where they regulate transcription. In addition to the SxS phosphorylation, Smad2/3 can also be phosphorylated at their linker region. Smad2/3 are comprised of two highly conserved MH1 and MH2 domains connected by an unstructured linker that contains several phosphorylatable serine and threonine residues. Specifically, there are proline-directed linker threonine (LT) and serine (LS) residues that are phosphorylated by various kinases such as PI3K/mTORC2, MAPKs, Rho/ROCK, GSK3-β, CDKs etc. to regulate Smad2/3 activity by altering their subcellular localisation, transcription, and protein stability. LT and LS are closely linked and are perceived to have similar functions in TGF-β signalling. However, a study in our lab showed that they are differentially regulated, suggesting they may also have different functions in TGF-β signalling. Therefore, this study aims to dissect the individual roles of LS and LT in regulating TGF-β signalling by using various cell models such as human embryonic stem cells (hESCs), mouse embryonic stem cells (mESCs), and PC3 cells for mechanistic and functional studies. LS was found to be phosphorylated by CDK8/9 while LT was not much affected. Inhibition of LS phosphorylation (pLS) delayed the deactivation of Smad2, resulting in their nuclear accumulation and augmented transcriptional activity. Conversely, inhibition of pLS in inactivated Smad2 after withdrawing the agonist, resulted in Smad2 proteasomal degradation. These findings reveal two distinct mechanisms by which pLS can regulate TGF-β signalling, which will greatly impact our understanding of effects of non-canonical Smad signalling on canonical TGF-β signalling and also provides potential insights into ways TGF-β responses could be manipulated for therapeutic benefits.

Statement of originality

All the experiments in this thesis were conducted by me, Manjari Trivedi, unless otherwise stated in the text.

Copyright declarations

Acknowledgements

Firstly, I would like to thank my PhD supervisor, Dr Wei Cui in supporting me throughout my PhD. I have enjoyed discussing my research with her and I am grateful for her advice and supervision that have made me a better scientist. I would also like to express my gratitude to Dr Vasso Episkopou for taking such interest in my research work and for guiding me throughout my project, particularly for the work on mouse embryonic stem cells. I am also very thankful to all the present and past members of the lab who have contributed greatly to my scientific development and encouraged me when experiments didn't work as planned. Specifically, I would like to thank Siti, Jen, and Huihan for their tuition upon my initial arrival in this lab and Faiza B, Faiza F, Xiaolun, and Li for friendly lab discussions. I am also thankful to the students I supervised- Mingxia, Sofianna, and Yiling, to offer me a chance to teach them my topic of research and lab techniques. I would also like to say a big thanks to our neighbouring lab members Roshni, Tommy, and Dr Veronique Azuara for always helping me with the reagents our lab had exhausted and specially, Roshni for being my partner during lunch breaks and late evening experiments. I would also like to extend my thanks to my early- and late-stage assessors- Dr Kate Hardy and Dr Vasso Episkopou for their invaluable comments and suggestions. Also, I am grateful for the President's PhD scholarship offered to me by Imperial College London, that supported me during my PhD.

Lastly, I would like to thank my parents for their love and supporting me in every way they could. Special thanks to my sister, Mansi, to encourage me when I needed motivation. Also, thank you Naani, my grandmother. And the biggest thanks to my partner, Nils, who has been on this journey with me through all the ups and downs. His care and love and friendship has helped me power through with a smile on my face. I would like to thank my friends, both in London and abroad, who have always supported me and ensured I have fun also outside the lab. Also, a special mention of my friends Richa, Jeannie, Alison, Megha, Callum, Lorenzo, Sunil, Oliver, Angelika, Khanh, and Neeraj for their support and friendship throughout my PhD.

Contents

Tables and Figures

Chapter 1

Chapter 3

Chapter 4

Chapter 5

Chapter 6

Appendix

Abbreviations

AA	Activin A
ADE	Anterior Definitive Endoderm
ALP	Agonist-induced linker phosphorylation
ATF3	Activating transcription factor 3
APS	Ammonium persulphate
BAMBI	BMP and activin membrane-bound inhibitor
BCA	Bicinchoninic Acid Assay
bFGF	Basic fibroblast growth factor
BGLAP	Bone γ-carboxyglutamic acid-containing protein
BMP	Bone Morphogenetic Facor
bp	Base pair
BSA	Bovine serum albumin
°C	Degree Celcius
CAMKII	Calcium/calmodulin-dependent protein kinase II
cDNA	Complimentary DNA
CEBPB	CCAAT/enhancer binding protein β
Cer1	Cerberus-1
CDK	Cyclin Dependent Kinase
CHIP	C terminus of HSC70-Interacting protein
Chx	Cycloheximide
CKIγ2	Casein kinase 1 gamma 2
CIN85	Cbl-interacting 85-kDa protein
CLIC4	Chloride intracellular channel 4
CMV	Cytomegalovirus promoter
Co-Smad	Common partner Smad
cPML	Cytoplasmic promyelocytic leukemia
CREBP	CREB binding protein
CRM1	Chromosome region maintenance 1
Ct	Threshold cycle
CtBP	C-terminal binding protein
CQ	Chloroquine
CM	Conditioned medium
Dab2	Disabled-2
DAPI	4',6-diamidino-2-phenylindole
Daf4	Dauer formation-4

DE	Definitive endoderm
DHD	Dachshund homology domain
DMEM	Dulbecco's modified eagle serum
DMSO	Dimethyl sulphoxide
DNA	Deoxyribonucleic acid
dNTP	Deoxynucleotide triphosphate
DPBS	Dulbecco's phosphate buffered saline
Dpp	*Drosophila* decapentaplegic
DTT	Dithiothreitol
DUBs	Deubiquitylating enzymes
EBs	Embryoid Bodies
EEA1	Early endosomal antigen 1
ECL	Enhanced chemiluminescence substrate
ECM	Extracellular matrix
EDTA	Ethylenediaminetetraacetic acid
EGF	Epidermal growth factor
EMT	Epithelial to mesenchymal transition
Eomes	Eomesdermin
ER	Endoplasmic reticulum
Erk	Extracellular signal-regulated kinase
FBS	Foetal bovine serum
FKBP12	FK506 binding protein of 12 kDA
FGF2	Fibroblast growth factor-2
FVP	Flavopiridol
GARP	Glycoprotein A repetitions predominant
GDFs	Growth differentiation factors
GFP	Green fluorescent protein
GRK2	G protein-coupled receptor kinase 2
GSC	Goosecoid
GS domain	Glycine-serine domain
GSK3-β	Glycogen synthase kinase β
HATs	Histone acetyl transferases
HDACs	Histone deactylases
HGF	Hepatocyte growth factor
HEPES	4-(2-hydroxyethyl)-1-piperazineethanesulfonic acid
hESC	Human embryonic stem cells

HMGA2	High-mobility group A protein 2
HNF3β	Hepatocyte nuclear factor 3-β
HRP	Horseradish peroxidase
ICM	Inner cell mass
I-Smads	Inhibitory Smads
JNK	Jun Nuclear kinase
kb	Kilobase
kDa	Kilodalton
KO-DMEM	Knockout DMEM
KO	Knockout
KD	Knockdown
KSR	Knockout serum replacement
LAP	Latency-associated protein
LIF	Leukemia inhibitory factor
LLC	Large latency complex
LS	Linker serine
LT	Linker Threonine
LTBPs	Latent TGF-β-binding proteins
LY	LY2857785
MAD	Mothers against decapentaplegic
MAPK	Mitogen activated protein kinase
MEFs	Mouse Embryonic Fibroblasts
MEF-CM	Mouse Embryonic Fibroblast-Conditioned medium
mESC	Mouse embryonic stem cells
MH1/2	Mad Homology domain 1/2
miRNA	micro-RNA
MIS	Müllerian-inhibiting substance
MG	MG132
mRNA	Messenger ribonucleic acid
MTMR4	Myotubularin-related protein 4
mTORC	Mechanistic target of rapamycin complex
NEAA	Non-essential amino acids
NEB	New England Biolabs
Nedd4-2	Neural developmentally down-regulated 4-2
Nedd4L	Neural precursor cell expressed developmentally downregulated gene 4-like
NLK	Nemo-like kinase

NES	Nuclear export signal
NRP1	Neuropilin-1
NP-40	Nonidet P40
NLS	Nuclear localization signal
NurD	Nucleosome remodelling deacetylase
Oct4	Octamer-binding transcription factor 4
PAK4	Protein-activated kinase 4
P/CAF	p300/CBP-associated factor
PDGF	Platelet derived growth factor
PI3K	Phosphatidylinositide 3-kinases
pLS	Linker serine phosphorylation
pLT	Linker Threonine phosphorylation
PLL	Poly-L-Lysine
PPM	Protein phosphatase Mg2+/Mn2+-dependent
PTM	Post-translational modification
PVDF	Polyvinylidene fluoride
qRT-PCR	Quantitative real-time polymerase chain reaction
Ras	Rat sarcoma
RIPA	Radio Immunoprecipitation Assay Buffer
RNA	Ribonucleic acid
Rho	Rho Kinase Inhibitor/p160 rho-associated coiled-coil kinase
RNAPII	RNA polymerase II
ROCK	Rho associated protein kinase
ROS	Reactive oxygen species
rpm	Revolutions per minute
RPMI	Roswell park memorial institute
R-Smad	Receptor-Smads
SAD	Smad activation domain
SARA	Smad anchor for receptor activation
SBE	Smad-binding element
$SCF^{\beta TrCP/\ Fbw1A}$	Skp1-cullin-F-box
SETDB1	SET domain bifurcated histone lysine methyltransferase 1
SKI	Sloan Kettering Institute protein
SLC	Small latent complex
SCPs	Small c-terminal domain phosphatases
Smurf2	Smad specific E3 ubiquitin protein ligase 2

SRP	Signal recognition proteins
SB	SB431542
SD	Standard deviation
SDS	Sodium dodecyl sulphate
ShRNA	Small hairpin RNA
SNAI1	Snail Family Transcriptional Repressor 1
Sox	Sex determining region Y box
S/T-P	Proline-directed threonine and serine amino acid
TEADs	TEA domain family members
TEMED	Tetramethylethylenediamine
TBS-T	Tris Buffered Saline with Tween-20
TGF-β	Transforming Growth Factor-β
TGIF	Transforming growth-interacting factor
Tiul1	TGIF interacting ubiquitin ligase 1
TF	Transcription factor
TSC22	TGF-β-stimulated clone 22
TSO	TEADs, Smads, and Oct4
UPS	Ubiquitin-proteasome system
v/v	Volume/volume
w/v	Weight/Volume
WT	Wildtype
ZEB1	Zinc finger E-box-binding homeobox 1
ZNF451	Zinc finger protein 451

Chapter 1

Introduction

1.1 TGF-β superfamily

1.1.1 Overview

Transforming growth factor-β (TGF-β) superfamily proteins are encoded by 33 genes in mammals and include TGF-βs, activins, nodal, bone morphogenetic proteins (BMPs), growth differentiation factors (GDFs), and Müllerian-inhibiting substance (MIS). These proteins form homo- or heterodimeric polypeptides which activate various signalling pathways and regulate a wide variety of biological functions including embryonic development, cellular homeostasis, wound healing, immune regulation, and regeneration (Morikawa et al., 2016, Derynck and Budi, 2019). Thereby, disruption of TGF-β signalling is implicated in the pathogenesis of numerous diseases, such as fibrosis, cancer, neurodegenerative and connective tissue disorders (Massagué, 2012). The core components of the TGF-β signalling pathway are highly conserved in evolution, across multiple species from *Drosophila melanogaster* to *Caenorhabditis elegans* to mammals (Huminiecki et al., 2009).

All the TGF-β superfamily proteins are produced and secreted as precursor forms into the extracellular matrix where they mature as disulphide-linked dimeric polypeptide ligands by eliminating the LAP. These mature dimeric ligands are able to bind to the serine/threonine-containing receptor complexes and activate these receptors as well as the downstream effectors receptor-activated Smads (R-Smads) via their phosphorylation at specific regions (*Fig 1.1*) (Morikawa et al., 2016, David and Massagué, 2018, Derynck and Budi, 2019, Tzavlaki and Moustakas, 2020). Activated R-Smads form functional protein complexes with the common partner Smad (co-Smad)- Smad4, accumulate in the nucleus, where they interact with partner transcription factors, and regulate expression of target genes (Inman et al., 2002, Schmierer and Hill, 2005, Ross and Hill, 2008, Hill, 2016, Tzavlaki and Moustakas, 2020). Evidently, R-Smads are crucial components of TGF-β signalling pathways as they are both effectors and transcription mediators. Based on the ligand specificity to distinct receptors and the downstream R-Smads involved, the TGF-β superfamily is broadly divided into two major categories: the TGF-β/activin/nodal subfamily, briefed simply as TGF-β family hereafter, and

the BMP subfamily. Smad2 and Smad3 are the R-Smads of TGF-β family, whereas Smad1, 5 and 8 are the R-Smads belonging to the BMP subfamily (Shi and Massagué, 2003). In addition, there is another type of Smads, called inhibitory Smads (I-Smads), Smad6 and Smad7. Smad6 inhibits BMP subfamily signalling while Smad7 can inhibit both TGF-β- and BMP-mediated signalling (Hanyu et al., 2001, Heldin and Moustakas, 2012). The molecular structures of most of the TGF-β components have been established, contributing to better insights into the structural basis of their biological functions, specific interactions in the pathway and diverse regulatory mechanisms (Hinck et al., 2016, Derynck and Budi, 2019, Tzavlaki and Moustakas, 2020). Given that signalling pathways of TGF-β superfamily contain a large number of components with various regulatory mechanisms and have critical biological functions, TGF-β signalling is often dysregulated in various human diseases and therefore, present an effective target for therapeutic intervention. An overview of the signalling by TGF-β and BMP pathways is depicted (*Fig 1.1*).

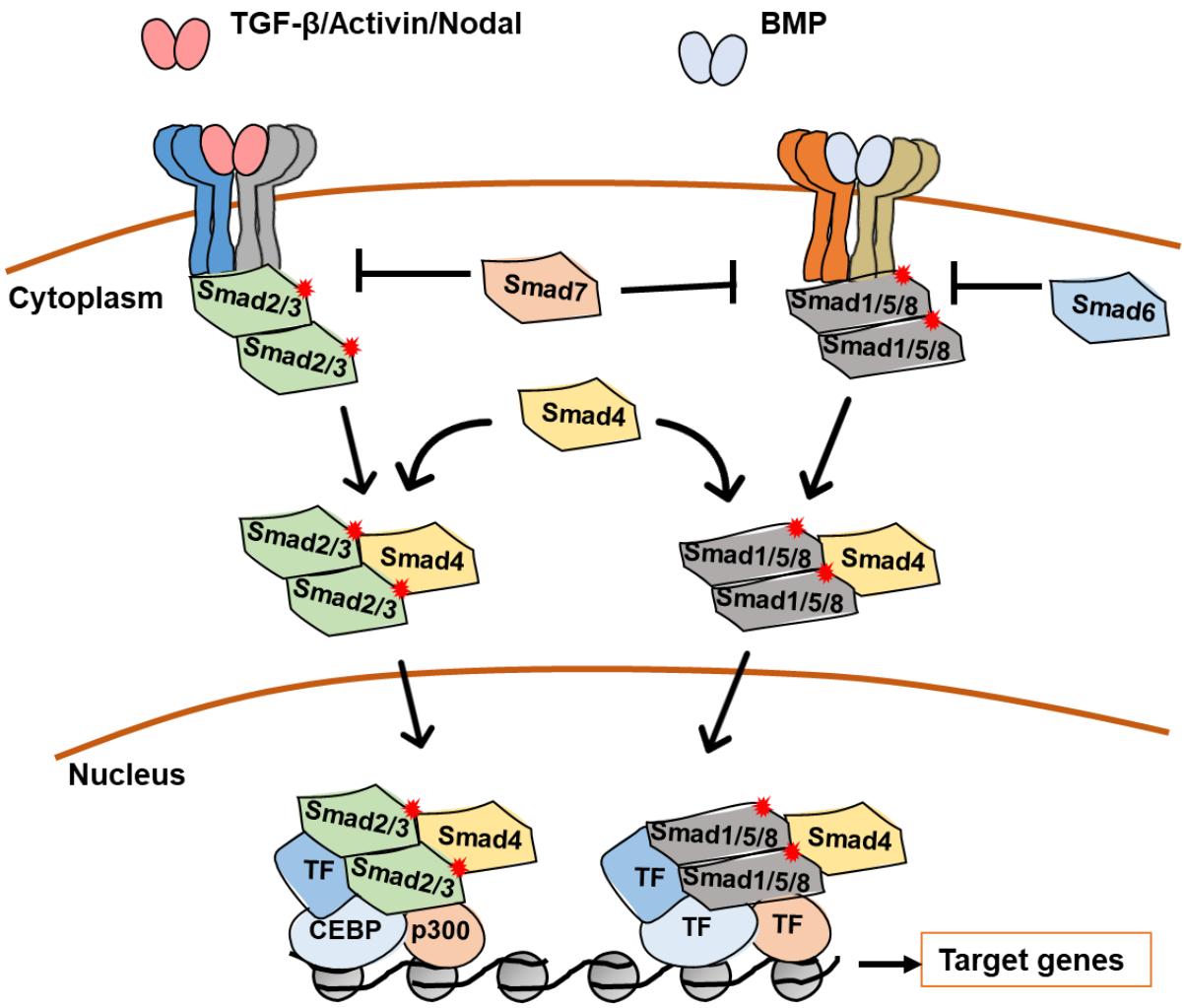

Figure 1.1: An overview of TGF-β and BMP signalling

Binding of TGF-β/Activin/Nodal to their receptor complex activate Smad2 and Smad3 (Smad2/3). Smad2/3 activation promotes their binding to Smad4 to form functional complexes that accumulate in the nucleus to induce target gene expression. Similarly, BMP binding to its receptor complex activate Smad1/5/8 to promote their interaction with Smad4 and nuclear accumulation. Smad6 and Smad7 are inhibitory Smads that negatively regulate the two branches of TGF-β signalling as shown. '✸' represents phosphorylation.

1.1.2 Historical perspective of TGF-β signalling

TGF-β was discovered in the early 1980s as a growth factor secreted by transformed mouse fibroblasts and identified to have both transforming activity for anchorage-independent cell growth in soft agar and bind to epidermal growth factor (EGF) receptors (de Larco and Todaro, 1978). It was later purified from tumour cells but lost its transforming property when subjected to the extraction procedure that could be completely restored if EGF was added to the assay (Roberts et al., 1980, Roberts et al., 1981, Anzano et al., 1982), indicating that it

constituted more than one synergizing component, which was later found to be TGF-α (now identified as EGF) that could not induce soft agar colonies, and TGF-β that could remarkably induce many, large colonies but only in the presence of small amount of EGF. This, in my opinion, is an early indicator of importance of crosstalk of TGF-β signalling with other signalling pathways in defining its role in health and disease. Further, TGF-β could also be purified from normal tissues like platelets, human placenta, and bovine kidney, strongly suggesting a role of TGF-β in both normal physiology and malignancy (Assoian et al., 1983, Frolik et al., 1983, Roberts et al., 1983). More studies confirming the bifunctional role of TGF-β showed that similar concentrations of TGF-β could induce both enhancement and inhibition of colony formation in different cell types (Tucker et al., 1984, Roberts et al., 1985). Moreover, the same cell type could have contrasting effects of TGF-β, depending on the availability of other growth factors in the culture system (Roberts et al., 1985). Together, these early findings strongly suggest the significance of the cellular context and signalling crosstalk in defining TGF-β activity. Many subsequent *in vivo* studies too demonstrated the growth-promoting and -inhibitory effects of TGF-β (Silberstein and Daniel, 1987, Jhappan et al., 1993, Pierce et al., 1993, Cui et al., 1996, Fowlis et al., 1996), prompting a perplex question that how TGF-β, can possess both of these functions. Extensive research into it has now established the consensus that effects of TGF-β superfamily ligands are highly dependent on the cellular context provided by the cell's transcriptional landscape and the activity of other signalling pathways in the cell (Morikawa et al., 2016, David and Massagué, 2018).

This chapter will provide you with an introduction on the fundamental concepts of TGF-β signalling pathway and also discuss the role and regulation of R-Smads in TGF-β signalling, mainly focusing on the Smad2/3-mediated TGF-β signalling and occasional mentions of the BMP pathway. Specially, I would like to introduce you to the important role of post-translational modifications (PTMs) such as phosphorylation and ubiquitination of Smad2/3 linker region in dictating their activity and regulating TGF-β signalling.

1.2 TGF-β family

1.2.1 Functional importance of TGF-β/activin/nodal signalling

1.2.1.1 Embryonic development

Signalling pathways of TGF-β family have important functions in various developmental processes (Jia and Meng, 2021). Nodal signalling is crucial for the induction of mesoderm and endoderm in vertebrates and critically involved in the left-right (LR) asymmetric development, dorso-ventral (DV) patterning and organogenesis of bone and lungs. Evidently, loss of nodal activity results in deficiency of mesodermal and endodermal tissues while the ectodermal tissues expand uncontrollably (Camus et al., 2006, Mesnard et al., 2006). A raise in nodal expression immediately post-implantation provides essential cues required for establishing the body plan and cell fate decisions in early mice embryos (Robertson, 2014, Hill, 2018). Moreover, in pre-implantation mouse embryos, nodal is essential for maintaining the expression of pluripotency genes such as Oct4 (*Pou5f1*) and Nanog (Vallier et al., 2009). In early mouse embryos, Smad2 has a more dominant role than Smad3 as Smad2 knockout mice exhibits early embryonic lethality at E7.5–12.5 while Smad3 knockout mice develops normally but has higher susceptibility to colorectal cancer and autoimmune disorders later in life (Brown et al., 2007). Also, in *Xenopus* embryos, Smad2 is expressed highly abundantly than Smad3 supporting a more important role of Smad2 in early embryonic development (Hill, 2018).

1.2.1.2 Embryonic stem cell (ESC) self-renewal and pluripotency

Fate of ESCs is determined by a complex signalling network determined by various factors like cellular microenvironment and cell-cell contact. Maintenance of ESC pluripotency is also regulated by intrinsic and extrinsic factors (Yilmaz and Benvenisty, 2019). Key intrinsic factors involved are the transcription factors Oct4, Nanog, and Sox2 which are highly expressed in ESCs and form the core transcription network that maintain pluripotency. On the other hand, extrinsic factors include growth factors, cytokines, and extracellular molecules, which act to maintain the proper expression of intrinsic factors through regulating signalling pathways.

Leukaemia inhibitory factor (LIF) in mouse ESCs (mESCs) as well as cooperative effect of fibroblast growth factor (FGF) and activin signalling in hESCs in conjunction with the intrinsic factors maintain ESC pluripotency and self-renewal (Ohtsuka et al., 2015, Mossahebi-Mohammadi et al., 2020, Vallier et al., 2005, Chng et al., 2011). In hESCs, nodal/activin signalling is required for both maintaining pluripotency and stem cell differentiation (Beyer et al., 2013a). Smad2/3 form complexes with key pluripotent factors like Nanog to suppress FGF mediated neuroectoderm differentiation (Vallier et al., 2009). Also, Smad2/3 can bind with Oct4, TEA domain family members (TEADs), and YAP/TAZ, together termed as the TSO complex (TEAD, Smad, and Oct4), to repress the expression of mesendodermal genes such as eomesdermin (EOMES), T-box transcription factor Brachyury, hepatocyte nuclear factor 3-β (HNF3β, or commonly called as FOXA2), and homeobox proteins MIXL1 and goosecoid (GSC) to maintain pluripotency (Beyer et al., 2013b). By contrast, high activin signalling is necessary for endoderm differentiation and Smad2/3 could possibly achieve these two distinct effects of activin signalling in hESCs by binding to different set of transcription partners during pluripotency maintenance and differentiation (Pauklin and Vallier, 2015)

1.2.1.3 Cancer

TGF-β has anti-proliferative role in healthy, non-malignant cells and early-stage tumours. It inhibits cell cycle progression and expression of oncogenes such as c-Myc (David and Massagué, 2018, Batlle and Massagué, 2019, Yu and Feng, 2019). Furthermore, TGF-β activity helps to maintain genetic stability and induces cell apoptosis in cells with damaged DNA (David and Massagué, 2018). However, its tumour-suppressive and pro-apoptotic roles are often lost when cells transform and become cancer cells. Instead, TGF-β promotes cancer progression in these cells as dictated by the genetic and epigenetic changes in the tumour cells. Although the exact mechanisms for this switch in the function of TGF-β is unclear, several potential mechanisms have been proposed, such as, direct binding of oncoproteins to activated Smad2/3 and induce PTMs in them thus, altering their role from anti-proliferative to tumour-promoting (Kretzschmar et al., 1999, Hough et al., 2012, Bae et al., 2014). For

example, elevated Erk/MAPK activation in cancer cells confers specific phosphorylation of Smad2/3 in their linker region and suppresses their growth-inhibitory effects by restricting their nuclear localisation and transcriptional activity (Kretzschmar et al., 1999). Also, TGF-β triggers expression of EMT-associated genes like ZEB-1, SNAI1, SLUG, and TWIST and hyperactive TGF-β signalling in cancer cells can cause deregulation of cell adhesion proteins to promote cell detachment and metastasis (Heldin et al., 2009). Also, some aggressive tumours and cancer stem cells begin expressing nodal which is not normally expressed in adult tissues, and contribute to the hyperactivation, EMT and metastasis of cancer cells. This paradox in the role of TGF-β in cancer progression complicates its therapeutic targeting but can be resolved by first assessing the role of TGF-β in a specific tumour type and then deciding if it needs to be inhibited or supported as part of the cancer therapy.

1.2.1.4 Fibrosis and other diseases

Fibrosis causes loss of normal tissue function and can occur as a response to repetitive injury and tissue damage. It is an imbalanced, hyper-responsive wound healing process and is characterized by modification of healthy parenchymal tissue in the extracellular matrix (ECM) and its replacement with collagen-rich ECM due to hyperactivated fibroblasts. TGF-β activation in these fibroblasts causes increased cell and nuclear sizes, upregulation in protein synthesis, changes in cellular metabolism, altered gene expression, and heightened ECM protein expression, especially an increase in collagen production which is a hallmark of fibrosis (Budi et al., 2021, Lodyga and Hinz, 2019). TGF-β is a potent mediator of fibrosis in many organs such as kidney, heart, lung, and liver. TGF-β signalling promotes inflammation and renal fibrosis to cause chronic kidney disease (CKD) in patients. It also causes pathogenesis of many liver diseases, such as hepatitis, cirrhosis, and hepatocellular carcinoma (Walton et al., 2017). TGF-β is also a master regulator of pulmonary health and disease and its dysregulation causes lung pathologies like pulmonary fibrosis and cystic fibrosis (Lederer and Martinez, 2018, Kramer and Clancy, 2018). TGF-β also induces cardiac fibrosis via its canonical and non-canonical signalling pathways and can cause chronic heart failure. Overall,

an upregulation of mediators of TGF-β signalling and downregulation of its antagonists characterize the molecular basis of TGF-β-mediated fibrosis. Development of therapeutic targets that inhibit TGF-β signalling can be used in the treatment of fibrosis.

In addition to cancer and fibrosis, TGF-β signalling is dysregulated in many other human diseases including cardiovascular diseases, neurological conditions, neurodegenerative diseases, auto-immune disorders, and aging-related conditions (David and Massagué, 2018, Goumans and ten Dijke, 2018, Kashima and Hata, 2017, Tominaga and Suzuki, 2019, Hammond et al., 2019). The reason TGF-β signalling is implicated in so many diseases, is that it has crucial roles in maintaining cellular homeostasis in adult cells and tissues. Therefore, any disruption of its functions can easily cause an imbalance in the cellular metabolic and transcriptional landscape and present pathological conditions.

1.2.2 TGF-β biosynthesis and activation

Like other members of the TGF-β superfamily, a TGF-β family ligand is synthesised as a ~50 kDa precursor protein, containing a C-terminal shorter mature TGF-β ligand and an N-terminal covalently bound pro-segment, known as the latency-associated protein (LAP) (*Fig 1.2A*) (Derynck et al., 1985, Robertson and Rifkin, 2016). The LAP aids in correct protein folding, stabilisation, PTMs, and further processing of the TGF-β precursor in the ER lumen (Gray and Mason, 1990). The LAP also directly masks the amino acid residues of the C-terminal amino acids of the mature TGF-β ligand, to prevent binding to the receptors (Shi et al., 2011). Moreover, the signal peptide at the N-terminal of the LAP is recognized by signal recognition proteins (SRP) and associated SRP receptors, helping in the transportation of the TGF-β precursor into the ER lumen (Gentry et al., 1988). In the ER lumen, TGF-β precursors dimerise via three disulphide bonds, two in the pro-segment and one in the mature domain, to form the small latent complex (SLC) (*Fig 1.2B*) (ten Dijke and Arthur, 2007).

Concomitantly, large multidomain glycoproteins called as latent TGF-β-binding proteins (LTBPs) are also translated in the ER lumen and associate with the SLC via a pair of disulphide bonds with the LAP to from the large latency complex (LLC) (*Fig 1.2B*) (Miyazono et al., 1991, Gleizes et al., 1996, Saharinen et al., 1996). However, in immune cells, SLC crosslinks with glycoprotein A repetitions predominant (GARP) to form the LLC (Wang et al., 2012, Liénart et al., 2018). LLC is then cleaved by the furin family proteases at the junction of the LAP and the mature TGF-β in the Golgi complex but the precursor TGF-β dimers still remain bound to each other and to the LTBPs via disulphide bonds (Dubois et al., 1995). These furin-cleaved LLC accumulates in secretory vesicles and undergoes exocytosis, to be deposited in the ECM, until its activation (*Fig 1.2C and D*) (Robertson and Rifkin, 2016).

Many ECM proteins can bind with the LLC via the LAP or the mature TGF-β to keep the latent TGF-β tethered to the ECM. For example, collagen, fibronectin, fibrillin, and thrombospondin in the ECM, can bind to and sequester TGF-β (Robertson and Rifkin, 2016). Proteolytic disruption of the ECM activates TGF-β, releasing the mature ligands for

subsequent receptor binding and downstream signal transduction. Other factors, including pH, reactive oxygen species (ROS), thrombospondin-1 and integrins, are also reported to be able to activate TGF-β (Robertson and Rifkin, 2016). Particularly, integrins play a major role in activating TGF-β. During inactive state, integrins remain bound to the RGD sequence in LAP and in turn preserve LAP structure to prevent the release of mature TGF-β (Munger et al. 1999; Annes et al. 2004). However, integrin-mediated traction between cell and ECM can change LAP structure, freeing mature TGF-β ligands (Annes et al. 2004). In addition, study by Mu et al., suggests that integrins may also interact with proteases such as matrix metalloproteinase 1 (MMP1) to cleave LAP structure and release mature TGF-β ligands as inhibiting MMPs blocked TGF-β activation (Mu et al., 2002). Moreover, a mice model with modified RGD sequence exhibited phenotype similar to TGF-β-1-null mice, highlighting the importance of integrins in activating TGF-β (Aluwihare et al. 2009).

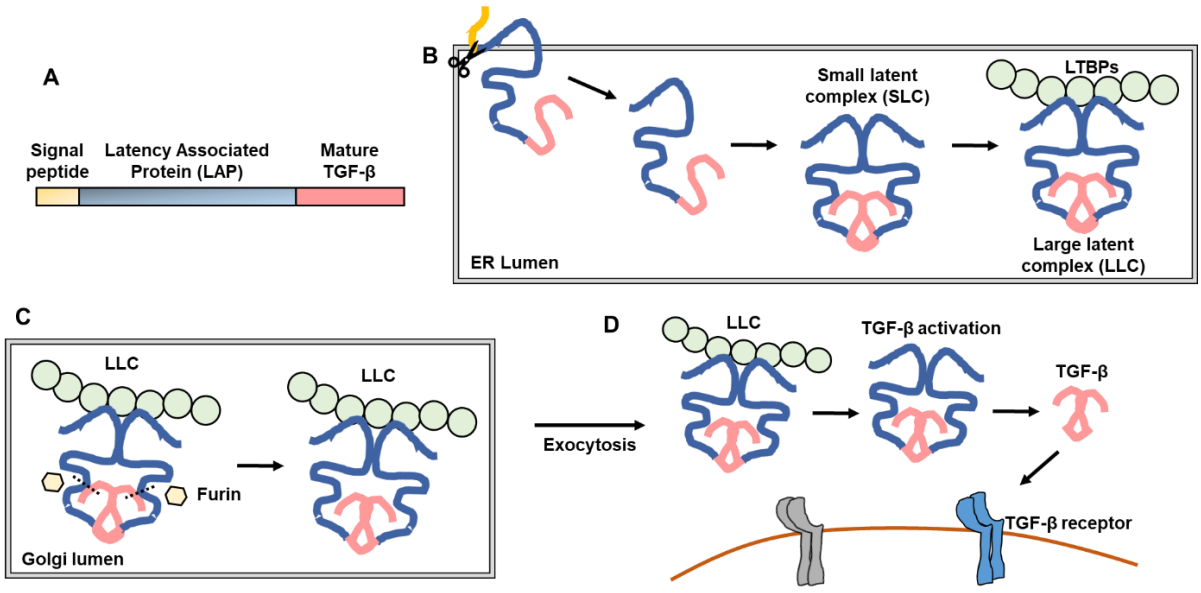

Figure 1.2: Ligand processing and presentation to the receptors

A) TGF-β is secreted as a precursor form (pro-TGF-β) comprised of an N-terminal signal peptide, LAP, or the pro-domain, and mature TGF-β. **B)** Pro-TGF-β is processed in the ER lumen after the removal of the signal peptide, where it undergoes dimerisation and further binds to LTBPs to form LLC. **C)** LLC is transported to the trans-Golgi apparatus where furin enzyme cleaves it at the junction of LAP and mature TGF-β. **D)** Cleaved LLC is exocytosed via secretory vesicles and is deposited in the ECM until activated. On activation, mature TGF-β is released from its scaffold and is free to bind to available receptors on the cell surface.

1.2.3 TGF-β receptor activation

Mature TGF-β can bind to cell surface localised TGF-β receptors and initiate the downstream cascade of signal transduction. TGF-β receptors are composed of type I and type II receptors, which are somewhat structurally similar to each other and have an extracellular glycosylated N-terminal domain, an α-helical trans-membrane domain, a small juxta-membrane domain, and a C-terminal cytoplasmic kinase domain (Chaikuad and Bullock, 2016). Both type I and II receptors are ATP-dependent, dual-specificity protein kinases, having both serine/threonine and tyrosine kinase activities, which is a distinct feature from most other receptors as they only have tyrosine kinase activities (Lawler et al., 1997). However, they differ from each other in that type I receptor has a glycine-serine-rich (GS) domain but type II receptors not (Huse et al., 1999). The canonical TGF-β signalling occurs via the serine/threonine kinase receptor activity, while the weaker tyrosine kinase activity of the receptor complex relays the non-canonical TGF-β signalling pathway (Manning et al., 2002). In the absence of ligands, these receptors exist as monomers, homo- or even heterodimers, conferring a strong need for a ligand for downstream signalling activation (Huang et al., 2011, Ehrlich et al., 2012). Only upon ligand binding, type I and type II receptors form stabilised, functional receptor hetero-tetrameric complexes (Hart et al., 2002, Groppe et al., 2008). A single dimeric TGF-β ligand binds with two type I and two type II receptors via distinct structural domains, forming a symmetrical 2:2:2 conformation and offering additional stability to the ligand-receptor complex by bringing the two receptors together. There are seven type I and five type II receptors in mammals. Individual TGF-β subfamily ligands bind to distinct receptor complexes (David and Massagué, 2018). Although it has not been deeply studied but it is considered that different receptor combinations may confer variability to downstream signalling activity (Heldin and Moustakas, 2016). Various type I and type II receptors for the TGF-β family is listed in the following page (*Table 1.1*).

Table 1.1: Receptors involved in Smad2/3-mediated canonical TGF-β signalling

TGF-β family member	Type I receptor	Type II receptor	Smad
TGF-β1	TGFBR1 (ALK5)	TGFBR2	Smad2/3
TGF-β2	TGFBR1	TGFBR2	Smad2/3
TGF-β3	TGFBR1	TGFBR2	Smad2/3
Activin A	ACVR1B (ALK4) and ACVR1C (ALK7)	ACVR2 (ActRII) and ACVR2B (ActRIIB)	Smad2/3
Activin B	ACVR1B and ACVR1C	ACVR2 and ACVR2B	Smad2/3
Nodal	ACVR1B and ACVR1C	ACVR2 and ACVR2B	Smad2/3
GDF1	ACVR1B and ACVR1C	ACVR2 and ACVR2B	Smad2/3
GDF3	ACVR1B and ACVR1C	ACVR2 and ACVR2B	Smad2/3
Myostatin (GDF8)	ACVR1B and TGFBR1	ACVR2	Smad2/3
GDF9	ACVR1B	BMPR2	Smad2/3
GDF11	ACVR1B and TGFBR1	ACVR2 and ACVR2B	Smad2/3
Activin C	unknown	unknown	unknown
Activin E	unknown	unknown	unknown

Abbreviations: TGFBR1/2- TGF-β receptor type I/II, ALK4/5/7- activin receptor-like kinase 4/5/7, ACVR1B/1C/2/2B- activin A receptor type 1B/1C/2/2B, ActRII/IIB- activin receptor type 2/2B, and BMPR2- bone morphogenetic protein receptor type II.

Mature TGF-β/activin/nodal molecules have a strong affinity to the homodimers of type II receptors (Groppe et al., 2008, Hart et al., 2002, Radaev et al., 2010). Type II receptors are constitutively active which auto-phosphorylate at specific serine (S213 and S409), tyrosine (Y259, Y336, and Y424) and some threonine residues (Luo and Lodish, 1997, Lawler et al., 1997). Ligand-type II receptors interaction causes receptor conformational changes, inducing formation of another high affinity binding site for type I receptor homodimers. Type II receptors can then phosphorylate type I receptors at their serine residues in the glycine-serine (GS) subdomain located in the juxta-membrane domain, just upstream of the cytoplasmic kinase domain (Wrana et al., 1994). Many serine residues of the GS domain are known to be phosphorylated by the type II receptors, and it only requires a certain threshold of phosphorylation to be achieved for activation (Heldin and Moustakas, 2016). The GS domain phosphorylation result in dissociation of a negative regulator chaperone of the type I receptors,

called FK506 binding protein of twelve kDA (FKBP12) and finally permit the formation of a tightly bound complex containing the ligand dimer, two type II receptors, and two type I receptors (Wang et al., 1996, Chen et al., 1997b, Huse et al., 1999). These interactions facilitate additional changes in the conformation of the transmembrane and cytoplasmic domains of both the receptors thus, enabling recruitment and phosphorylation of downstream signal transducers, Smad2/3 for TGF-β signalling activation (Huse et al., 2001).

1.2.4 Smad2/3 activation

1.2.4.1 Smad structure and function

As introduced in section 1.1.1, there are total eight Smad proteins in humans, which are categorised in three groups, R-Smads, Co-Smad and I-Smads according to their structure and functions. All Smad proteins, except I-Smads, consist of two highly conserved domains, the mad homology 1 (MH1) and MH2, separated by a non-conserved, unstructured, and flexible linker region, whereas I-Smads lack a distinct MH1 domain and only possess an MH2 domain (*Fig 1.3*). The MH1 and MH2 domains of Smad2/3 are very similar to each other while the other R-Smads share sequence similarities among them (Shi et al., 1998, Shi, 2001). Smad2/3 are 467 and 425 amino acid residues long, respectively, and both contain a nuclear localisation signal (NLS), and a β-hairpin structure in their N-terminal MH1 domain for DNA binding. However, the most expressed form of Smad2 has two other structural motifs in its MH1 domain, called insert 1 (ist1) and exon3 (E3), that disrupt Smad2 NLS and its interaction with poly (ADP-ribose) polymerase-1 (PARP-1), and most importantly, the conformation held by the E3 insert determines the extent of Smad2 interaction with the Smad binding elements (SBE) sequence (Shi et al., 1998, Yagi et al., 1999, Aragon et al., 2019). Therefore, MH1 domain is generally considered to help Smads with their DNA binding. Smad4 too has an NLS and the β-hairpin motif in its MH1 domain in addition to a nuclear export signal (NES) just upstream of the linker region, which are essential for its translocation within the subcellular spaces, DNA binding, and transcriptional activity (Xiao et al., 2003).

The MH2 domain of both Smad2/3 has an NES, nucleopore signal (NPS), the L3 loop, and the C-terminal serine-x-serine (SxS) motif (*Fig 1.3*) (Shi, 2001, Macias et al., 2015). The SxS motif and the L3 loop play essential roles in TGF-β-mediated Smad2/3 activation (Chacko et al., 2001). The L3 loop recruits Smad2/3 to the activated type I receptor (Lo et al., 1998) which phosphorylates their SxS motif and allows Smad2/3 formation of functional oligomeric complexes with Smad4 to further relay the signal into the nucleus (Chaikuad and Bullock, 2016). Smad4 too has the L3 loop structure that allows its interaction with Smad2/3 following their activation, in addition to having an NPS upstream of its L3 loop, but no SxS motif, which prohibits its direct activation through activated type I receptors (Shi et al., 1997). Smad7 too has an NPS, NES, and the L3 loop in its MH2 domain but no SxS motif (Murayama et al., 2020), which together, allow Smad7 translocation to the cytoplasm or nucleus but no activation by the receptors. Overall, MH2 domain of Smad2/3 and Smad4 presents a versatile protein interacting unit as well as contains cellular localisation signals for various Smad functions.

The linker region of Smad2/3 connects the MH1 and MH2 domains and does not have a specific structure. It contains several phosphorylatable serine and threonine residues which are substrates of kinases belonging to other signalling pathways. Increasing evidence suggests that the linker region of Smad2/3 has important regulatory roles in TGF-β signalling, which will be discussed in detail in the later sections of this chapter.

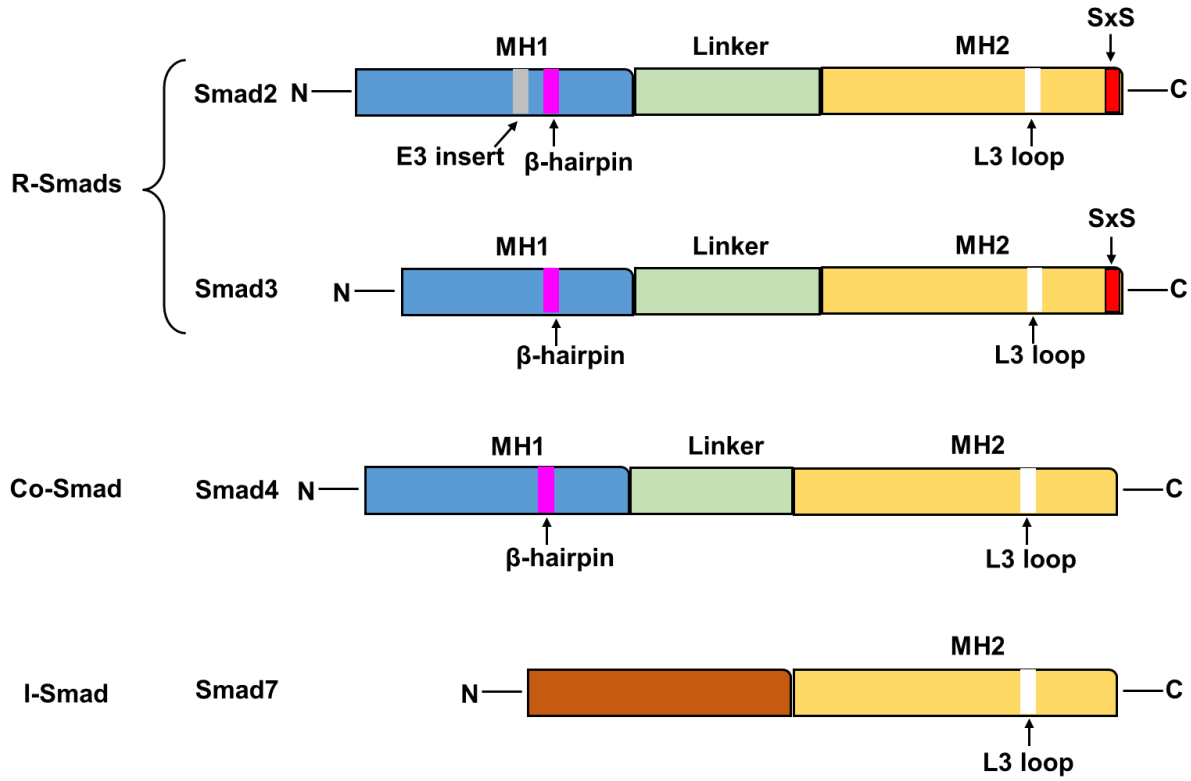

Figure 1.3: Schematic representation of important features of Smad2, Smad3, Smad4 and Smad7

Both R-Smads and Co-Smad have the MH1 and MH2 domain flanked by a linker region. They also have the β-hairpin structure in their MH1 domain for DNA binding and L3 loop in their MH2 domain that helps in their protein interactions. Only R-Smads have the SxS motif in their MH2 domain for type I receptor-mediated phosphorylation and activation. I-Smad, Smad7 does not have a distinct MH1 domain but only an MH2 domain with L3 loop for its protein binding.

1.2.4.2 Smad activation

Smad2/3 are activated upon activation of TGF-β receptor complexes, in which Smad2/3 chaperone protein, an FYVE domain-containing Smad anchor for receptor activation protein (SARA) in the endosomal membranes, presents Smad2/3 to the activated type I receptors to enable their interaction (Tsukazaki et al., 1998, Penheiter et al., 2002). Once bound, type I receptors activate Smad2/3 through phosphorylating their C-terminal SxS motif, resulting in conformational changes in their structures that allow their dissociation from the receptors and from SARA to create new binding sites for Smad4 (Chaikuad and Bullock, 2016). Smad4 associates with activated Smad2/3 to form functional oligomeric complexes containing either heterodimer or homodimer of Smad2/3 with Smad4 for subsequent TGF-β signalling (Chacko et al., 2001). Complexes containing a combination of activated Smad2 and Smad3, but no Smad4 have also been observed but their biological function has not been clearly described yet (Kawabata et al., 1998, Lucarelli et al., 2018).

1.2.5 Smad2/3 nucleocytoplasmic shuttling

Smad2/3-Smad4 functional oligomeric complexes translocate and accumulate in the nucleus to enable their interaction with their transcription partners and target genes for subsequent action (Hill, 2016). However, regardless of TGF-β-induced activation, individual Smads can also translocate in and out of the nucleus, as they undergo constant nucleocytoplasmic shuttling by various mechanisms such as RanGTPase-dependent nuclear import and export or direct interaction with nucleoporins (*Fig 1.4*). As a result of different rates of the nucleocytoplasmic shuttling of Smad2/3 and Smad4, Smad2/3 are more cytoplasmic while Smad4 remains evenly distributed in the cell in the absence of signal activation (Pierreux et al., 2000, Funaba and Mathews, 2000). Nevertheless, inactivated Smad3 localises in the nucleus more than Smad2 and remains bound to the SBEs to prime target gene expression when the signalling is activated (Liu et al., 2016, Aragon et al., 2019). Smad3 can also interact directly with importin-β through its NLS in the MH1 domain for its nuclear import whereas, Smad4 uses the same conserved NLS for its importin-α/β-dependent nuclear import (Xiao et

al., 2000a, Xiao et al., 2000b, Kurisaki et al., 2001, Xiao et al., 2003). In contrast, Smad2 NLS may be affected by E3, as mentioned previously, which prevents its nuclear localisation in the absence of signal activation (Shi et al., 1998, Aragon et al., 2019). Moreover, other importins, Importins 7 and 8 can also import Smad2/3 into the nucleus (Xu et al., 2007). Interestingly, Smad4 can also be exported out of the nucleus via chromosome region maintenance 1 (CRM1), also called as exportin1, but not Smad2/3 as CRM1 inhibition retains only Smad4 in the nucleus (Pierreux et al., 2000). Additionally, another completely different mechanism by which Smad2/3/4 can be transported between the cellular compartments is through the nucleoporins CAN/Nup214/Nup153, contributing to their constitutive nucleocytoplasmic shuttling (Xu et al., 2002, Xu et al., 2003). In particular, Smad2 cytoplasmic and nuclear retention proteins compete with Nup214 and Nup153, respectively, to mediate its translocation to the other compartment.

However, if these Smads are already capable to be in the nucleus even in the absence of any stimulation, what ensures their sustained nuclear presence on TGF-β stimulation? To answer this, evidence via mathematical modelling and *in vitro* studies suggest that activated Smad2/3 simply have reduced export rate from the nucleus, likely due to diminished rate of interaction with their nuclear export proteins as well as their SxS phosphorylation-mediated conformational changes and protein interactions (Schmierer and Hill, 2005, Schmierer et al., 2008). They enter the nucleus at the same rate as before TGF-β activation but can exit the nucleus at a much slower rate. Concomitantly, Smad4 also undergoes its nucleocytoplasmic shuttling and detects activated Smad2/3, and due to their strong affinity to bind with activated Smad2/3, Smad4 forms oligomeric complexes with them and prevent itself and bound Smad2/3 from nuclear export. These events, along with decreased mobility because of enhanced DNA binding, consequently, result in net accumulation of Smad2/3-Smad4 complexes in the nucleus (*Fig 1.4*). Another mechanism by which functional Smad complexes are retained in the nucleus is by WW-domain-containing transcription regulator 1 (WWTR1 or commonly known as TAZ) (Varelas et al., 2008). In the presence of TGF-β activation, TAZ

can bind to functional Smad2/3 complexes to promote their nuclear accumulation and interaction with the transcriptional machinery to induce target gene expression (Varelas et al., 2008). Interestingly, despite TGF-β activation, individual dephosphorylated Smads can exit the nucleus, indicating a dynamic process that allows constant nucleocytoplasmic shuttling of Smad2/3 for swift sensing of receptor activation or deactivation and regulating subsequent rounds of TGF-β signalling (Inman et al., 2002, Schmierer and Hill, 2005, Schmierer et al., 2008).

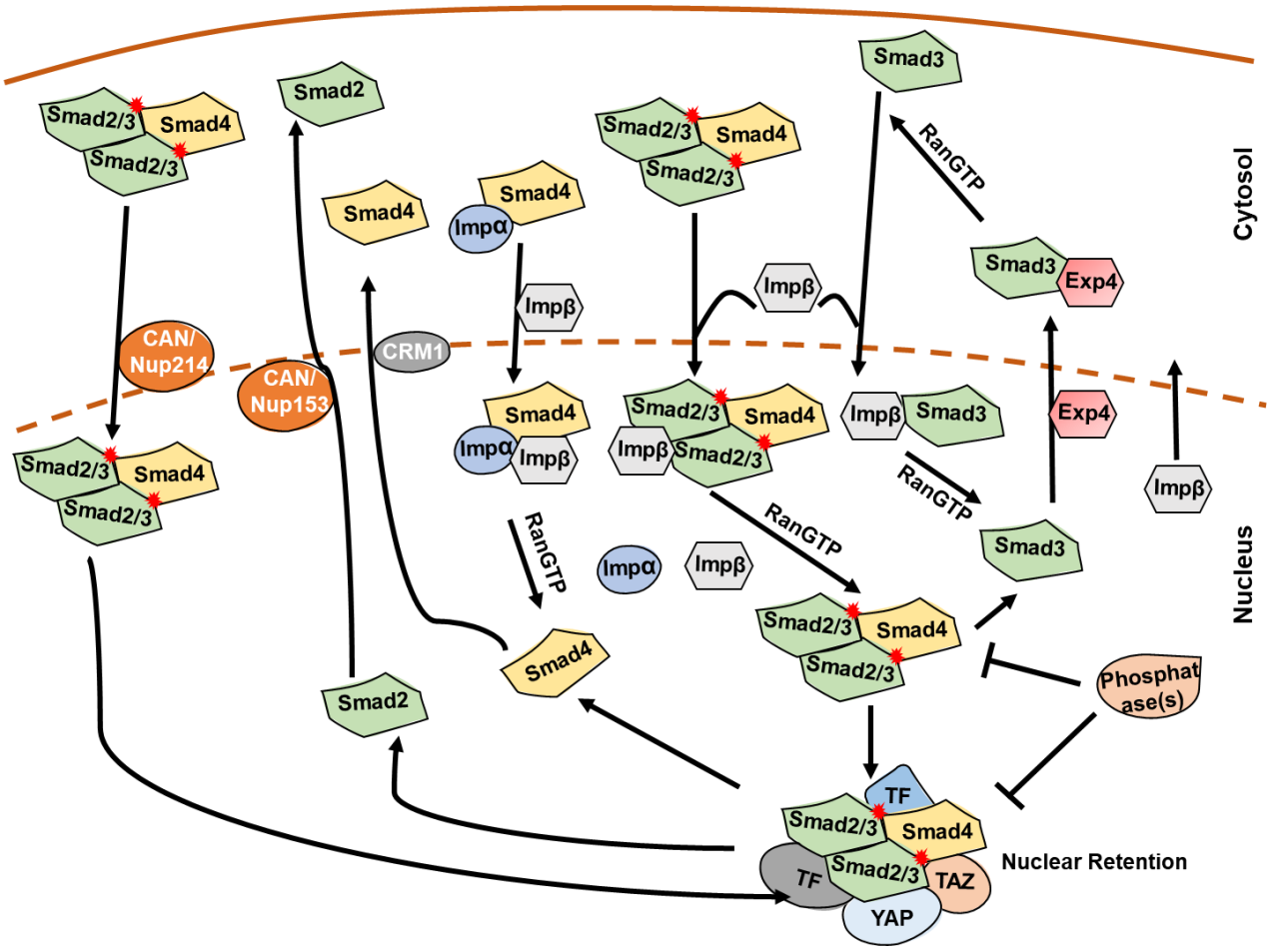

Figure 1.4: A model for importin/exportin- and nucleoporin-mediated nucleocytoplasmic shuttling of Smad2, Smad3, and Smad4 Functional oligomeric complexes containing activated Smad3 associate with importin-β to enter the nucleus. Its association with nuclear retention proteins aids in nuclear accumulation of the functional oligomeric complexes while phosphatases can result in dissociation of the complex into individual Smads. Smad3 can exit the nucleus via its association with exportin4 or directly through nucleoporins CAN/Nup153. Smad2 can also translocate to the cytoplasm via CAN/Nup153 or to the nucleus via CAN/Nup214. Smad4 can exit the nucleus through CRM1, unlike Smad2/3.'✸' represents phosphorylation.

1.2.6 Smad2/3-mediated transcription

Accumulation of Smad oligomeric complexes in the nucleus regulate the expression of TGF-β target genes. Smad2/3 and Smad4 are capable of direct interaction with specific DNA motif called the Smad-binding element (SBEs) via their β-hairpin structure in the MH1 domain (Shi et al., 1998, Zawel et al., 1998, Morikawa et al., 2013, Aragon et al., 2019). SBEs are available abundantly throughout the genome and are defined by the sequence 5'-CAGAC-3' or its reverse complement 5'-GTCTG-3'. However, more recent studies indicate that just like the R-Smads of BMP subfamily, Smad2/3 can also bind to GC rich motifs and therefore, they can also recognise the common consensus sequence of 5'-GGC(GC)(CG)-3' (Martin-Malpartida et al., 2017). As described before, presence of an E3 insert in Smad2 makes it slightly structurally different from Smad3 and these intrinsic structural differences in Smad2/3 determine differences in their transcriptional activity and cellular localisation (Liu et al., 2016, Aragon et al., 2019). Upon signal activation, the DNA-binding ability of the Smad oligomeric complexes is considerably enhanced when they interact with other transcriptional cofactors and chromatin modifiers, and their cooperation dictates the target genes that are expressed or repressed (Hill, 2016). Since these transcriptional cofactors can be cell- and lineage-specific as well as potential targets of other signalling pathways, their interaction with functional Smad complexes help to provide the cell-dependent context for the outcome of TGF-β signalling (Mullen et al., 2011).

Furthermore, there are some classic transcriptional partners of Smad2/3 which enhance their recruitment to DNA. For example, Forkhead box protein H1 (FoxH1), the first transcription factor identified to interact with activated Smads in *Xenopus laevis* embryos and subsequently in other species as well (Chen et al., 1996, Chen et al., 1997a). In hESCs, nodal/activin signalling is required for both maintaining pluripotency and stem cell differentiation (Beyer et al., 2013a). Activated Smad2/3 form complexes with key pluripotency factors Oct4 and Nanog to suppress FGF-mediated neuroectoderm differentiation and remain in the TSO complex to repress the expression of mesendodermal genes such as EOMES, T-box transcription factor

Brachyury, hepatocyte nuclear factor 3-β (HNF3β, or commonly called FOXA2), and homeobox proteins MIXL1 and goosecoid (GSC), likely with the help of a co-repressor nucleosome remodelling deacetylase (NuRD), to maintain pluripotency (Beyer et al., 2013b, Vallier et al., 2009). Activated Smad2/3, on the other hand, cooperate with FoxH1 to lift the repression of mesendoderm transcription factors, enable their upregulation, and facilitate stem cells exit from their pluripotency state (Beyer et al., 2013a). Recruitment of activated Smad2/3 to FoxH1 sites is facilitated by a RING finger domain containing E3 ubiquitin ligase, Ectodermin/TIF1γ/TRIM33 to drive mesendodermal differentiation (Dupont et al., 2005). Another class of forkhead transcription factor with which activated Smad2/3 interact with is the FoxO family which synergise with SBE-bound activated Smad2/3 complexes by binding to adjacent sequences and driving expression of the cyclin-dependent kinase (CDK) inhibitors $p21^{Cip1}$ to inhibit cell cycle progression (Seoane et al., 2004, Gomis et al., 2006a).

Complexes of activated Smad2/3 also remodel the chromatin by interacting with histone acetyl transferases (HATs) and co-activators like p300, CREB binding protein (CREBP), GCN5, and p300/CBP-associated factor (P/CAF) to enhance TGF-β signalling (Ross et al., 2006). In addition, other transcription factors like high-mobility group A protein 2 (HMGA2) and CCAAT/enhancer binding protein β (CEBPB) facilitate activated Smad2/3 to enhance the expression of zinc finger protein- SNAI1 and $P15^{Ink4b}$ as well as repress c-Myc expression, associated with EMT and cell cycle regulation (Gomis et al., 2006b, Thuault et al., 2008). In addition to c-Myc, other target genes that are repressed by Smad2/3 activity are bone γ-carboxyglutamic acid-containing protein (BGLAP) and activating transcription factor 3 (ATF3), which are mediated by recruiting histone deacetylases (HDACs) to the DNA binding sites and have functions in osteoblastic differentiation and cellular stress response, respectively (Alliston et al., 2001, Kang et al., 2003, Kang et al., 2005). In addition to histone acetylases and deacetylases, activated Smad complexes can also interact with histone methyltransferases like SET domain bifurcated histone lysine methyltransferase 1 (SETDB1), for example, to repress transcription of SNAI1, generating negative feedback for TGF-β signal

(Du et al., 2018). Smads can also suppress transcription by binding with co-repressors such as transforming growth-interacting factor (TGIF), C-terminal binding protein (CtBP) and zinc finger protein 451 (ZNF451) which inhibit activated Smad2-mediated transcription by recruiting HDACs and disabling Smad2/3 interaction with HAT p300 (Derynck and Budi, 2019). Some other co-repressors that activated Smad2/3 and Smad4 can interact with are protooncogenes Sloan Kettering Institute protein (SKI) and the related SKI-like protein (SKIL, previously called as SnoN), their action of repression and regulating TGF-β signalling is discussed in greater detail in the following sections. Altogether, Smad2/3 transcriptional activity is governed by their transcription partners as well as the epigenetic regulation via co-repressors and co-activators that define the net outcome of TGF-β signalling. An overview of all the events of Smad2/3-mediated TGF-β signalling discussed so far is summarised (*Fig 1.5*).

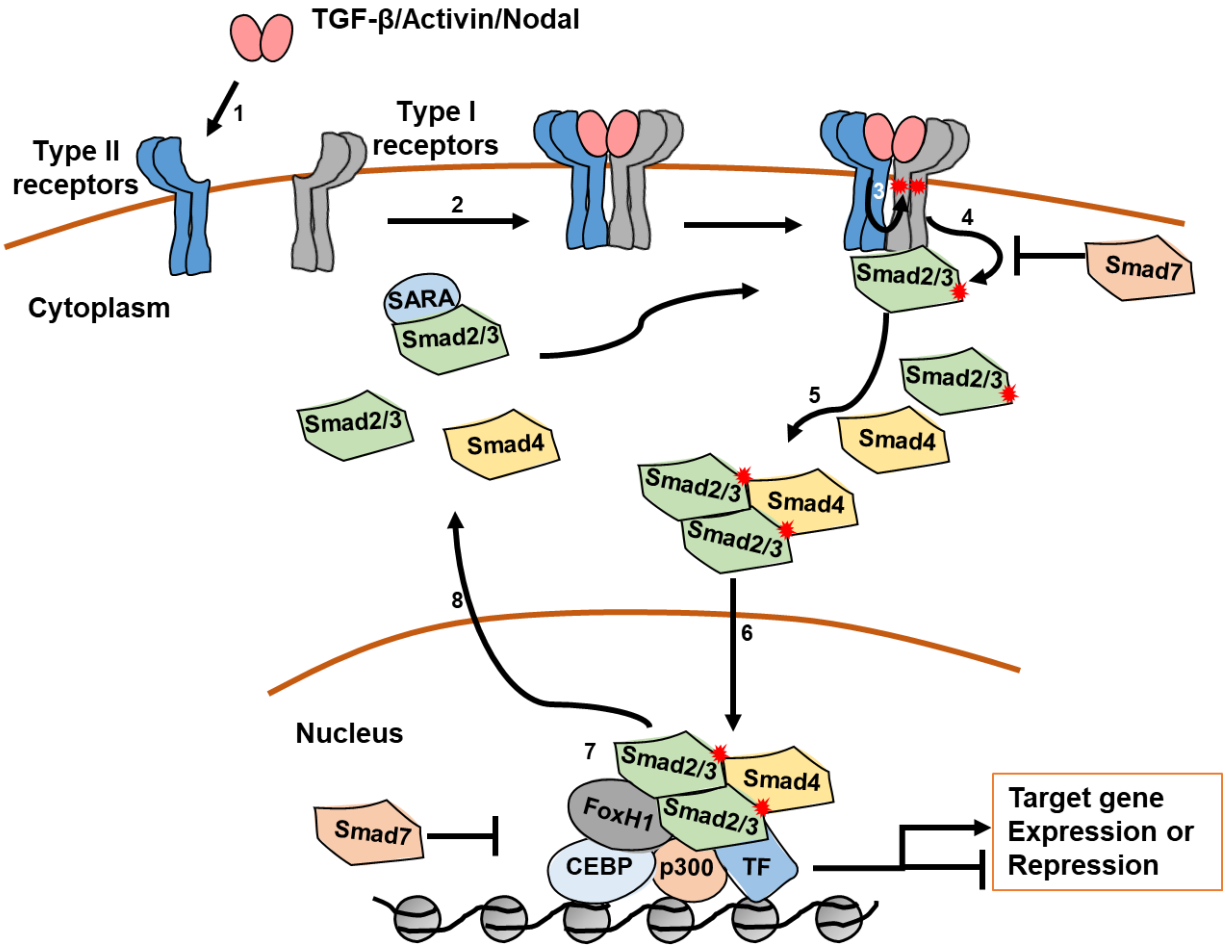

Figure 1.5: An overview of TGF-β signalling

TGF-β signalling is initiated when it binds to type II receptors (1) to form receptor complex with type I receptors (2) inducing type I receptor phosphorylation (3), as indicated by the red star. Activated type I receptor phosphorylates Smad2/3 (4) to facilitate their binding with Smad4 and form functional oligomeric complexes (5) which accumulate in the nucleus (6) and interact with other transcription partners to induce target gene expression or repression (7). Smad2/3 is dephosphorylated and dissociates from the complex to translocate back to the cytoplasm (8). Smad7 inhibits Smad2/3 transcriptional activity and also, compete with them to bind to activated type I receptors and thus, preventing formation of functional oligomeric complexes. '✸' represents phosphorylation.

1.3 Regulation of TGF-β family signalling

Since TGF-β signalling plays important roles in embryonic development and adult tissue homeostasis, abnormality in this signalling is associated with many pathological conditions. Proper control of it is crucial for normal health which is often dysregulated in diseases. Therefore, many factors are involved at multiple levels along the signalling pathway, from ligands to effectors, in regulating TGF-β signalling.

1.3.1 Regulation of ligand availability and binding to receptors

1.3.1.1 Ligand bioavailability

The ECM generally contains more latent TGF-β than required for cellular functions so that its active form can be rapidly released when necessary, during early embryonic development or in adult tissue homeostasis or in pathological conditions (Robertson and Rifkin, 2016, Doyle et al., 2012). Several mechanisms can control TGF-β/activin/nodal ligand availability to modulate their downstream signalling. For example, biosynthesis of TGF-β ligands can be negatively regulated by proteins like E-selectin-ligand-1 that bind to intracellular TGF-β precursor protein and inhibit its processing and secretion into the ECM, thus, preventing its deposition into the ECM (Yang et al., 2013). Another way to control ligand availability is via the action of proteases and/or integrins on LTBPs to strictly regulate the amount of active TGF-β released (Robertson and Rifkin, 2016). Moreover, many proteins required for TGF-β activation in the ECM are also its transcriptional targets such as integrins, MMPs, collagen, and fibronectin which help in a positive feedback regulation of TGF-β signalling (Yan et al., 2017).

1.3.1.2 Ligand competition

TGF-β signalling can also be regulated by competition of active ligands with other secretory factors like follistatin to bind to the receptors, especially during early embryonic development and in reproductive health. Follistatin hinders activin and myostatin binding with the type II receptors to inhibit downstream signalling necessary for mesoderm induction during embryonic development and stimulating follicle-stimulating hormone (FSH) secretion from the pituitary (Chen and Meng, 2004). It can also form complexes with BMPs to inhibit their activity during embryonic development (Iemura et al., 1998). Another protein that inhibits nodal signalling by competition for receptor binding is Lefty which directly binds to nodal to prevent its receptor interaction (Chen and Shen, 2004). During gastrulation in mouse development, Lefty prevents nodal signalling and causes an expanded primitive streak whereas its inactivity results in excessive mesodermal induction (Chen and Meng, 2004). Similarly, overexpression of Lefty1 in zebrafish embryos suppresses mesodermal induction and inhibits head and trunk formation which can be reversed by increasing the availability of activin/nodal ligands or by overexpressing their receptors (Chen and Meng, 2004). Furthermore, Lefty suppresses activin/nodal signalling also via a negative feedback loop as its expression is dependent on nodal signalling. Another structurally related protein to activin is inhibin, which with the help of a TGF-β co-receptor betaglycan, antagonises activin's role in FSH secretion, erythroid differentiation, and chondrogenesis by competing with it for receptor binding (Lewis et al., 2000, Vale et al., 1990). Other proteins like Cerberus, Dan and Charon also play an important role in negatively regulating both TGF-β/activin/nodal and BMP pathways by impeding their receptor interaction and affect left-right patterning (Piccolo et al., 1999, Hashimoto et al., 2004).

1.3.2 Regulation at the level of receptors

1.3.2.1 Regulation via membrane trafficking of TGF-β receptors

Receptor internalisation is a normal event in any cell signalling where cell surface receptors are trafficked inside the cell via endocytic vesicles for further processing such as receptor degradation or their recycling back to the plasma membrane. TGF-β receptors are rapidly internalised upon ligand binding but they can undergo endocytosis even in the absence of any ligands (Mitchell et al., 2004, Doré et al., 2001). There are two separate mechanisms with which activated ligand-bound TGF-β receptors can undergo endocytosis: 1) clathrin-coated pits and 2) cholesterol-enriched caveolar vesicles (*Fig 1.6*) (Hayes et al., 2002, Di Guglielmo et al., 2003, Razani et al., 2001). It is not yet known what determines the mechanism adopted for receptor internalisation, but it may be dictated by the cell type, cell polarity, and cell-cell junctions (Heldin and Moustakas, 2016, Vander Ark et al., 2018).

Clathrin-coated pits are responsible for internalisation of ligand-bound receptors into endosomes enriched with early endosomal antigen 1 (EEA1) and SARA and promote canonical TGF-β signalling (Tsukazaki et al., 1998, Penheiter et al., 2002). Another adaptor protein called disabled-2 (Dab2) and a tumour suppressor protein called cytoplasmic promyelocytic leukaemia (cPML) regulate the interaction between Smad2/3 and type I receptors in these endosomes (Hocevar et al., 2001, Lin et al., 2004). Perturbing these protein interactions or the clathrin-dependent receptor internalisation process, severely hampers downstream Smad signalling (Hayes et al., 2002, Di Guglielmo et al., 2003). Most receptors trafficked via clathrin-coated pits are effectively recycled back to the plasma membrane via activity of Rab11 small GTPase, Dab2, and Cbl-interacting 85-kDa protein (CIN85) that facilitate subsequent rounds of ligand interaction and thus, positive regulation of TGF-β signalling (Mitchell et al., 2004, Penheiter et al., 2010, Yakymovych et al., 2015). Contrarily, receptor internalisation in the caveolar vesicles is associated with receptor degradation, recycling, and non-canonical TGF-β signalling, hence, overall, negative regulation of canonical TGF-β signalling. In the caveolar vesicles, CD109, a TGF-β co-receptor, interacts with

caveolin-1 to enable receptor-Smad7 interaction and recruitment of E3 ubiquitin ligase, Smad specific E3 ubiquitin protein ligase 2 (Smurf2) for receptor degradation via the proteasome or mediate their lysosomal degradation, thus, negatively regulating TGF-β signalling (Bizet et al., 2011, Razani et al., 2001). In addition to type I and type II receptors, TGF-β co-receptor, betaglycan, can also undergo endocytosis via clathrin-coated pits or caveolar vesicles and its internalisation can promote both Smad-mediated canonical TGF-β signalling and p38/mitogen activated protein kinase (MAPK)-associated non-canonical TGF-β signalling (Finger et al., 2008). Moreover, these vesicles can maintain substantial intracellular pool of inactive TGF-β receptors, allowing their quick mobilisation to the cell surface whenever required for activation (Wu and Derynck, 2009). An overview of TGF-β-induced receptor internalisation is depicted (*Fig 1.6*).

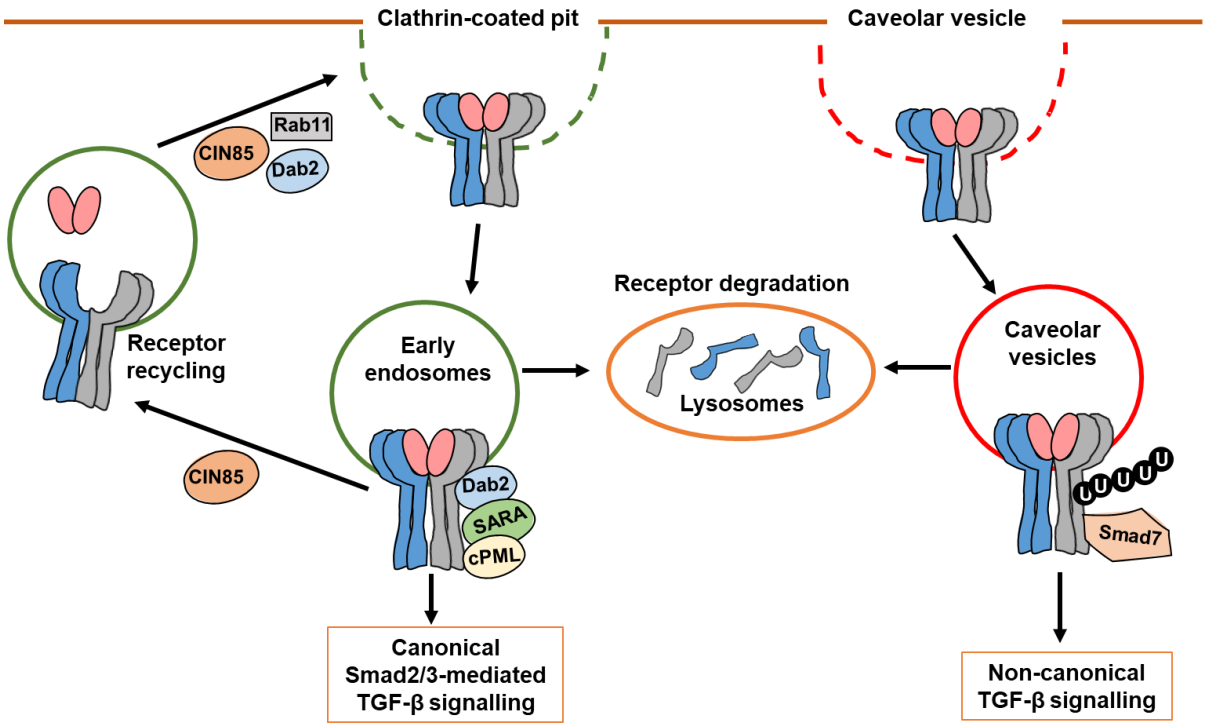

Figure 1.6: Internalisation of TGF-β receptors upon ligand binding and activation

TGF-β binding can induce receptor internalisation via two vesicle types- clathrin-coated pits and caveolar vesicles. Receptor internalisation via clathrin-coated pits supports canonical Smad2/3-mediated TGF-β signalling in association with other adaptor proteins like SARA, Dab2, and cPML whereas, internalisation of receptors in caveolar vesicles promotes Smad7-mediated receptor degradation as well as facilitates non-canonical TGF-β signalling. Receptors in both the vesicle types can be directed towards lysosomes for their degradation. Receptor recycling mainly occurs in the clathrin-coated pits in association with other proteins like CIN85, Dab2 and Rab11 GTPase.

1.3.2.2 Regulation via co-receptors of TGF-β family

Co-receptors are usually expressed on the cell surface and their binding with TGF-β ligands may either function to enhance or restrict downstream signalling. Several TGF-β co-receptors can regulate TGF-β signalling such as betaglycan (TGF-β type III receptor), endoglin, Cripto, BMP and activin membrane-bound inhibitor (BAMBI), CD109, and neuropilin-1 (NRP1). They can regulate TGF-β signalling by presenting free ligands to the receptors or by sequestering them away from the receptor complexes or cause intracellular trafficking of the receptors, thus making them unavailable to activate downstream Smad2/3. Betaglycan, structurally similar to TGF-β type I and II receptors, can bind to all three TGF-βs1-3 and present them to the TGF-β receptors to enhance TGF-β signalling (Mendoza et al., 2009). Conversely, soluble form of betaglycan negatively regulates TGF-β signalling by sequestering TGF-βs1-3 away from the receptors (López-Casillas et al., 1994). It can also bind with other TGF-β family proteins like BMP2/4, GDF5 and Inhibin as well as fibroblast growth factor-2 (FGF2) thus, offering a broad range of control and crosstalk between various signalling pathways (Wiater et al., 2006, Lee et al., 2009, Knelson et al., 2013).

Another TGF-β co-receptor, endoglin (CD105) exists as two spliced forms, the long form (L) and the short form (S) (Barbara et al., 1999, Guerrero-Esteo et al., 2002, Lebrin et al., 2004, Scherner et al., 2007, Ray et al., 2010, Velasco et al., 2008). L-endoglin antagonises TGF-βs1-3-mediated signalling through TGFBRI receptors whereas S-endoglin promotes TGF-β signalling (Velasco et al., 2008). Conversely, soluble endoglin prevents TGF-β signalling by sequestering TGF-β/activin/nodal away from the receptors (Venkatesha et al., 2006, Malhotra et al., 2013). Another co-receptor, Cripto, also known as Cripto-1/FRL-1/Cryptic (EGF–CFC), enhances nodal signalling by promoting its binding to the receptors (Yan et al., 2002). Interestingly, Cripto enhances nodal but not activin signalling, suggesting distinct roles of activins and nodal during embryogenesis. It can also bind with TGF-β1 to limit its receptor access during cancer onset thus, acting as a negative regulator (Gray et al., 2006). Moreover, Cripto can also coordinate with EGF and Wnt signalling pathways thereby,

providing a platform for signalling crosstalk at the receptor level (Nagaoka et al., 2012). There are some more TGF-β co-receptors, all summarised below (*Table 1.2*).

Table 1.2: Summary of TGF-β family co-receptors, their key characteristics, effect on TGF-β signalling, and mode of action

TGF-β co-receptors	Co-receptor characteristics	Effect on TGF-β signalling	Mode of action	References
Betaglycan	transmembrane proteoglycan, GAG chains	both negative and positive	presents TGF-β1-3 to the receptors, sequesters TGF-β away from the receptors	(López-Casillas et al., 1991, 1993, 1994, Mendoza et al., 2009)
Endoglin (CD105)	transmembrane glycoprotein, expressed by endothelial cells, exists as L- and S-forms	L-endoglin-negative and S-endoglin-positive	sequesters TGF-β away from the receptors, L-form antagonises TGF-β and promotes BMP signalling, S-form supports TGF-β signalling	(Barbara et al., 1999, Guerrero-Esteo et al., 2002, Lebrin et al., 2004, Scherner et al., 2007, Ray et al., 2010, Velasco et al., 2008)
Cripto	GPI-linked co-receptor	both negative and positive	promotes nodal signalling over activin, limits access of TGF-β1 to type I receptors	(Yan et al., 2002, Gray et al., 2006)
BAMBI	Truncated transmembrane type I receptor	negative	sequesters activins and BMPs, synergises with Smad7 for receptor inactivation	(Onichtchouk et al., 1999, Grotewold et al., 2001, Sekiya et al., 2004, Xi et al., 2008, Yan et al., 2009)
CD109	GPI-anchored, α2-macroglobulin family	negative	role in TGF-β receptor internalisation	(Lin et al., 2002, Finnson et al., 2006, Bizet et al., 2011)
NRP-1	transmembrane glycoprotein	both negative and positive	affects Smad2/3 activation	(Glinka and Prud'homme, 2008, Cao et al., 2010, Glinka et al., 2010, Aspalter et al., 2015)

Abbreviations: BAMBI- BMP and activin membrane-bound inhibitor, NRP-1- Neuropilin-1, GAG-glycosaminoglycan, GPI- glycosylphosphatidylinositol.

1.3.2.3 Regulation via Smad7

Smad7 plays a crucial role in regulating TGF-β signalling by modulating its receptor availability. In the absence of TGF-β activation, Smad7 is localised in the nucleus (Itoh et al., 1998). However, Smad7 is ubiquitinated at lysine residues K64 and K70 by a nuclear E3 ubiquitin ligase, Smurf2 upon TGF-β activation to induce cytoplasmic localisation of Smad7-Smurf2 complex (Kavsak et al., 2000). In the caveolar vesicles located in the cytoplasm, Smad7 competes with activated Smad2/3 to bind to phosphorylated type I receptors and in this process, Smad7 recruits Smurf2 to induce both proteasomal and lysosomal degradation of activated type I receptors, thereby, limiting subsequent TGF-β signalling (Kavsak et al., 2000, Hanyu et al., 2001, Di Guglielmo et al., 2003). At the same time, Smad7 competition with activated Smad2/3 to bind to type I receptors also prevents further phosphorylation and activation of Smad2/3 (Kavsak et al., 2000). Furthermore, Smad7 can hamper TGF-β activity by also recruiting another E3 ubiquitin ligase, neural precursor cell expressed, developmentally down-regulated 4-2 (Nedd4-2 or Nedd4L) to the activated type I receptors and promote receptor degradation (Kuratomi et al., 2005). On the other hand, TGF-β activation also initiates PTMs of Smad7 such as methylation at its arginine residues 57 and 67 by protein arginine methyltransferase-1 (PRMT1) that decreases its association with the type I receptors which rather enhances TGF-β signalling (Katsuno et al., 2018). An overview of Smad7 action on receptor stability is shown (*Fig 1.7*).

In the absence of TGF-β activation, nuclear Smad7 remains bound to transcriptional co-activators and HATs like p300 (Itoh et al., 1998, Gronroos et al., 2002). p300 stabilises Smad7 in the nucleus by acetylating its lysine residues K64 and K70, the Smurf2 ubiquitination sites, thereby making them inaccessible for Smurf2-mediated ubiquitination and protecting Smad7 from pre-mature degradation (Simonsson et al., 2005, Kavsak et al., 2000). On the contrary, upon TGF-β activation and nuclear accumulation of activated Smad2/3-Smad4 complexes, p300 dissociates from Smad7 and binds to the activated Smad complexes, freeing Smad7 to bind to Smurf2 (Kavsak et al., 2000). HDACs like NAD-dependent protein deacetylase sirtuin-

1 (SIRT1) remove p300-mediated K64 and K70 acetylation that further permits Smurf2-mediated ubiquitination of these lysine residues (Kume et al., 2007). Hence, a fine balance between Smad7 acetylation, deacetylation, and ubiquitination dictates its role in TGF-β signalling (*Fig 1.7*).

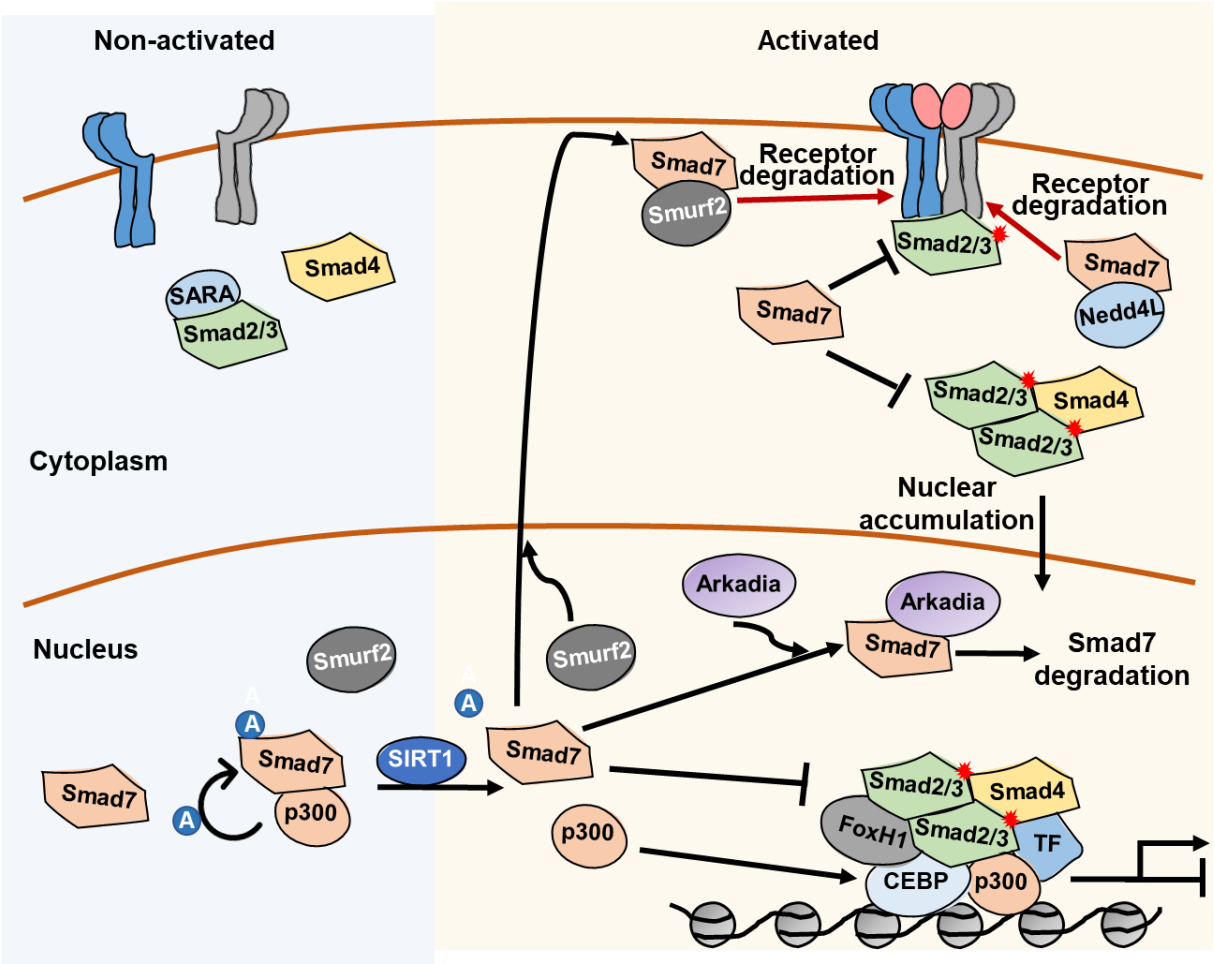

Figure 1.7: Overview of regulation of TGF-β signalling by Smad7

Smad7 regulates TGF-β signalling by various mechanisms that affect both receptors and activated Smad2/3. '✸' represents phosphorylation. 'A' represents acetylation.

1.3.3 Regulation at the level of effectors

1.3.3.1 Regulation of Smad2/3 via Smad7

In addition to Smad7 function in degradation of activated TGF-β type I receptors, it also hinders TGF-β signalling by competing with Smad4 to bind to activated Smad2/3 thereby, preventing the formation of functional oligomeric complexes and eventually, activation of TGF-β target genes (*Fig 1.7*) (Zhang et al., 2007). Moreover, functional Smad complexes are inhibited from binding with SBEs as nuclear Smad7 competes with them for the same binding sites and thus, prevents Smad2/3 transcriptional activity (Zhang et al., 2007). Smad7 itself is a direct target of TGF-β signalling and its mRNA levels increase after TGF-β activation thus, offering a direct negative feedback loop to regulate TGF-β signalling (Nakao et al., 1997b). Another target is TGF-β-stimulated clone 22 (TSC22) which balances the negative regulation of TGF-β by Smad7 by competing with it to bind to TGFBR1 and protect the receptor from degradation (Yan et al., 2011). Furthermore, E3 ubiquitin ligases like Arkadia ubiquitinate Smad7 upon TGF-β activation and cause Smad7 degradation thus, enhancing TGF-β signalling (*Fig 1.7*) (Koinuma et al., 2003).

1.3.3.2 Regulation of Smad2/3 via SKI and SKIL

Proto-oncogenes SKI and SKIL (SKI/SKIL) are implicated in the negative regulation of TGF-β signalling by various mechanisms that antagonise Smad2/3 activity. Both SKI/SKIL lack an innate catalytic activity and perform their functions on Smad2/3 by interacting with other transcription factors (Deheuninck and Luo, 2009). SKIL is itself a target of TGF-β signalling and its expression increases after about two hours of TGF-β stimulation, resulting in its activation and negative regulation of Smad2/3 activity (Stroschein et al., 1999). SKI/SKIL can simultaneously bind with activated Smad2/3 and Smad4 via distinct domains and disrupt the functional oligomeric complexes (Stroschein et al., 1999, Wu et al., 2002). SKI also competes with activated Smad2/3 to bind to Smad4 at the same site and displaces them from the functional complex, thereby restricting Smad2/3 transcriptional activity (Wu et al., 2002). Furthermore, SKI/SKIL also hinder Smad2/3 interaction with their transcription factors

p300/CEBPB and instead recruit transcriptional co-repressor complex comprising of HDAC, nuclear receptor co-repressor (N-Cor), and mammalian Sin3A (mSin3A) to the SBEs, therefore, preventing Smad2/3-mediated gene expression (Akiyoshi et al., 1999, Wu et al., 2002, Stroschein et al., 1999, Luo et al., 1999). In this process, Smad2/3-Smad4 complexes containing SKI/SKIL are stabilised at the SBEs, blocking further recruitment of functional Smad complexes (Suzuki et al., 2004). Conversely, various E3 ubiquitin ligases such as Arkadia, Smurf2, and anaphase promoting complex (APC) can ubiquitinate and mediate proteasomal degradation of SKI/SKIL bound to Smad complexes stabilised at the SBEs, ensuring their repression of TGF-β target genes is lifted off (Sun et al., 1999, Bonni et al., 2001, Wan et al., 2001, Nagano et al., 2007).

1.3.3.3 Regulation of Smad2/3 via non-coding RNAs

Smad2/3 activity can also be negatively regulated by a variety of non-coding RNAs (ncRNA) that are themselves targets of Smad2/3 transcriptional activity. Upon TGF-β activation, activated Smad2/3 enhance or repress micro-RNA (miRNA) expression which in turn negatively affect their DNA-binding capacity and thus, Smad2/3 target gene expression (Blahna and Hata, 2012). For example, miR-140 suppresses TGF-β signalling by targeting Smad3 protein (Pais et al., 2010) while miR-21 suppresses Smad7 activity and supports TGF-β signalling (Marquez et al., 2010). Also, some of the long ncRNAs (lncRNAs) that are expressed as a result of TGF-β activation, can regulate its response by upregulating EMT-related genes such as ZEB1, SNAI1, SLUG, and TWIST and affecting mRNA levels of cell adhesion proteins like E-cadherin and N-cadherin in cancer cells (Janakiraman et al., 2018, Yuan et al., 2014).

1.3.4 Regulation of Smad2/3 via PTMs

Post-translational modifications (PTMs) of Smad2/3, such as phosphorylation, ubiquitination, sumoylation, acetylation, poly-ADP-ribosylation and neddylation, can also control TGF-β signalling by regulating their stability, cellular localisation, and transcriptional activity (Tzavlaki and Moustakas, 2020). Multiple signalling pathways including TGF-β itself can confer PTMs to Smad2/3 thus positively or negatively regulating TGF-β signalling (Xu et al., 2016). For example, phosphorylation and phosphorylation-directed ubiquitination of Smad2/3 linker region has emerged to have important roles in regulating TGF-β activity by directing Smad2/3 activity and their protein interactions. In the following sections, I would like to discuss some important PTMs of Smad2/3 with a special focus on their regulation via linker region phosphorylation. A summary of known phosphorylation and dephosphorylation events in Smad2/3 induced by various factors is shown (*Fig 1.8*).

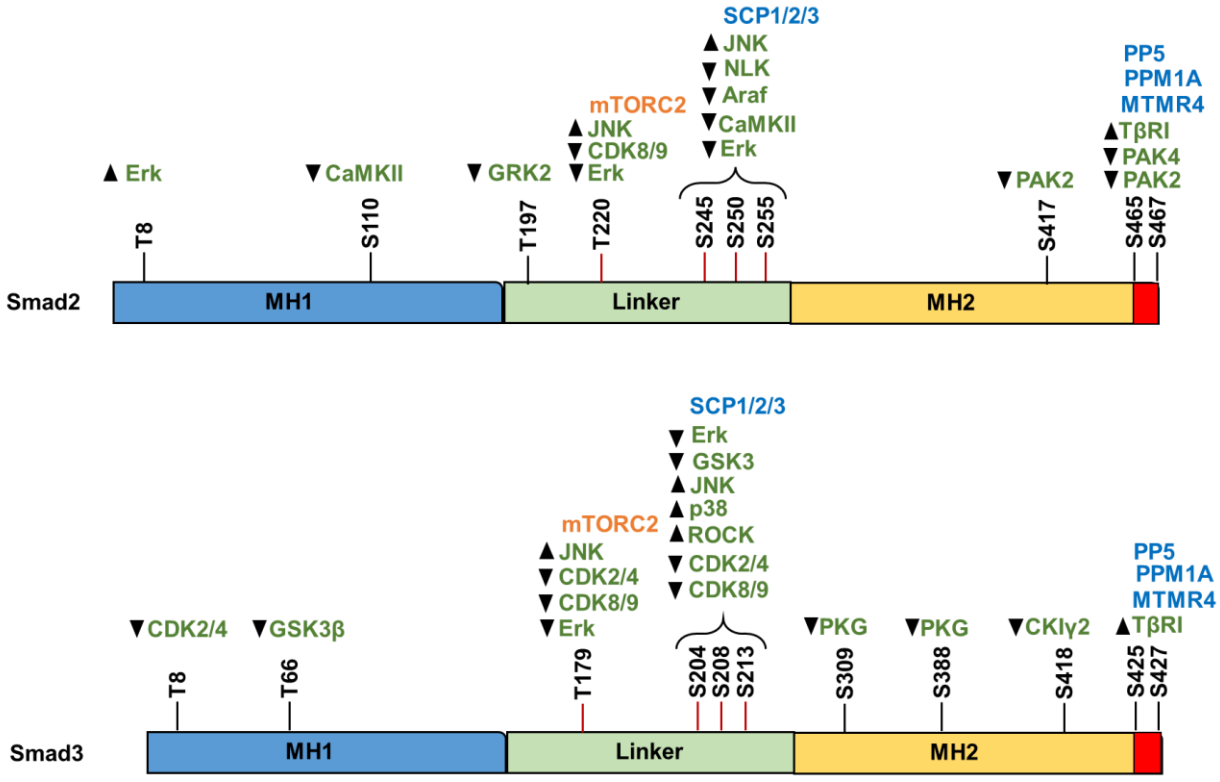

Figure 1.8: Summary of phosphorylation and dephosphorylation events in Smad2/3

Kinases that directly phosphorylate threonine and serine residues are written in green. Kinases that indirectly regulate Smad2/3 phosphorylation are written in orange. Phosphatases that target linker serine residues and SxS motif are in blue. The red line preceding an amino acid residue indicates proline-directed threonine or serine and the black line is for all other residues. The upward-facing black triangle just before a kinase indicates the positive role of that kinase in TGF-β signalling, while the downward-facing black triangle indicates the negative role of that kinase in TGF-β signalling.

1.3.4.1 Dephosphorylation of SxS motif of activated Smad2/3

Phosphorylation of C-terminal SxS motif of Smad2/3 is the most important PTM in response to ligand-induced receptor kinase activation in TGF-β signalling as it determines subsequent steps in the signalling pathway. However, there are other kinases too which can induce phosphorylation of serine residues in the SxS motif of Smad2 and/or Smad3, but whether they activate Smad pathway needs to be investigated further. For example, Smad2/3 SxS motif can be phosphorylated by a mitotic progression kinase, Mps1 after Smad4 binds to Mps1 and activates it (Zhu et al., 2007) or just the S465 of the SxS motif in Smad2 can be phosphorylated by p21 protein-activated kinase 4 (PAK4) that induces Smad2 proteasomal degradation (Wang et al., 2014). But most importantly, it is the dephosphorylation of the SxS motif which is one of the mechanisms that timely terminates TGF-β signalling or facilitates nuclear export of individual, dephosphorylated Smad2/3 for dynamic recognition of an active receptor and engage in subsequent rounds of signalling. There are phosphatases that can dephosphorylate Smad2/3 SxS motif, such as, protein phosphatase Mg^{2+}/Mn^{2+}-dependent 1A (PPM1A) and protein phosphatase 5 (PP5). These phosphatases have been reported to interact with activated Smad2/3 in the nucleus and dephosphorylate them to facilitate their nuclear export thus, limiting TGF-β signalling (*Fig 1.8*) (Lin et al., 2006, Bruce et al., 2012). However, some studies found cytoplasmic localisation of PPM1A thus, questioning its role in Smad2/3 dephosphorylation in the nucleus (Yu et al., 2015, Bruce et al., 2012). Interestingly, the integral inner nuclear envelop protein MAN1 was found to bind to both PPM1A and activated Smad2 to facilitate their interaction, which may explain how PPM1A could dephosphorylate Smad2/3 SxS motif (Bourgeois et al., 2013). But further validation of the relationship between PPM1A, Smad2, and MAN1 is required through performing *in vivo* experiments. Smad2/3 SxS motif can also be dephosphorylated by myotubularin-related protein 4 (MTMR4) associated with early endosomes that functions to attenuate TGF-β signalling by preventing them to form oligomeric complexes with Smad4 (Yu et al., 2010). Such diverse control for phosphorylation

and dephosphorylation of the SxS motif of Smad2/3 helps to strictly regulate the intensity and duration of TGF-β signalling.

1.3.4.2 Phosphorylation of Smad2/3 MH domains

In addition to C-terminal SxS motif phosphorylation and dephosphorylation, MH1/2 domains of Smad2/3 can also be the targets of various kinases and phosphatases that contribute to regulating TGF-β signalling. For instance, T66 in the MH1 domain of Smad3 (but not Smad2) can be phosphorylated by Axin/GSK3β to induce ubiquitination and degradation of non-activated Smad3 thus, limiting the amount of Smad3 available for TGF-β signalling (Guo et al., 2008a). On the other hand, phosphorylation of T8 in Smad2 MH1 domain via Erk enhances its transcriptional activity, at least partly by stabilising the Smad2 protein (Funaba et al., 2002). T8 is also a substrate for CDK activity, which in combination with linker region phosphorylation, inhibits TGF-β-mediated transcription (Matsuura et al., 2004). Moreover, MH2 domain S309/S388 and S418 phosphorylation by a cGMP-dependent protein kinase PKG and casein kinase 1 gamma 2 (CKIγ2), respectively, negatively regulates TGF-β signalling by facilitating Smad3 ubiquitination and degradation (Saura et al., 2005, Guo et al., 2008b). However, it is not clear for most of MH1/2 domains phosphorylation whether they exert their effects on Smad2/3 activity independently or in conjunction with other PTMs of Smad2/3, such as the linker region phosphorylation and ubiquitination.

1.3.5 Regulation of Smad2/3 via PTMs of its linker region

As previously mentioned, Smad2/3 linker is an unstructured, flexible, serine/threonine-rich region that contains several phosphorylatable residues which are substrates of kinases belonging to multiple signalling pathways (Kamato et al., 2013, Xu et al., 2016). Therefore, these sites are hotspots for crosstalk between TGF-β signalling and other signalling pathways, which help in fine-regulation of TGF-β signals by affecting Smad2/3 cellular localisation, protein stability, and transcriptional activity (Feng and Derynck, 2005, Kamato et al., 2013). Linker phosphorylation of Smad2/3 is emerging to be a critical and important mechanism to regulate TGF-β signalling (Xu et al., 2016). Protein kinases that have been identified to regulate Smad2/3 linker phosphorylation, whether directly or indirectly, include mitogen activated protein kinases (MAPKs), cyclin dependent kinases (CDKs), glycogen synthase kinase 3β (GSK3β), Rho/Rho associated protein kinase (ROCK), calcium/calmodulin-dependent protein kinase II (CaMKII), a RAF kinase Araf, nemo-like kinase (NLK), G protein-coupled receptor kinase 2 (GRK2), and phosphoinositide-3 kinase/mechanistic target of rapamycin complex 2 (PI3K/mTORC2) and their target sites are summarised (*Fig 1.8*) (Kretzschmar et al., 1999, Wicks et al., 2000, Funaba et al., 2002, Mori et al., 2004, Matsuura et al., 2004, Ho et al., 2005, Kamaraju and Roberts, 2005, Yoshida et al., 2005, Matsuura et al., 2005, Millet et al., 2009, Alarcon et al., 2009, Burch et al., 2010, Hough et al., 2012, Liu et al., 2013, Yu et al., 2015, Liang et al., 2021).

These kinases can be activated following ligand binding to the TGF-β type I-type II receptor complex which activates both canonical serine/threonine kinase activity and non-canonical tyrosine kinase activity of the receptors (Derynck and Budi, 2019, Tzavlaki and Moustakas, 2020). For instance, MAPKs like Erk1/2, JNK1/2/3, and p38 are activated after phosphorylation of tyrosine residues of TGF-β receptor that further induces activation of Ras/Raf-Erk1/2 via ShcA phosphorylation, as well as tumour necrosis factor receptor associated factor 4/6 (TRAF4/6) and TGF-β activated kinase 1 (TAK1) for downstream activation of JNK and p38 (Lee et al., 2007, Sorrentino et al., 2008, Yamashita et al., 2008).

Activated MAPKs can then phosphorylate various Smad2/3 linker sites to modulate TGF-β signalling and integrate its response with other signalling pathways. A specific phosphorylatable residue in Smad2/3 linker can be the substrate for multiple kinases and similarly, a particular kinase can also phosphorylate more than one residue in Smad2/3-linker. Furthermore, out of five phosphorylation sites in Smad2/3-linker region, there are four proline-directed threonine and serine (S/T-P) residues (*Table 1.3 and Fig 1.8*) that have more important roles in regulating TGF-β signalling than other non-S/T-P linker sites. Since these Smad2/3 linker S/T-P sites can be phosphorylated by different kinases in a spatial- and temporal-dependent manner in TGF-β signalling, different phospho-isoforms of Smad2/3 can exist, which may affect Smad2/3 activity by inducing conformational changes in them. These changes subsequently modulate Smad2/3 interaction with other proteins, resulting in various outcomes of TGF-β signalling.

Table 1.3: Smad2/3 linker S/T-P phosphorylation sites

R-Smads	Proline-directed Ser/Thr linker phosphorylation sites			
Smad2	T220	S245	S250	S255
Smad3	T179	S204	S208	S213

1.3.5.1 Smad2/3 linker S/T-P phosphorylation

Specific Smad2/3 linker S/T-P residues that are phosphorylated by some of the important kinases upon TGF-β activation is shown (*Table 1.4*). Erk1/2- and CDK2/4-mediated linker phosphorylation inhibits TGF-β signalling by suppressing Smad2/3 transcriptional activity and their nuclear localisation (Kretzschmar et al., 1999, Matsuura et al., 2005, Matsuura et al., 2004, Alarcon et al., 2009), thus, inhibiting anti-proliferative effects of TGF-β signalling and enhancing cell cycle progression. Conversely, phosphorylation of the same linker residues by JNK, p38, and ROCK augments Smad2/3 transcriptional activity, because they enhance Smad2/3 nuclear accumulation (Funaba et al., 2002, Mori et al., 2004, Kamaraju and Roberts, 2005). However, how phosphorylation of the same residues but through different upstream kinases can determine opposite effects is unclear. On the other hand, CDK8/9-mediated linker

phosphorylation upon TGF-β activation, maximises Smad2 transcriptional activity while also priming them for future degradation via the ubiquitin-proteasome system (UPS), thus, eventually, terminating TGF-β signalling (Alarcon et al., 2009, Gao et al., 2009). In addition to CDK8/9, linker threonine phosphorylation induced by PI3K/Akt/mTORC2 pathway also primes Smad2/3 for proteasomal degradation (Yu et al., 2015). Increased activated Smad2/3 transcription and their subsequent degradation orchestrated by the same linker region is the result of sequential protein interactions of Smad2/3 which determines their fate (Alarcon et al., 2009, Aragon et al., 2011). Phosphorylation of the latter two linker serine residues promotes binding of a peptidyl-prolyl cis/trans isomerase, NIMA-interacting-1 protein (Pin1) at the PPxY motif located downstream of phosphorylated linker threonine, maximising Smad2/3 transcriptional activity (Matsuura et al., 2009, Nakano et al., 2009, Aragon et al., 2011). But at the same time, these phosphorylation events prime GSK3β-mediated linker serine phosphorylation, which instead diminishes Smad2/3-Pin1 binding and increases Smad2/3 affinity to bind to WW domain HECT E3 ubiquitin ligases such as Smurf2 and Nedd4L (Millet et al., 2009, Gao et al., 2009, Tang et al., 2011, Lin et al., 2000, Zhang et al., 2001, Aragon et al., 2011) thus, initiating Smad2/3 degradation via the UPS.

Table 1.4: Kinases that phosphorylate Smad2/3 linker S/T-P residues upon TGF-β activation

Kinases	Smad2				Smad3			
	T220	S245	S250	S255	T179	S204	S208	S213
Erk1/2	✓	✓	✓	✓	✓	✓	✓	×
JNK	✓	✓	✓	✓	✓	✓	✓	✓
P38	×	-	-	-	×	✓	✓	×
ROCK	✓	-	-	-	✓	✓	✓	×
CDK2/4	-	-	-	-	✓	×	×	✓
CDK8/9	-	-	-	-	✓	×	✓	✓
GSK3β	-	-	-	-	×	✓	×	-
PI3K/mTORC2	✓	×	×	×	✓	×	×	×

Different signs in the table indicate the following, ✓: positive phosphorylation by the kinase, ×: not phosphorylated by the kinase, -: not clearly known.

1.3.5.2 Smad2/3 linker ubiquitination and degradation

Smad2/3 linker phosphorylation and associated ubiquitination concertedly determine net Smad2/3 activity and therefore, duration and intensity of TGF-β signalling. Smad2/3 linker T220/T179 phosphorylation in response TGF-β activation, facilitates recruitment of Smurf2 and Nedd4L to the PPxY domain via their WW domain (Gao et al., 2009, Tang et al., 2011, Aragon et al, 2011). Both Smurf2 and Nedd4L promote Smad2/3 degradation via the UPS to inhibit TGF-β signalling (Kuratomi et al., 2005, Gao et al., 2009, Lin et al., 2000, Zhang et al., 2001). Smurf2 is a predominantly nuclear protein and Smurf2-mediated Smad2/3 degradation can account for terminating TGF-β signalling. However, Nedd4L is exclusively cytoplasmic protein (Kuratomi et al., 2005), which means that rather than terminating TGF-β signalling, its function is to attenuate it by regulating the amount of activated Smad2/3 reaching the nucleus. Moreover, Smurf2 can also induce mono-ubiquitination of multiple residues of Smad3 that impedes the formation of Smad functional complexes and ultimately, attenuates TGF-β signalling (Tang et al., 2011).

In addition to Nedd4L and Smurf2 mediated Smad2/3 degradation, there are several other E3 ubiquitin ligases as well such as, Arkadia, Itch3, TGIF interacting ubiquitin ligase 1 (Tiul1), c-terminus of HSC70-Interacting protein (CHIP), and ROC1, a subunit of Skp1-cullin-F-box ($SCF^{\beta TrCP/\ Fbw1A}$), that can also ubiquitinate Smad2 and regulate its protein stability (Fukuchi et al., 2001, Mavrakis et al., 2007, Bai et al., 2004, Seo et al., 2004, Xin et al., 2005). Of note, Smad2/3 ubiquitination by E3 ubiquitin ligases other than Nedd4L and Smurf2 do not occur as a result of S/T-P linker phosphorylation but regulate TGF-β signalling via other mechanisms.

1.3.5.3 Smad2/3 linker dephosphorylation and deubiquitination

Notably, these linker phosphorylation and ubiquitination events are not permanent and can be reversed by the action of phosphatases and deubiquitinating enzymes (DUBs), respectively. Some of the phosphatases identified to dephosphorylate Smad2/3 linker region are small C-terminal domain phosphatases-1/2/3 (SCP1/2/3) and they have no effect on the

C-terminal SxS motif phosphorylation (Sapkota et al., 2006, Wrighton et al., 2006). Intriguingly, they can remove linker serine but not linker threonine phosphorylation (*Fig 1.8*). In mammalian cells and *Xenopus* embryos, SCP1/2/3 remove linker serine phosphorylation in order to achieve maximal transcriptional activity of Smad2/3 upon TGF-β activation. Gain of function studies of SCP1/2/3 show an increase in Smad2/3-transcription while SCP knockdown resulted in higher linker serine phosphorylation and lower Smad2/3 transcriptional responses. Furthermore, a variety of DUBs such as ubiquitin specific peptidases (USPs), ubiquitin C-terminal hydrolases (UCHs), and OTU family DUBs such as OTU domain-containing ubiquitin aldehyde-binding protein 1 (OTUB1), CYLD, and A20 can reverse the effects of ubiquitination and can either upregulate or downregulate TGF-β signalling and thus, provide an additional level of regulation (Kim and Baek, 2019). These events of linker phosphorylation and dephosphorylation in addition to other PTMs of Smad2/3 have a huge impact on the final outcome of TGF-β signalling.

1.4 Aims and Hypothesis

Phosphorylation and phosphorylation-directed ubiquitination of Smad2/3 S/T-P linker residues are highly inter-connected events and play a crucial role in regulating TGF-β signalling. These phosphorylation events heavily control Smad2/3 activity by regulating their interaction with other proteins, their cellular localisation, and transcriptional activity which in turn, fine-tunes the net effect of TGF-β signalling. Linker phosphorylation also serves as a hotspot for crosstalk of TGF-β signalling with other signalling pathways. Most Smad2/3 linker phosphorylation studies that investigate the role of linker S/T-P residues: T220 and S245/S250/S255 in Smad2 and T179 and S204/S208/S213 in Smad3 do not distinguish between them and perceive them all to be similarly regulated to generate the same effect on TGF-β signalling. However, interestingly, in a previous study from our lab, it was identified that phosphorylation of linker threonine (LT) and linker serine residues (LS) can be differentially regulated by different kinases in human embryonic stem cells (hESCs) (Yu et al., 2015). When MAPKs and PI3K activities were inhibited by small molecule inhibitors, agonist-induced Smad2 LT phosphorylation (pLT) was suppressed, while its LS phosphorylation (pLS) was hardly affected (*Fig 1.9A*). On the other hand, when CDKs activity was inhibited by using a pan-CDK inhibitor, flavopiridol (FVP), the major effect of the inhibitor was observed on pLS with little effect on pLT (*Fig 1.9A*). This data suggest that different signalling pathways/kinases can have varying propensities for LT and LS as their substrate. More importantly, we observed a significant drop in total Smad2/3 levels in hESCs when treated with FVP for a longer duration of 6 hours, hinting towards a role of pLS in Smad2/3 stability (*Fig 1.9B, last column*) (Yu et al., 2015). Studying these phosphorylation of Smad2/3 linker S/T-P residues will help us to clearly understand their role in physiological and pathological processes of TGF-β signalling as well as allow us to manipulate its responses for therapeutic interventions in various pathological conditions. Moreover, so far, mostly the role of canonical TGF-β signalling has been studied in embryonic development. Therefore, studying Smad2/3 linker phosphorylation in hESCs will

contribute to our knowledge of how non-canonical TGF-β signalling can regulate canonical TGF-β signalling during embryonic development.

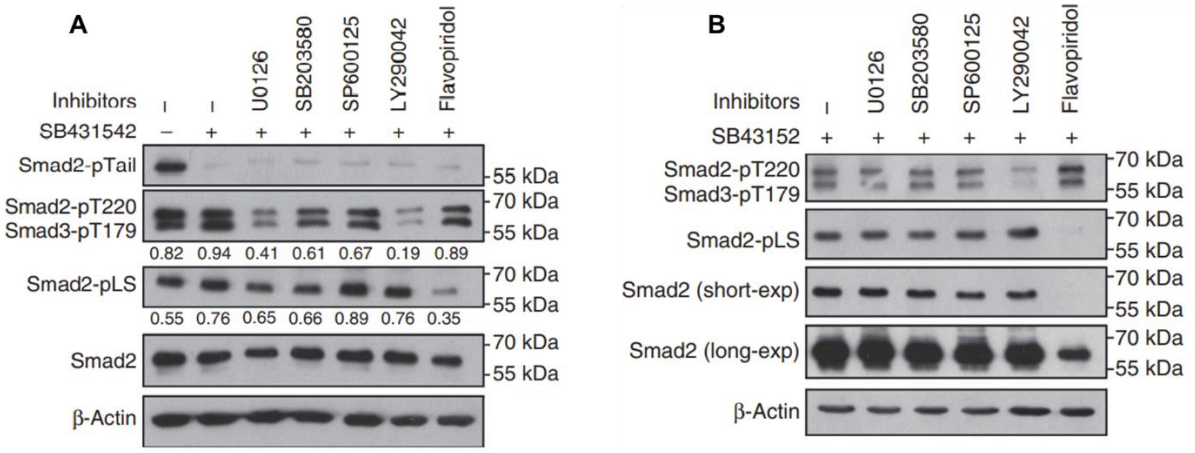

Figure 1.9: Differential regulation of Smad2/3 linker phosphorylation (Part of figure 5 taken from Yu et al., 2015, Nature Communications)

Immunoblots of Smad2/3 linker threonine and serine phosphorylations (pLT and pLS) in human embryonic stem cells (hESCs) that were pre-treated with activin A followed by simultaneous treatment with TGF-β type I receptor inhibitor SB431542 and with indicated inhibitors for **A)** 1 hour and **B)** 6 hours. Targets of the inhibitors are: U0126- MEK1/2, SB203580- p38 MAPK, SP600125- JNK, LY290042- PI3K, Flavopiridol- CDKs 1/2/4/6/8/9.

Given that Smad2/3 LT and LS exhibited a differential regulation of their phosphorylation in hESCs, the current study is based on the hypothesis that pLT and pLS may also have different functions in regulating TGF-β signal and I would aim to achieve the following objectives in this thesis:

1) to understand the role of CDKs in regulating the phosphorylation of Smad2/3 LT and LS.

2) to specifically understand the role of Smad2-pLS in regulating TGF-β signalling.

3) the biological function of Smad2/3-pLS in development, health, and disease.

Chapter 2

Materials and methods

2.1 Tissue culture

2.1.1 Materials

2.1.1.1 Cell lines

All the cell lines used in this research work were cultured at 37°C with 5% CO_2.

Cell types	Source
PC-3 cells	Grade IV prostate adenocarcinoma cell line derived from bone metastasis site from a 62-year-old male Caucasian, obtained from ATCC (CRL-1435), kindly gifted by Dr R. M. Krypta's lab, Imperial College London.
HEK293T cells	Fetal embryonic kidney cell line containing the SV40 T-antigen derived from HEK293 cells, obtained from ATCC (CRL-3216).
Smad2 knockout and control HEK293T cells	HEK293T cells in which SMAD2 gene has been disrupted using CRISPR-Cas9 system, kindly gifted by Dr C. S. Hill's lab, Francis Crick Institute, London (Gori et al., 2021).
H1 hESCs (WA-01)	Male human embryonic stem cell distributed by WiCell (Thomson et al., 1998).
Esc (26) V9 Hex-GFP mESCs	Mouse embryonic stem cells reporter cell line to generate GFP fluoresecence on Hex expression, kindly gifted by Dr V. Episkopou's lab, Imperial College London.
KT 15 Smad2 knockout mESCs	Mouse embryonic stem cells isolated using standard procedures (Robertson, 1987) from delayed blastocysts obtained from $Smad2^{Robm1/+}$ females crossed to $Smad2^{Robm1/+}$, Rosa26/+ males. KT 15 Smad2 knockout mESCs are LacZ+, $Smad2^{Robm1}$ homozygous ES cell line, kindly gifted by Dr V. Episkopou's lab, Imperial College London.

2.1.1.2 Growth factors and Inhibitors

Reagent	Target of action	Supplier, Catalogue #	Diluent for stock preparation	Working concentration
Activin A	Activates TGF-β signalling	Peprotech, 120-14E	0.1% BSA-PBS	1-100 ng/ml
TGF-β	Activates TGF-β signalling	Peprotech, 100-21	100 mM Citric Acid	1-10 ng/ml
BMP4	Activates BMP signalling	Peprotech, 120-05ET	4 mM HCl	3 ng/ml
bFGF	Activates FGF signalling	Peprotech, 100-18B-500	0.1% BSA-PBS	10 ng/ml
Heat stable bFGF	FGF signalling	Gibco, PHG0367	0.1% BSA-PBS	10 ng/ml

Flavopiridol	Inhibits CDK2/4/6/7/8/9	Selleckchem, S1230	DMSO	1 µM
ROCKi	Inhibits ROCK activity	Stratech, A3773-APE	DMSO	10 µM
LY2857785	Inhibits CDK8/9	Selleckchem, S7511	DMSO	0.5 µM
Torin-2	Inhibits mTORC	Tocris, 4248	DMSO	10 nM
LY294002	Inhibits PI3K signalling	Cell Signalling, 9901	DMSO	20 µM
U0126	Inhibits Erk1/2 signalling	Reagents Direct, 84-P22	DMSO	10 µM
SB431542	Inhibits ALK4/5/7	Tocris, 1614	DMSO	10 µM
LDN-193189	Inhibits BMP receptors	Stratech, A8685-APE	DMSO	250 nM
MG132	Inhibits 26S proteasome	Abcam, ab141003	DMSO	10 µM
Cycloheximide	Inhibits protein translation	Abcam, ab120093	DMSO	20 µg/ml
Chloroquine	Inhibits lysosomal activity	Sigma Aldrich, C6628	DMSO	100 µg/ml
Puromycin	antibiotic	Sigma, P8833	Water	0.5-1 µg/ml
G418	antibiotic	Sigma, G8168	Water	1 µg/ml
mLIF (2019 batch)	Suppresses differentiation in mouse ES cells	Selfmade (V. Azuara lab)	DMEM	1:1000

2.1.1.3 Media components

Components	**Supplier, Catalogue #**
200 mM L-Glutamine	Thermo Scientific, 25030024
100X Penicillin-Streptomycin	Sigma, P0781
20% Bovine Serum Albumin (BSA)	Sigma, F9665
Dulbecco's Modified Eagle AQ Media (DMEM-AQ)	Sigma, D0819
DMEM, high glucose, pyruvate, no glutamine	Gibco, 21969035
Heat-inactivated Foetal Bovine Serum (FBS)	Sigma, F9665
FBS-ES-12A (Lot# CP18-2223)	Generon, FBS-ES-12A
Knockout DMEM	Life Technologies, 10829018
Knockout Serum Replacement (KSR)	Life Technologies, 10828028

Opti-MEM® Reduced Serum Medium	Life Technologies, 11058-021
Roswell Park Memorial Institute AQ-Media 1640 (RPMI-AQ)	Sigma, R2405
50 mM β-mercaptoethanol	Life Technologies, 31350-010
Non-essential Amino Acids (NEAA)	Sigma, N7145
50X B27 Supplement	Life Technologies, 17504-044

2.1.1.4 Disassociation enzymes

Enzymes	Supplier, Catalogue #
Trypsin-EDTA	Merck, T3924
Collagenase IV	Life Technologies, 17104019
Accutase	Merck, A6964
TrypLE	Life Technologies, 12604013

2.1.1.5 Chemicals, kits, and coating reagents

Reagent	Supplier, Catalogue #
2% Gelatin in PBS	Sigma, G1393
Calcium Phosphate Transfection Kit	Sigma, CAPHOS-1KT
Dimethyl sulphoxide (DMSO)	Sigma, D2650
Dual-Glo® Luciferase Assay Kit	Promega, E2920
Dulbecco's Phosphate Buffered Saline (DPBS)	Merck, D1408
LipofectamineTM LTX with PLUSTM Reagent	Fisher, 15338030
Matrigel® Matrix Growth Factor Reduced	SLS, 354230
Water Tissue Culture Grade (TC-H2O)	Merck, W3500
Poly-L-Lysine (PLL)	Sigma, P4707

2.1.2 Methods

2.1.2.1 Media Composition

Medium name (Application)	Media composition
Anterior Definitive Endoderm (ADE) differentiation medium (mESCs differentiation to ADE)	Gibco DMEM supplemented with: 20% KSR 1% Penicillin-Streptomycin 10 ng/ml bFGF 50 ng/ml Activin A
DMEM (HEK293T cell culture)	DMEM-AQ supplemented with 10% FBS
KSR (Knockout Serum Replacement) medium (MEF-CM preparation)	KO-DMEM supplemented with: 20% KSR 1 mM L-glutamine 1% NEAA 0.1 M β-mercaptoethanol 1% Penicillin-Streptomycin 4ng/ml bFGF
MEF medium (mouse embryonic fibroblasts (MEF) culture)	DMEM supplemented with: 10% FBS 2mM L-glutamine 1% Penicillin-Streptomycin
MEF-CM medium (H1 hESCs culture)	KSR medium supplemented with: 1 mM L-glutamine 10 ng/ml bFGF 1% Penicillin-Streptomycin
mESC medium (mESC culture)	DMEM supplemented with: 10% ES-FBS 2 mM L-Glutamine 0.5% Penicillin-Streptomycin 0.1 mM NEAA 0.1 mM β-mercaptoethanol 1:1000 mLIF
RPMI medium (PC3 cells culture)	RPMI-AQ medium supplemented with 10% FBS
RPMI/B27 medium (H1 hESCs serum starvation)	RPMI-AQ supplemented with 1x B27
Starvation medium 1 (serum starvation of HEK293T cells)	DMEM-AQ supplemented with 1% FBS
Starvation medium 2 (serum starvation of PC3 cells)	RPMI-AQ medium (No supplements)

2.1.2.2 Culture and propagation of hESCs

i) Isolation of mouse embryonic fibroblasts (MEFs)

A pregnant female CD1 mouse (E13.5) was sacrificed by cervical dislocation in accordance with the UK Home office protocols. Its uterine horns were dissected out and washed three times with DPBS containing 2% Penicillin/Streptomycin. Each embryo was then dissected out, viscera was removed, and carcass was disassociated into single cells with trypsin-EDTA at 37°C in a sterile Bijou tube. The single cells were then transferred into a T75 flask and incubated at 37°C overnight in DMEM medium. The medium was refreshed the next day and cells checked for any bacterial contamination. When they reached ~90% confluency, they were trypsinised and frozen at $1x10^7$ cells per cryovial in MEF medium containing 10% DMSO as passage P0.

ii) Generation of MEF-conditioned medium (MEF-CM)

Frozen MEFs were thawed, grown, and propagated at 1:6 ratio maximum in DMEM to passage P3/P4. Cells were then trypsinised into single cells and collected in 2-4x 50 ml falcon tubes. The cells were mitotically inactivated by being irradiated at 40 Gy in an IBL-637 Cell irradiator equipment (CIS-Bio International). Irradiated MEFs (i-MEFs) were then seeded in 0.5%-gelatin-coated T225 flasks at ~20-25 $x10^6$ cells per flask. Next day, the cells were rinsed with DPBS and DMEM was replaced with KSR medium supplemented with 4 ng/ml bFGF freshly at 150 ml per flask. After 24 hours, this conditioned KSR medium, called MEF-CM, was collected in cryo-storage bottles, and stored at -80°C until needed, while new 150 ml KSR medium was added into the flask. This procedure was repeated for 6-7 days depending on the MEF health. Before applying to hESCs, two bottles of frozen MEF-CMs were thawed, mixed in pairs, D1+D6, D2+D5, D3+D4, filtered to remove cellular debris, and supplemented with 2 mM L-glutamine and 1% Pen/Strep. It was stored at 4°C for up to 2 weeks.

iii) Preparation of Matrigel coated plates

Matrigel stock was thawed overnight on ice at 4°C. Knockout-DMEM (KO-DMEM) and plastics were also chilled at 4°C before use. Matrigel was diluted 1:2 with chilled KO-DMEM, aliquoted into 1 ml into 15 ml tubes and stored at -20°C for future use. One aliquot of Matrigel was thawed overnight in the refrigerator and further diluted 1:15 with chilled KO-DMEM., then used to coat the tissue culture plate. The Matrigel was allowed to set at least for ~10 hours at 4°C or ~3 hours at room temperature (for immediate use). Just before seeding hESCs, the Matrigel fluid was aspirated off and washed with DPBS.

iv) Propagation, culture and freezing of hESCs

H1 hESCs were routinely cultured in Matrigel-coated plates in MEF-CM, supplemented with freshly added 10 ng/ml bFGF with daily medium-change. The cells were passaged when either individual colonies become densely packed, or cells are getting confluent. 200 U/ml Collagenase IV solution was prepared by dissolving 20,000 units of collagenase IV in 100 ml of KO-DMEM and filtered before aliquoting and storing at 4°C for immediate use for up to 3 weeks and at -20°C for long term storage. It was applied to the cells for ~4-6 minutes and then the colonies were mechanically disassociated into smaller colonies of up to 50-100 cells in bFGF-supplemented MEF-CM. The plate was shaken gently up and down and left and right to evenly distribute the cells. Confluent cells were passaged at 1:3 ratio. For freezing hESCs, wells with >85% confluent cells were collagenase IV-treated and then mechanically disassociated in cold KSR. 10% v/v DMSO was added in a dropwise fashion before transferring the cells to a cryovial and storing them in a cryobox at -80°C prior to their storage in liquid nitrogen.

2.1.2.3 Culture and propagation of mESCs

ES26 Hex-GFP and Kt15 Smad2$^{-/-}$ mESCs were both routinely cultured on 0.1% gelatin-coated plates and in mESC medium. The plates were coated with gelatin at least 10 minutes before adding the cells and incubated at 37°C. The media was freshly supplemented with 1:1000 mLIF, just before applying on the cells. Medium was changed every day and the cells

were passaged when the colonies were ~80% confluent, usually every three days. 0.5 ml/10 cm^2 of accutase was used to disassociate the cells by incubating the cells at 37°C for 5-10 minutes. Cells were routinely split at a ratio of 1:10 and plates gently shaken for even distribution of cells. For freezing mESCs, mESC medium supplemented with 10% DMSO and an extra 10% ES-FBS was used.

2.1.2.4 Culture and Propagation of PC3 cells

PC3 cells were routinely cultured in RPMI medium and regularly passaged every 2-3 days at a ratio of 1:10 with Trypsin-EDTA. The cells were frozen in the same medium supplemented with 10% DMSO. For growth factors and inhibitor treatment experiments, the cells were serum-starved in RPMI-AQ medium for 16-20 hours/overnight.

2.1.2.5 Culture and propagation of HEK293T cells

HEK293T cells were routinely cultured in DMEM and regularly passaged every 2-3 days at a ratio of 1:10 with Trypsin-EDTA. The cells were frozen in the same medium supplemented with 10% DMSO. For growth factors and inhibitor treatments, HEK293T cells were starved in 1% FBS-DMEM-AQ for 16-20 hours/overnight, as they cannot survive in no-serum medium.

2.1.2.6 Cell transfection

i) Lipid-based transfection

Transient transfection of PC3 cells were performed by seeding the cells one day before transfection to get them to be ~70% confluent on the day of transfection in RPMI medium. Medium was refreshed 1-2 hours before transfection. Two tubes were labelled as tube A and B. For cells covering a 10 cm^2 area,150 µl OptiMEM and 2 µl Lipofectamine LTX were added to tube A and mixed by pipetting while 1-2 µg of purified plasmid DNA was mixed with 150 µl OptiMEM before adding PLUS reagent (the same volume as the DNA) were added to tube B and mixed. These mixtures were allowed to sit at room temperature for 5 minutes before mixing by pipetting the contents of tube B to tube A and incubate at room temperature for no longer than 30 minutes. This mixture was then evenly distributed on top of the cells in a

dropwise fashion. The plate was gently shaken and incubated at 37°C for 24-48 hours before using them for further experiments.

For hESCs, the cells were transfected while in suspension, at the time of splitting. Same volumes of reagents for tube A and tube B were mixed as in PC3 cells and incubated for 5 minutes. The cells were disassociated using accutase during this incubation period. Then, the contents of tube A and B were mixed and incubated at room temperature for up to 30 minutes while counting the cells. The lipofectamine-DNA mixture was added to the cells in a dropwise fashion and mixed before seeding the cells on to the desired Matrigel-coated tissue culture dish.

For mESCs, the cells were transfected while in suspension, at the time of splitting. Same volumes of reagents for tube A and tube B were mixed as in hESCs and incubated for 5 minutes. The cells were disassociated using accutase during this incubation period. Then, the contents of tube A and B were mixed and incubated at room temperature for up to 30 minutes while counting the cells. The lipofectamine-DNA mixture was added to the cells in a dropwise fashion and mixed before seeding the cells on to the desired gelatin-coated tissue culture dish.

ii) Calcium phosphate transfection

This method of transfection was used for HEK293T cells. Antibiotic-free medium was used, and cells were seeded to be ~70% confluent the following day for transfection. Media was refreshed 1-2 hours before transfection. The transfection mix was prepared in two tubes, tube A and B. For each 10 cm^2 area, 15 µl of $CaCl_2$ was added to tube A, followed by 0.5-2 µg purified plasmid DNA and TC grade water to make the total volume to 150 µl and mixed gently by pipetting. 150 µl 2x HeBs buffer was added to tube B and bubbled using a hand-held pipette gun fitted with a 20 µl micropipette tip while tube A contents were added to it in a dropwise fashion. The mixture was incubated at room temperature for no longer than 30 minutes before evenly distributing on the cells drop by drop. The cells were transfected for 24-48 hours before treating them as required.

2.1.2.7 Luciferase assay

Luciferase assay was conducted in hESCs and mESCs. The cells were transfected in suspension while splitting in antibiotic-free medium. Co-transfection with firefly (pGL3-$CAGA_{12}$-MLP-Luciferase), renilla (pRL-T7) (both CAGA-Luc and renilla constructs were kindly gifted by Dr Vasso Episkopou) and Smad2-WT/LA (pCS5-Flag-Smad2-WT/LA) was done at a ratio of 10:1:10. Lipofectamine LTX was used for transfection and Tubes A and B were prepared and transfection carried out the same as explained in section 2.1.2.6 i). A firefly and renilla only control with GFP-transgene was used as a no-Smad2 control. The cells were seeded on Matrigel/gelatin-coated plates and transfected for 36 hours before refreshing the media (Day 2). On Day 3, the cells were pre-treated with 10 μM SB431542 for 2 hours before treatment with 5 ng/ml activin A or continued with SB431542 for 20 hours before performing the luciferase assay using Promega dual luciferase assay kit as per manufacturer's instructions.

Cells were harvested using trypsin and each well was equally dispensed into 3 wells of a 96-well luminometer plate. Cells were lysed using the Dual-Glo luciferase assay reagent for 10 minutes on a shaker followed by detecting luminescence using PHERAstar microplate reader by BMG labtech. The lysate was then treated with Dual-Glo-Stop & Glo reagent to quench the firefly luciferase signal and activate renilla luminescence. Firefly luminescence readings were normalized with corresponding renilla luminescence readings to account for differences in transfection efficiencies.

2.2 Molecular biology- DNA/RNA techniques

2.2.1 Materials

2.2.1.1 Reagents, chemicals, and kits

Reagent	Supplier, Catalogue #
2-Log DNA ladder	NEB, N3200
50 bp DNA ladder	NEB, N3236
6X DNA loading buffer	NEB, B7024
Agarose (molecular biology grade)	Sigma, A9539
Ampicillin sodium salt	Sigma, A0166
Kanamycin sulfate	Sigma, 60615
Chloroform:Isoamyl Alcohol	Sigma, 25666
DH5α Competent E. coli	Fisher, 18265017
Ethanol	VWR chemicals
Isopropanol	Fisher, BP2618212
SafeGreen nucleic acid stain	NBS biologicals, NBS-SG1
HiSpeed Midiprep Kit	Qiagen, 12643
Molecular Grade Water	Fisher, 11430615
Murine RNAse Inhibitor	Fisher, EO0381
Oligo(dT)12-18	Fisher, 10753741
Deoxynucleotide mix (dNTP)	Fisher, R0191
NEB Monarch Gel extraction kit	NEB, T1020S
SYBR® Green JumpstartTM Taq Ready Mix	Merck, KCQS02
Tri Reagent ®	Sigma, T9424
Q5 Site Directed Mutagenesis Kit	NEB, E0552S

2.2.1.2 Buffers and solutions

Buffers	Recipe
50X Tris-Acetate-EDTA Buffer (TAE)	242 g Tris Base 57.1 ml Acetic Acid 18.6 g EDTA Autoclaved water to 1 L
10X Tris-Borate-EDTA Buffer (TBE)	108 g Tris Base 55 g Boric Acid 9.3 g EDTA Autoclaved water to 1 L
Tris-EDTA Buffer (TE)	1 ml Tris-HCL pH 8.0 (10mM) 200 µl of 0.5M EDTA pH 8.0 (1mM) Autoclaved water to 100 ml
Lysogeny Broth (LB) Medium	10 g Bacto-tryptone 5 g Yeast extract 10 g NaCl Autoclaved water to 1 L
LB Agar	5 g Bacto-tryptone 2.5 g Yeast extract 5 g NaCl 7.5 g Agar Autoclaved water to 500 ml
P1 Resuspension Buffer (Qiagen)	50mM Tris-HCl pH 8.0 10mM EDTA 100 µg/ml RNAse A
P2 Lysis Buffer (Qiagen)	200mM NaOH 1% Sodium Dodecyl Sulphate (SDS)
P3 Neutralisation Buffer (Qiagen)	3M Potassium acetate pH 5.5
SOC Media	20 g Bacto-tryptone 5 g Yeast extract 2 ml of 5M NaCl 2.5 ml of 1M KCl 10 ml of 1M MgCl2 20 ml of 1M glucose Autoclaved water to 1 L
Oligos annealing buffer	400 µl Tris-HCl pH 7.5 (10mM) 80 µl of 0.5M EDTA pH 8.0 (1mM) 400 µl of 5M NaCl (50mM) Molecular grade water to 50 ml

2.2.1.3 Plasmids

Plasmids	Source	Plasmid code
pCS2-Flag-Smad2-WT	Addgene, 14042	C39
pCS2-Flag-Smad2-3LSA	Lab-made	L156
pCS2-Flag-Smad2-T220V	Lab-made	L57
pCMV-Flag-Smad2-EPSM	Addgene, 14933	C40
pCMV-Flag-Smad2-3LSA	Lab-made	L61
pCMV-Flag-Smad2-3LSD	Lab-made	L152
pCMV-GFP-Smad2-WT	Gift from Prof C. S. Hill	G86
pCMV-GFP-Smad2-3LSA	Lab-made	L150
pCMV-GFP	Clonetech	C18
pCAG-Flag-Smad2-WT-IRES-Puro	Lab-made	L158
pCAG-Flag-Smad2-3LSA-IRES-Puro	Lab-made	L159
pCAG-Flag-Smad2-T220V-IRES-Puro	Lab-made	L160
pCAG-IRES-Puro	Lab-made	L157
pCAG-GFP-IRES-Puro	Gift from Prof. Meng Li	G35
pGL3-CAGA12-MLP-luc	Gift from Prof. V. Episkopou	G54
pRL-TK-Renilla	Promega, AF025846	C20

2.2.1.4 Primers

All primers were re-constituted in molecular grade water to a concentration of 100 μM and stored in -20°C.

Primer	Forward strand 5'→3'	Reverse strand 5'→3'
Flag-Smad2	GGACTACAAGGACGACGATGA	TCACTGCTTTCTCACACCACT
RPL22	TCGCTCACCTCCCTTTCTAA	TCACGGTGATCTTGCTCTTG
β-actin	TGTCTGGCGGCACCACCATG	AGGATGGAGCCGCCGATCCA

Brachyury	TGCTTCCCTGAGACCCAGTT	GATCACTTCTTTCCTTTGCATCAAG
Eomes	AGGAATTCTTGCTTTGCTAATTCTG	CGAAGAAACAGCAAGAGCAGC
FoxA2	GGGAGCGGTGAAGATGGA	TCATGTTGCTCACGGAGGAGTA
Goosecoid	GAGGAGAAAGTGGAGGTCTGGTT	CTCTGATGAGGACCGCTTCTG
MixL1	CCGAGTCCAGGATCCAGGTA	CTCTGACGCCGAGACTTGG
Nanog	TGATTTGTGGGCCTGAAGAAAA	GAGGCATCTCAGCAGAAGACA
Oct4	TCGAGAACCGAGTGAGAGGC	CACACTCGGACCACATCCTTC
Rex1	TCACAGTCCAGCAGGTGTTT	GCCATCACATAAGGCCCACA
Sox17	GGCGCAGCAGAATCCAGA	CCACGACTTGCCCAGCAT
Sox2	GCCGAGTGGAAACTTTTGTCG	GCAGCGTGTACTTATCCTTCTT
GATA6	ACTTGAGCTCGCTGTTCTCG	CAGCAAAAATACTTCCCCCA
Twist	AGCTACGCCTTCTGGTCT	CCTTCTCTGGAAACAATGACATC
E-cadherin	AGCCCTTACTGCCCCCAGAG	GGGAAGATACCGGGGGACAC
N-cadherin	CAACGGGGACTGCACAGATG	TGTTTGGCCTGGCGTTCTTT
Snail1	GCTGCAGGACTCTAATCCAGA	ATCTCCGGAGGTGGGATG
CTGF	CTGCAGGCTAGAGAAGCAGAG	GATGCACTTTTTGCCCTTCT
SKIL	GAGGCTGAATATGCAGGACAG	CTATCGGCCTCAGCATGG
c-Myc	TCGGAAGGACTATCCTGCTG	GTGTGTTCGCCTCTTGACATT
Smad7	GGCCGGATCTCAGGCATTC	TTGGGTATCTGGAGTAAGGAG
Slug	TGGTTGCTTCAAGGACACAT	GCAAATGCTCTGTTGCAGTG
Zeb1	GCACCTGAAGAGGACCAGAG	TGCATCTTGGTGTTCCATTTT
Nedd4L	TCCAATGGTCCTCAGCTGTTTA	ATTTTCCACGGCCATGAGA
Smad2	ATTCCAGAAACGCCACCTCC	GCTATTGAACACCAAAATGCAGG
Mouse-FoxA2	CCATCAGCCCCACAAAATG	CCAAGCTGCCTGGCATG
Mouse-Hex	GAGGTTCTCCAACGACCAGA	GTCCAACGCATCCTTTTTGT
Mouse-Cer1	AGGAGGAAGCCAAGAGGTTC	CATTTGCCAAAGCAAAGGTT
Mouse-Sox17	GGTCTGAAGTGCGGTTGG	TGTCTTCCCTGTCTTGGTTGA

Mouse -S17	ATGACTTCCACACCAACAAGC	GCCAACTGTAGGCTGAGTGAC
Mouse-L19	TGATCTGCTGACGGAGTTG	GGAAAAGAAGGTCTGGTTGGA

2.2.1.5 Nucleic acid-modifying Enzymes

Enzyme	Supplier, Catalogue #
DNAse I	Fisher, EN0521
RNAse A	Fisher, 10174711
Jumpstart™ Taq Polymerase	Sigma, D9307
ProtoScript II Reverse Transcriptase	NEB, M0368
Restriction endonucleases	NEB, various RE
T4 DNA ligase	NEB, M0202
T4 Salt DNA ligase	NEB, M0467

2.2.2 Methods

2.2.2.1 Plasmid construction and subcloning

i. Restriction Endonuclease digestions and gel DNA extraction

Plasmid DNA (pDNA) was used to digest with restriction endonucleases (RE) either to verify the sequence identity or for subcloning. Typically, 2 µg of pDNA was used in a 10-20 µl reaction volume containing the compatible buffer and the amount of RE added was maintained to be less than 10% v/v of the reaction volume, usually 10-20 U enzyme per reaction. The same approach was used for sequence verification but with reduced pDNA- up to 0.5 µg. RE reactions were either inactivated by incubating for 10 minutes at 65°C or by adding 6x NEB loading buffer. The digested pDNA was analyzed by agarose gel electrophoresis and imaged using safe-view UV illuminator. The samples were run alongside a suitable NEB DNA ladder at 135 V for 30-45 minutes through 0.8% agarose gel dissolved in 1x TAE or TBE buffer. Safe green was added to cooled molten agarose gel at a 1:20,000 concentration before allowing it

to set. For subcloning, the gel DNA fragments were excised using a clean scalpel and purified using Monarch DNA gel extraction kit by NEB. DNA fragments were typically eluted in 10 µl.

ii. DNA dephosphorylation

After purification, digested vectors were dephosphorylated by Antarctic phosphatase to eliminate the possibility of re-ligation of single-digested plasmids. Typically, 1/10th volume of 10x Antarctic phosphatase buffer and 5 U Antarctic Phosphatase was added to 1-5 µg of digested vector and incubated for 30-60 minutes to dephosphorylate 5' or 3' extensions. Enzyme activity was heat-inactivated for 5 min at 70°C before further use.

iii. Oligo annealing and phosphorylation

Sense and anti-sense strands were added at an equimolar ratio to achieve an annealing reaction volume of 100 µl and a final concentration of 10 µM of oligo. The reaction tube was placed in a heating block at 95°C for 5 minutes before removing the block away from the heating unit and allowing it to cool gradually at room temperature to promote oligo annealing. Nanodrop was used to measure oligo concentration and the oligos were then used for further applications.

iv. Ligation

Vector and Insert ligation reactions were set up using T4 DNA ligase of T4 Salt DNA ligase according to manufacturer's instructions. A vector to insert molar ratio of 1:3 was used in a 10 µl reaction volume containing no more than 1 µl ligase and 1 µl of 10x T4 ligase buffer and incubated overnight at 16°C before heat-inactivating the reaction for 10 minutes at 65°C. Total DNA concentration in the ligase reaction was maintained to be 1-10 ng/µl. The ligated DNA was then used for bacterial transformation.

v. Bacterial transformation

Competent DH5α *E.coli* was thawed on ice for ~10 minutes before adding ~10-50 ng of ligated product or a plasmid DNA. It was mixed gently by tapping. The reaction tube was incubated on ice for 30 minutes before performing heat-shock at 42°C for 45 seconds. The

cells placed on ice to recover for 5 minutes before adding SOC media or LB broth to a total volume of 1 ml. They were then incubated at 37°C for 1 hour with shaking at 200-220 rpm. Transformed bacteria was then pelleted by centrifugation at 15,000 g for 1 minute, all but 100 µl of the supernatant was discarded. The cells were resuspended and evenly plated onto LB agar plates containing the right selection antibiotic (100 µg/ml ampicillin or 50 µg/ml kanamycin). Plates were incubated at 37°C overnight to allow the bacterial growth.

vi. Plasmid Amplification and Purification

Transformed colonies were picked from LB agar plates and cultured in 5 ml of antibiotic supplemented LB broth and cultured for either 6 hours or overnight at 37°C with shaking at 200-220 rpm. The grown cultures were then pelleted by centrifugation at 15,000 g for 1 minute and resuspended in 140 µl Qiagen buffer P1 containing RNase, by vigorous vortexing. An equal volume of buffer P2 was added for alkaline lysis of the cells, and it was gently mixed by inverting 4-6 times to obtain a clear, viscous solution. 140 µl of buffer P3 was then added and mixed by inverting ~10 times to neutralize the reaction. The tube containing the lysed cells was placed on ice for 5-30 minutes before centrifugation at 15,000 g for 2 minutes. Supernatant was collected in a fresh tube and an equal volume of isopropanol (~450 µl) was mixed with it to precipitate the DNA. It was then centrifuged for 2 minutes at 15,000 g before a quick 70% Ethanol wash by centrifugation at 15,000 g for 1 minute. Ethanol was quickly removed after the spin and the pellet allowed to air-dry for ~10 minutes at room temperature. 25-50 µl of molecular grade water was used to resuspend the DNA pellet. DNA concentration and purity were measured by nanodrop spectrophotometer (Thermo Fisher) for use in further applications.

For more purified and large-scale DNA amplification, the transformed colonies were picked from LB agar plates and cultured like before for 6 hours in 5 ml antibiotic supplemented LB broth. It was then used to inoculate 50-100 ml of fresh LB broth with the appropriate antibiotic for Midiprep, which was incubated overnight at 37°C with shaking at 200-220 rpm. Plasmid DNA was then isolated using Qiagen HiSpeed Midiprep kit according to manufacturer's

instructions and DNA was eluted in 400-750 µl of sterile, endotoxin-free TE buffer. DNA quantification was performed using nanodrop and it was stored at -20°C until required.

vii. Site-directed mutagenesis

NEB Q5 site-directed mutagenesis kit was used to introduce point mutations in the DNA templates. Non-overlapping primers were designed using NEBasechanger™ application with 5' ends annealing back-to-back, through which single nucleotide mutation(s) could be introduced to change the resulting amino acid residue(s) from serine to alanine or alanine to asparagine. The following templates were used to introduce the required mutations.

Template	Forward and Reverse primers 5'→3'	Final product
pCS2-Flag-Smad2-WT (C39)	**Forward:** TCCTACTACTCTTGCCCCTGTTAATCATAGCTTGGATTTAC **Reverse:** GCTAGTTCTGCTGGAGCGCCTGTGTCCATACTTTGATTC	pCS2-Flag-Smad2-LA (L156)
pCMV-Flag-Smad2-3LSA (L61)	**Forward:** TCCTACTACTCTTGACCCTGTTAATCATAGCTTGG **Reverse:** TCTAGTTCTGCTGGATCGCCTGTGTCCATACTTTG	pCMV-Flag-Smad2-3LSD (L152)
pCMV-GFP-Smad2-WT (G86)	**Forward:** TCCTACTACTCTTGCCCCTGTTAATCATAGCTTGGATTTAC **Reverse:** GCTAGTTCTGCTGGAGCGCCTGTGTCCATACTTTGATTC	pCMV-GFP-Smad2-3LSA (L150)

PCR was carried out with the appropriate template and primer pairs as follows:

Reaction components	**25 µl reaction**	**Final concentration**
Q5 Hot Start High-Fidelity 2x Master Mix	12.5 µl	1x
10µM F primer	1.25 µl	0.5 µM
10µM R primer	1.25 µl	0.5 µM
Template DNA (10 ng)	1 µl	10ng
Nuclease-free water	9 µl	-

and cycling conditions in a Bio-Rad Dyad DNA Engine thermocycler as follows:

Step	**Temp**	**Time**
Initial denaturation	98°C	30 sec
25 cycles	98°C	10 sec
	61°C	30 sec
	72°C	20–30 seconds/kb
Final extension	72°C	2 min
Hold	4-10°C	Forever

1 µl of this amplified PCR product was treated with Kinase-Ligase-DpnI (KLD) enzyme mix to digest the template and ligate the new plasmid. This reaction was carried out for ~20 minutes at room temperature after which, 5 µl of this product was used for bacterial transformation. Clones obtained were confirmed by sanger sequencing, service offered by Genewiz, UK.

2.2.2.2 Gene expression analysis

i. RNA isolation and extraction

To obtain RNA samples, cells were lysed using 1 ml TRI reagent per 10 cm^2 surface area of at least 85% confluent cells. The sample was either stored at -80°C for RNA isolation at a later period within a month or the next steps were followed immediately. 0.2 ml of chloroform:isoamyl alcohol was used per 1 ml TRI reagent after allowing the lysate to stand at room temperature for 5 minutes. The sample was shaken vigorously for 15 seconds before incubating again for 2-15 minutes at room temperature. Then, the sample was centrifuged at 12,000 g for 15 minutes at 4°C. The clear, aqueous phase was collected in a fresh tube, taking care to prevent contamination from other phases. The sample was incubated at room temperature for 5-10 minutes after adding 0.5 ml isopropanol per 1 ml of TRI reagent. It was centrifuged again at 12,000 g for 10 minutes at 4°C. The RNA pellet was washed with 0.5 ml of 75% ethanol and vortexed before centrifugation again at 7,500 g for 5 minutes at 4°C. The RNA pellet was allowed to air-dry, after which, it was resuspended in 16 µl of nuclease-free water.

ii. DNAse I treatment

To remove any trace contamination of DNA, 16 µl of RNA sample was incubated with 2 µl of DNAse I and 2 µl of reaction buffer for 30 minutes at 37°C. Then, 2 µl of EDTA stop solution was added and the reaction carried out at 65°C for 10 minutes to inactivate DNAse activity. RNA concentration was measured using nanodrop spectrophotometer.

iii. cDNA synthesis

The purified RNA sample obtained from the above step was used to synthesize cDNA using reverse transcription. 1 µg of RNA was incubated with 5 µM of oligo dT and 1 mM of dNTP mix in a reaction volume of 10 µl at 65°C for 5 minutes after which, it was briefly spun and placed on ice. Then, 4 µl of 5x protoscript II buffer was added to it along with 0.01 M DTT, 10 U/µl of protoscript II reverse transcriptase enzyme, 0.4 U/µl RNAse inhibitor and nuclease free water to make the total volume to 20 µl. This mix was then incubated at 42°C for 1 hour

and the reaction was inactivated at 65°C for 20 minutes. 180 µl nuclease free water was added to it and the pure cDNA sample was stored at -20°C until use. Two tubes per sample were made, one with and the other without reverse transcriptase enzyme for control.

iv. Quantitative Real-Time PCR (qRT-PCR)

cDNA efficacy was verified by standard PCR before using them for qRT-PCR. 1 µl of cDNA, 0.5 µM of each primer, 5 µl SYBR Green Jumpstart™ Taq ready mix and 3 µl of nuclease free water was used for the qRT-PCR reaction. Each reaction was setup up in triplicates for each gene, with each cDNA sample analyzed thrice on separate occasions to generate n=9. C_t value was calculated for each of the samples for a given gene. Reactions were run on a Bio-Rad Opticon2™ DNA Engine Real-time fluorescence thermocycler with the following conditions:

Step	Temperature	Time
Initial denaturation	94°C	2 minutes
Denaturation	94°C	15 seconds
Annealing	60°C	30 seconds
Extension	72°C	30 seconds
Real-time fluorescence read/sec	75-84°C	+3°C/sec
40 Cycles		
Melting curve read/sec	67-91°C	+0.3°C/sec

Production of double stranded product was tracked in real-time by measuring the SYBR Green fluorescence. Melting curve was performed at the end of the reaction for each primer set to ensure the formation of a single PCR product. Analysis was done using the Opticon software and using the comparative $2\Delta\Delta C_t$ method. In brief, raw C_t value of the sample was normalized to the C_t value of endogenous house-keeping gene, RPL22/β-actin/S17/L19, to generate the ΔC_t value. For $\Delta\Delta C_t$ calculation, ΔC_t was normalized to the control. The relative

gene expression or the fold-change was calculated by taking the $\Delta\Delta C_t$ value as the exponential function of 2. The standard deviation was calculated from at least three qRT-PCR data obtained from three independent experiments. Primer sequences are listed in section 2.2.1.4.

2.3 Molecular biology- Protein techniques

2.3.1 Materials

2.3.1.1 Reagents, chemicals, and kit

Reagent	Supplier, Catalogue #
Protease Inhibitor Cocktail	Sigma, P8340
Sodium orthovanadate (Na_3VO_4)	Sigma, S6508
Sodium fluoride (NaF)	Sigma, 450022
Sodium deoxycholate	Sigma, D6750
Phenylmethanesulfonylfluoride (PMSF)	NEB, 8553S
Pierce BCA assay Kit	Thermo Fisher, 23227
30% Acrylamide/Bis-acrylamide	Sigma, A3699
β-mercaptoethanol	Sigma, M6250
4-(2-hydroxyethyl)-1-piperazineethanesulfonic acid (HEPES)	Sigma, 54457
Ammonium persulfate (APS)	Merck, A3678
Tetramethylethylenediamine (TEMED)	Merck, T7024
Bromophenol blue	Sigma, B0126
Bovine Serum Albumin (BSA)	Sigma, A9647
Xray films	SLS, MOL7016
Clarity Western Enhanced chemiluminescence substrate (ECL)	BioRad, 1705061
Immobilon Forte Western HRP substrate	Millipore, WBLUF0500
Goat serum	Merck, G9023
Ethylene glycol tetraacetic acid (EGTA)	Sigma, E4378
Ethylenediaminetetraacetic acid (EDTA)	Sigma, E6635
Glycerol	Sigma, G5516
Immobilon® polyvinylidene fluoride (PVDF) membrane	Fisher, IPVH00010
Methanol	VWR, MFCD00004595

Ethanol	VWR, MFCD00003568
Isopropanol	Fisher, C3H80
Mowiol 4-88	Calbiochem, 475904
Nonidet P-40	Anachem, E109
Prestained Protein Ladder	Abcam, ab-116028
Pierce™ 16% Formaldehyde	Thermo, 23227
Protein A/G Dynabeads®	Invitrogen, 10003D
Sodium azide (NaN_3)	Sigma, S2002
Triton X-100	Sigma, T8787
Tween-20	Sigma, P1379
Glycine	Sigma, G8898

2.3.1.2 Buffers and solutions

Immunoblotting buffers	**Composition**
Radio Immunoprecipitation Assay Buffer (RIPA)	25 ml 1 M Tris-HCl pH 8.0 (50 mM) 15 ml 5 M NaCl (150 mM) 5 ml NP-40 (1% v/v) 2.5 g Sodium deoxycholate (0.5% w/v) 0.5 g SDS (0.1% w/v) Autoclaved water to 500 ml
5x Sample buffer (5x Laemmeli buffer)	1.25 ml 0.5 M Tris-HCl pH 6.8 (50 mM) 2.5 ml glycerol (25 % v/v) 2 ml 10% SDS (2% w/v) 400 µl 0.5% bromophenol blue (0.02 % w/v) 500 µl β-mercaptoethanol (715 mM) Autoclaved water to 10 ml
Sodium Orthovanadate stock	183.9 mg Na_3VO_4 (200 mM) Adjust pH to 10.0 Boil solution until colorless Cool and readjust pH back to 10.0 Repeat boil/cool cycles until solution remains colorless at pH 10.0

4% Polyacrylamide Stacking Gel	2.5 ml 0.5 M Tris-HCl pH 6.8 (125 mM) 1.3 ml 30% Acrylamide/Bis (4% v/v) 100 µl 10% SDS (1% v/v) 75 µl 12% APS (0.09% v/v) 10 µl TEMED (0.1% v/v) Autoclaved water to 10 ml
7.5% Polyacrylamide Running Gel	2.5 ml 0.5 M Tris-HCl pH 8.8 (125 mM) 2.5 ml 30% Acrylamide/Bis (7.5% v/v) 100 µl 10% SDS (1% v/v) 75 µl 12% APS (0.09% v/v) 10 µl TEMED (0.1% v/v) Autoclaved water to 10 ml
SDS Running Buffer	3 g Tris base (25 mM) 14.4 g Glycine (0.2 M) 5 ml 20% SDS (0.1%) Autoclaved water to 1 L
TBS-T Buffer	20 ml Tris-HCl pH 7.6 (20 mM) 26 ml NaCl (130 mM) 1 ml Tween-20 (0.1% v/v) Autoclaved water to 1 L
Transfer Buffer	5.82 g Tris base (48 mM) 2.93 g Glycine (39 mM) 3.75 ml 10% SDS (0.04% w/v) 200 ml methanol (20% v/v) Autoclaved water to 1 L
Blocking buffer	5 g BSA or non-fat skimmed milk (5% w/v) 100 ml TBS-T buffer

Cell fractionation buffers	**Composition**
Cytoplasmic extraction buffer	50 ml 1 M Tris-HCl pH 7.5 (50 mM) 5 ml Triton X-100 (0.5%) 27.5 ml 5 M NaCl (137.5 mM) 100 ml Glycerol (10%) 10 ml 0.5 M EDTA (5 mM) Autoclaved water to 1 L
Nuclear extraction buffer	50 ml 1 M Tris-HCl pH 7.5 (50 mM) 5 ml Triton X-100 (0.5%) 27.5 ml 5 M NaCl (137.5 mM) 100 ml Glycerol ((10%)

	10 ml 0.5 M EDTA (5 mM) 50 ml 10% SDS (10% v/v) Autoclaved water to 1 L

Immunocytochemistry buffers	Composition
Fixation buffer	10 ml 16% PFA solution 30 ml PBS
Blocking/permeabilizing buffer	1 ml goat serum (10% v/v) 0.25 g BSA (2.5% w/v) 30 µl Triton X-100 (0.3% v/v) PBS to 10ml
Mowiol 4-88 mounting solution	12 ml 200 mM Tris-HCl pH 8.5 (135 mM) 6 g glycerol 2.4 g Mowiol 4-88 6 ml autoclaved water Tubes heated at 60°C to dissolve Mowiol 4-88

2.3.1.3 Antibodies

Antigen target	Supplier, Catalogue #	Application and Dilution
Flag	Sigma, F1804	WB- 1:1000 IF- 1:500
Smad2/3	Cell Signalling, 3102	WB- 1:1000
Smad2/3	Cell Signalling, 8685	WB- 1:1000 IF- 1:800
Smad2	Thermo Fisher, 436500	WB- 1:1000
Phospho-Smad2 S465/467	Cell Signalling, 3108	WB- 1:1000
Phospho-Smad2 S465/467	Cell Signalling, 18338	WB- 1:1000 IF- 1:800
Phospho-Smad2 S245/250/255	Cell Signalling, 3104	WB- 1:1000
Phospho-Smad2 T220	Sigma, SAB4300252	WB- 1:1000- 1:2000
Smad4	Cell Signalling, 46535	WB- 1:1000
Nedd4L	Cell Signalling, 4013	WB- 1:1000
Smurf2	Cell Signalling, 12024	WB- 1:1000
Smad1	Cell Signalling, 6944	WB- 1:1000

Phospho-Smad1/5/9	Cell Signalling, 13820	WB- 1:1000
Lamin B	Millipore, MAB3536	WB- 1:1000
β-actin	Sigma, A5441 Proteintech, 66009	WB- 1:50000
α-tubulin	Cell Signalling, 3873	WB- 1:3000 IF- 1:1000
GAPDH	Santa Cruz, 365062	WB- 1:5000
Mouse IgG-HRP	Jackson Labs, 115-035-174	WB- 1:5000- 1:10000
Rabbit IgG-HRP	Fisher, 31460	WB- 1:5000- 1:10000
Rabbit IgG-Alexa Fluor® 488	Life Technologies, #A11055	IF- 1:400
Rabbit IgG-Alexa Fluor® 568	Life Technologies, #A11011	IF- 1:400
Mouse IgG-Alexa Fluor® 488	Life Technologies, #A11001	IF- 1:400
Mouse IgG-Alexa Fluor® 568	Life Technologies, #A11004	IF- 1:400

2.3.2 Methods

2.3.2.1 Protein extraction and quantification

Cultured cells were subjected to treatment with appropriate growth factor/ inhibitor for a given time to collect cell lysate for protein expression analysis. The media was aspirated, and cells were washed with chilled PBS before adding 100 µl RIPA buffer per 10 cm^2 surface area of cells. In some cases, the cells were trypsinised, collected in a tube, pelleted by centrifugation at 13000 g for 1 minute before washing with chilled PBS and adding RIPA buffer as before. RIPA buffer was always supplemented with protease inhibitor cocktail (1:1000), NaF (1:100), PMSF (1:100) and Na_3VO_4 (1:100) right before cell lysis. The lysate was incubated on ice for 10 minutes, vortexed to break the pellet and passed through a 21G syringe or pipetted several times using 10 µl tip to eliminate DNA contamination. The lysates were then centrifuged at ~13000 g for 10 minutes at 4°C. The supernatant was collected in a fresh

tube and protein quantification was done using Pierce BCA assay kit, following the manufacturer's instructions. In brief, BSA protein standards ranging from 0 µg/ml to 2000 were prepared (which could be stored at 4°C long-term until exhausted) and required volume of working reagent (WR) was made by mixing reagents A and B in the ratio of 50:1. 5 µl of each sample was mixed with 100 µl of WR in separate wells of a clear flat-bottom 96-well plate. The samples were gently shaken for 30 seconds for mixing before placing the plate at 37°C for 30 minutes. Protein absorbance was read at a wavelength of 562 nm on an Optimax Tuneable microplate reader (Bio-Rad).

2.3.2.2 Immunoblotting

Protein samples were prepared for immunoblotting by boiling a mixture of 3-20 µg protein, 5x SB and autoclaved water in a suitable volume at 98°C for 5 minutes in order to denature the protein and impart it with negative charge. The samples were carefully loaded into the wells of a self-prepared gel for stacking and resolving by applying 120 V for 1.5 hours. Either wet transfer or semi-dry transfer method was used for the next step to transfer the resolved proteins from gel on to an activated PVDF membrane. PVDF membrane was activated by immersing it in methanol for 10 seconds, quickly washing it with autoclaved water and then allowing it to equilibrate in 1x TB for at least 10 minutes before using. Gel-PVDF membrane sandwich was prepared between buffer-soaked filter papers and thick pads such that gel faces the black side (negative charge) and the membrane towards the red side (positive charge). Care was taken to prevent any bubble formation. Wet transfer was performed in the cold room at 100 V for 1 hour whereas, semi-dry transfer was performed at 20 V for 1 hour at room temperature but with chilled buffer to keep the system from over-heating. The membrane was then blocked in 15 ml of 5% milk-1x TBS-T blocking buffer for 30-60 minutes on a shaker at room temperature before overnight primary antibody incubation on tube-roller in the cold room. The following day, the membrane was washed with ~10 ml 1x TBS-T for 10 minutes three times before incubating with 10-15 ml of an appropriate secondary antibody at room temperature on shaker. The membrane was washed again three times with 10 ml of 1x TBS-

T, 10 minutes each before incubation with ECL reagent and exposing X-ray film to the membrane in the dark room to develop and record protein expression/signal on the film. These films were scanned and saved as .jpg files and analyzed using Image J software. Note: immunoblots were first probed with phospho-antibodies (pCS, pLS, and pLT) overnight at 4°C and developed using ECL reagent followed by 10-30 minutes 1xTBST wash at room temperature on the shaker. The blots were then probed with anti-Smad2/3 antibody overnight at 4°C to be developed before similarly probing with antibody for loading control proteins - β-Actin, GAPDH, or β-Tubulin.

2.3.2.3 Cytoplasmic/nuclear fractionation

The cells were grown on a larger surface area, usually on a 10 cm dish, treated appropriately and trypsinised. These cells were collected in 15 ml falcon tube and pelleted at ~3500 g for 5 minutes at 4°C. Cells were washed with chilled PBS and 250 µl of cytoplasmic extraction buffer per 55 cm^2 surface area of grown cells was added and sample incubated on ice for 10 minutes to lyse the plasma membrane only but preserve intact nuclei in the sample. The sample was vortexed at medium speed setting 2-3 times for 15 seconds each or until the pellet had dissolved before centrifugation at ~13000 g for 10 minutes. The supernatant was collected in a fresh tube as cytoplasmic fraction. The whitish pellet, which is the nuclear pellet, was washed twice with chilled cytoplasmic extraction buffer and then lysed using 50 µl nuclear extraction buffer per 55 cm^2 surface area of cells on ice for 10 minutes and vortexed vigorously. The nuclear lysate was passed through 21G needle to denature the DNA contamination after which, the sample was centrifuged again at ~13000 g for 10 minutes to collect the supernatant as the nuclear fraction. These fractions were analysed via immunoblotting as described in the previous sections.

2.3.2.4 Quantitation and statistical analysis of immunoblotting

The densitometry of immunoblots was measured using Image J software. Gel analysis tool was used to assign a value to measure the expression level on each blot. The expression level of target protein was normalised to the loading control and then normalised again to the

control sample to calculate the fold-change. All the results in this thesis are presented as the average of at least three separate experiments and standard deviation calculated and indicated in the figures. The statistical analysis was done using two-tailed unpaired Student's t-test and p-value < 0.05 was considered statistically significant.

2.3.2.5 Immunostaining

Cells were split and cultured on coverslips or chamber slides until the desired confluency was reached. hESCs were cultured on Matrigel-coated coverslips and HEK293T cells on poly-L-lysine-coated cover slips. Cells were then washed with PBS and fixed for 20 minutes with 4% formaldehyde solution at room temperature. Excess formaldehyde was removed by 1x PBS-T wash three times and then the coverslips were incubated in blocking/permeabilisation buffer for 1 hour followed by an overnight incubation with primary antibody at the appropriate dilution at 4°C with tilting. The following day, coverslips were subjected to three 10 minutes washes with 1x PBS-T followed by 1 hour incubation with the appropriate fluorophore-conjugated secondary antibody in the dark. Coverslips were then subjected to two more 10 minutes PBS washes followed by one 10 minutes PBS+DAPI wash with DAPI at a final concentration of 1:1000 to counterstain the nuclei, also performed in the dark. Slides were mounted on microscope slides using Mowiol 4-88 solution and allowed to air-dry overnight. Slides were then visualised using a Leica SP5 II confocal fluorescent microscope typically at 64x magnification.

2.4 Software and online tools

Computer software
Leica LAS AF Lite
Image J (FIJI)
Serial Cloner
Sequence scanner 2
Opticon Monitor 3
Adobe Photoshop CS6

Online tools	Website link
Basic Local Alignment Search Tool (BLAST)	https://blast.ncbi.nlm.nih.gov/Blast.cgi
Clustal OMEGA Protein Alignment Tool	https://www.ebi.ac.uk/Tools/msa/clustalo/
Genebank® DNA Sequence Database	https://www.ncbi.nlm.nih.gov/nucleotide/
UniProt Protein Database	https://www.uniprot.org/
NEB Double Digest Finder	http://nebcloner.neb.com/#!/redigest
NEBasechanger	https://nebasechanger.neb.com/
NEBioCalculator™	https://nebiocalculator.neb.com/#!/ligation
Endnote Web	https://access.clarivate.com/login?app=endnote

Chapter 3

Results

Suppression of CDK8/9-induced Smad2-pLS extends half-life of activated Smad2

3.1 Introduction

Smad2/3 linker is an unstructured region which contains several phosphorylatable residues including the proline-directed threonine and serine residues (S/T-P) (Kamato et al., 2013, Xu et al., 2016). Phosphorylation of the linker region of Smad2/3 alter their protein-binding affinities (Chaikuad and Bullock, 2016), changing their interacting partners to modulate Smad2/3 subcellular localisation, transcriptional activity, and prime them for degradation, thereby further enhancing or attenuating TGF-β signalling. Linker phosphorylation can be carried out by various kinases that are associated with different signalling pathways; therefore, they can integrate canonical TGF-β signalling with the activity of other signalling pathways to establish crosstalk (Kamato et al., 2013, Xu et al., 2016). Numerous kinases such as PI3K/mTORC2, GSK3β, Erk1/2, JNK, p38, CDKs, NLK, CaMKII, ROCK etc. have been reported to be able to phosphorylate Smad2/3 linker region, directly or indirectly, underscoring the significance of linker phosphorylation in regulating TGF-β signalling (Kretzschmar et al., 1999, Wicks et al., 2000, Funaba et al., 2002, Mori et al., 2004, Matsuura et al., 2004, Kamaraju and Roberts, 2005, Yoshida et al., 2005, Matsuura et al., 2005, Millet et al., 2009, Alarcon et al., 2009, Burch et al., 2010, Hough et al., 2012, Yu et al., 2015, Liang et al., 2021).

Smad2/3 nuclear translocation and transcriptional activity can be inhibited by agonist-induced phosphorylation of linker S/T-P residues via Erk1/2 and CDK8/9 (Kretzschmar et al., 1999, Funaba et al., 2002, Hough et al., 2012, Matsuura et al., 2005, Alarcon et al., 2009). Conversely, it is enhanced by JNK and p38 mediated linker phosphorylation (Kamaraju and Roberts, 2005). Interestingly, dephosphorylation of linker serine residues by the SCPs counter-effect Erk1/2 and CDK8/9-induced phosphorylation and enhance Smad2/3 transcription (Wrighton et al., 2006, Sapkota et al., 2006). Subsequently, GSK3β phosphorylates linker serine (LS) and promotes binding of WW domain E3 ubiquitin ligases such as Nedd4L and Smurf2, that recognise linker threonine phosphorylation (pLT) and can prime Smad2/3 for proteasomal degradation to cease transcription (Millet et al., 2009, Gao et al., 2009, Tang et al., 2011, Aragon et al, 2011).

Evidently, the functions of Smad2/3 pLS and pLT are inter-connected. They are frequently perceived as one single unit, having similar functions, and generating similar effects on TGF-β signalling. However, a previous study in our lab identified that linker proline-directed threonine (LT) and serines (LS) can be regulated by different kinases in hESCs (Yu et al., 2015). The study showed that a pan-CDK inhibitor, flavopiridol (FVP) predominantly suppresses Smad2/3 linker serine phosphorylation (Smad2/3-pLS) while PI3K inhibitor, LY294002 mainly inhibits Smad2/3 linker threonine phosphorylation (Smad2/3-pLT) without any clear effect on Smad2/3-pLS (*Fig 1.9A*). This finding suggests that Smad2/3 LT and LS can be differentially regulated by different signalling pathways and that distinct linker phosphorylation patterns may have distinct functions in modifying Smad2/3 protein stability and activity, thereby differentially affecting TGF-β signalling.

In this chapter, I further validate the differential phosphorylation of Smad2-LS and -LT identified in hESCs and in another cell model to investigate the effect of Smad2-pLS on Smad2 protein activity as well as on TGF-β signalling.

3.2 Results

3.2.1 Inhibition of CDK8/9 predominantly suppresses Smad2-pLS

To interrogate the effect of CDK inhibition by FVP on Smad2-pLS and -pLT, I first confirmed our previous findings in hESCs. As expected, stimulating hESCs with activin A (AA) for an hour induced Smad2 C-terminal SxS phosphorylation (Smad2-pCS) and increased pLS and pLT signals, through agonist-mediated canonical and non-canonical signalling pathways, respectively (*Fig 3.1A lane 2 vs 1*). Applying AA to the cells showed significant increase in Smad2-pCS signal, regardless of FVP treatment (*Fig 3.1B*). In addition, application of FVP to the cells showed reduced Smad2-pLS signals, regardless of AA stimulation (*Fig 3.1A lane 3 vs 1 and 4 vs 2*) and under both conditions, the reduction in Smad2-pLS was significant (*Fig 3.1C*). On the other hand, FVP treatment in the absence of agonist stimulation did not show much effect on Smad2-pLT (*Fig 3.1A lane 3 vs 1*) while, in the presence of agonist, FVP exhibited some reduction in Smad2-pLT (*Fig 3.1A lanes 2 and 4*) which was not statistically significant (*Fig 3.1D*). These results confirm our previous findings that FVP-mediated inhibition of CDKs in hESCs mainly affect Smad2-pLS.

In order to show that effect of FVP on Smad2 is not restricted to a specific cell type, I performed similar experiments in PC3 cells, a prostate cancer tumour cell line. Cells were stimulated with TGF-β for an hour in the presence or absence of FVP after culturing them in serum-free medium for 16-18 hours. The results were similar to that in hESCs and inhibition of TGF-β receptor by SB431542 (SB) did not affect Smad2-pLS levels and FVP-mediated reduction in Smad2-pLS (*Fig 3.1 E-G*). These results confirm that FVP-mediated reduction in Smad2-pLS is not cell type-specific and also, suggest that FVP inhibits both agonist-induced and agonist-independent Smad2-pLS. In addition, the use of PC3 cells enabled us to perform further experiments in a more controllable and easier setting in comparison to hESCs as hESCs have more complicated and expensive culture requirements.

Given that FVP is a well-characterised CDK inhibitor, it is likely that CDKs play an important role in the regulation of Smad2-pLS (Shapiro, 2004, Chen et al., 2005). However, cells that

were concomitantly treated with FVP and TGF-β showed a much higher pLS signal than the cells treated with FVP alone (*Fig 3.1E lanes 4 and 5*), indicating a non-CDK-mediated pLS upon TGF-β stimulation. It has been previously reported that Erk can phosphorylate both pLS and pLT upon stimulation by agonist-induced non-canonical pathways (Kretzschmar et al., 1999, Funaba et al., 2002, Matsuura et al., 2005, Burch et al., 2010, Hough et al, 2012). Therefore, I applied Erk and CDK inhibitors individually as well as concomitantly in TGF-β-stimulated cells and investigated their effects on Smad2-pLS (*Fig 3.1H*). As expected, inhibition of CDKs by FVP diminished pLS signal in both serum-starved and TGF-β-stimulated PC3 cells (*Fig 3.1H lanes 3 and 5*), whereas inhibiting Erk alone with U0126 did not reveal much effect on pLS signal (*Fig 3.1H lanes 4 and 6*). However, inhibiting both Erk and CDKs in TGF-β-stimulated cells considerably suppressed pLS signal (*Fig 3.1H lane 7*). These results indicate that the extra non-CDK-induced Smad2-pLS is derived from agonist-induced Erk activation.

Although FVP-mediated inhibition on agonist-induced linker phosphorylation has been attributed to its inhibiting role on CDK8/9 (Alarcon et al., 2009), it is unclear whether its agonist-independent inhibition also resulted from CDK8/9 inhibition. Moreover, FVP at higher concentrations can also target GSK3β, which may interfere with the results (Leclerc et al., 2001). Therefore, to validate the specific CDKs involved, I used a potent CDK8/9 inhibitor, LY2857785 (LY) to study its effects on Smad2-pLS (*Fig 3.1I*) (Yin et al., 2014). Expectedly, TGF-β stimulation resulted in increased Smad2-pCS signal, along with an increase in Smad2-pLS and -pLT signals (*Fig 3.1I lanes 2 and 4*). Consistent with the effects of FVP, LY also decreased Smad2-pLS signals in both TGF-β-stimulated or non-stimulated cells without clear effects on pLT, (*Fig 3.1I, lanes 3 and 4*). These results suggest that it is indeed CDK8/9 that are mainly responsible to phosphorylate Smad2-LS and their inhibition leads to reduction in Smad2-pLS.

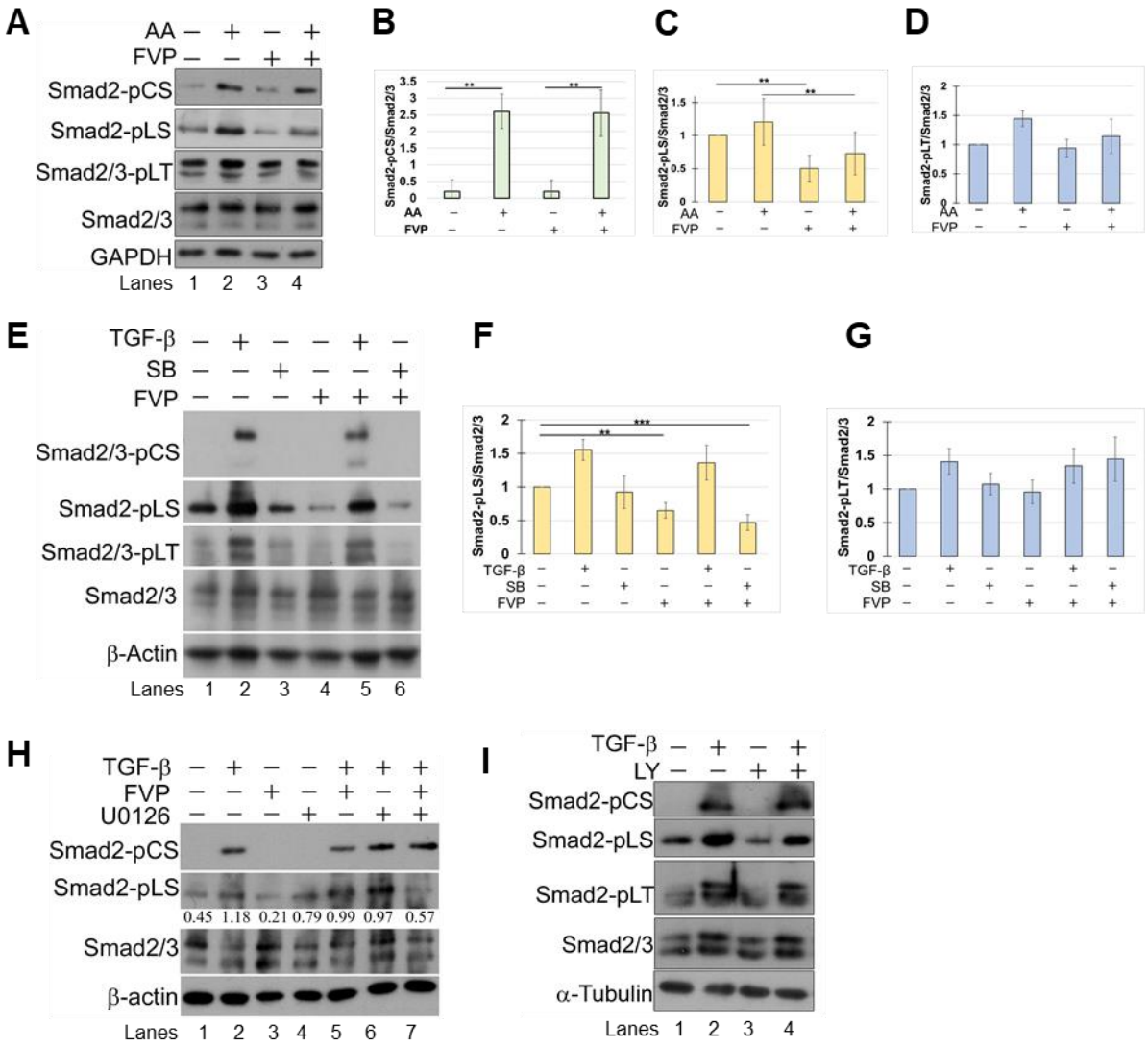

Figure 3.1: Differential effect of flavopiridol and LY2857785 on Smad2-pLS and Smad2-pLT

A) Immunoblot analysis of H1 hESCs treated with activin A and flavopiridol for 1 hour in RPMI/B27 medium after washing off MEF-CM, with antibodies against the indicated proteins (n=5). **B)** Quantification of Smad2-pCS in A **C)** Quantification of Smad2-pLS in A and **D)** Quantification of Smad2-pLT in A, all using means±s.d. densitometric measurements in H1 hESCs, normalised to total Smad2/3 protein. **E)** Immunoblot analysis of serum-starved PC3 cells treated with TGF-β, SB431542, and flavopiridol for 1 hour, with antibodies against indicated proteins (n=9). **F)** Quantification of Smad2-pLS in E and **G)** Quantification of Smad2-pLT in E, both using means±s.d. densitometric measurements in PC3 cells, normalised to total Smad2/3 protein. **H)** Immunoblot analysis of serum-starved PC3 cells treated with TGF-β, flavopiridol, and U0126 for 1 hour, with antibodies against indicated proteins (n=2). Numbers indicate densitometric measurements of Smad2-pLS, normalised against total Smad2/3. **I)** Immunoblot analysis of serum-starved PC3 cells treated with TGF-β, SB431542, and LY2857785 for 1 hour, with antibodies against indicated proteins (n=5). Targets of inhibitors used are: Flavopiridol-CDK2/4/6/7/8/9, SB431542-ALK4/5/7, LY2857785- CDK8/9, U0126- Erk1/2. Student t-test was done and '*', '**', and '***' indicate p<0.05, 0.01, and 0.001, respectively. Please refer to chapter 2- materials and methods (Pg-85) for how the immunoblots were acquired.

3.2.2 Agonist-induced Smad2 activation is prolonged by FVP and LY

In the hESCs experiments described earlier (*Fig 3.1*), the cells were collected for analysis after 1 hour of agonist-stimulation in the presence or absence of CDK inhibitor, FVP or LY, in which CDK inhibitor treatment did not show any difference on the levels of Smad2-pCS. Interestingly, after 6 hours of such treatments, agonist-induced Smad2-pCS signals were still clearly visible in FVP-treated cells, whereas no Smad2-pCS signal could be detected in the absence of FVP (*Fig 3.2A lane 4 vs 2*). Meanwhile, Smad2-pLS signals were lower in FVP-treated cells than non-FVP-treated ones under similar stimulation conditions, while Smad2-pLT was not affected by FVP treatment, as expected. Furthermore, no clear changes were observed in total Smad2/3 protein levels across all treatments (*Fig 3.2A*). These results suggest that FVP has a function in prolonging half-life of activated Smad2 in hESCs.

To verify if such effects of FVP is not cell-type specific, similar experiment was done in PC3 cells (*Fig 3.2B*). Like before, FVP maintained strong Smad2-pLS suppression and only had slight reduction in pLT signals (*Fig 3.2B lanes 4 and 6*). As expected, TGF-β-stimulated cells did not show any Smad2-pCS (*Fig 3.2B lane 2*) but FVP could maintain Smad2-pCS signals even 6 hours post stimulation (*Fig 3.2B lane 5*). Similar effect of FVP on agonist-induced Smad2 activation was also observed in HEK293T cells (*Fig A-IIG, lane 4*). These results match the observations in hESCs and confirms that FVP can extend agonist-induced Smad2 activation.

In order to further examine whether inhibition of CDK8/9 is likely to account for this prolonged activation by FVP, LY was used to replace FVP in the above experiments in PC3 cells (*Fig 3.2C*). Similar to the FVP treatment, LY treatment exhibited considerably stronger signal of TGF-β-induced Smad2-pCS than TGF-β alone stimulation (*Fig 3.2C lane 4 vs 2*). The Smad2-pLS signals were also lower in LY-treated cells as expected, while no clear difference was detected on Smad2-pLT levels (*Fig 3.2C lanes 3 and 4*). Taken together, these results demonstrate that inhibition of CDK8/9 by FVP or LY prolongs the duration of agonist-activated Smad2 in the cells, meanwhile maintains the suppression of Smad2-pLS.

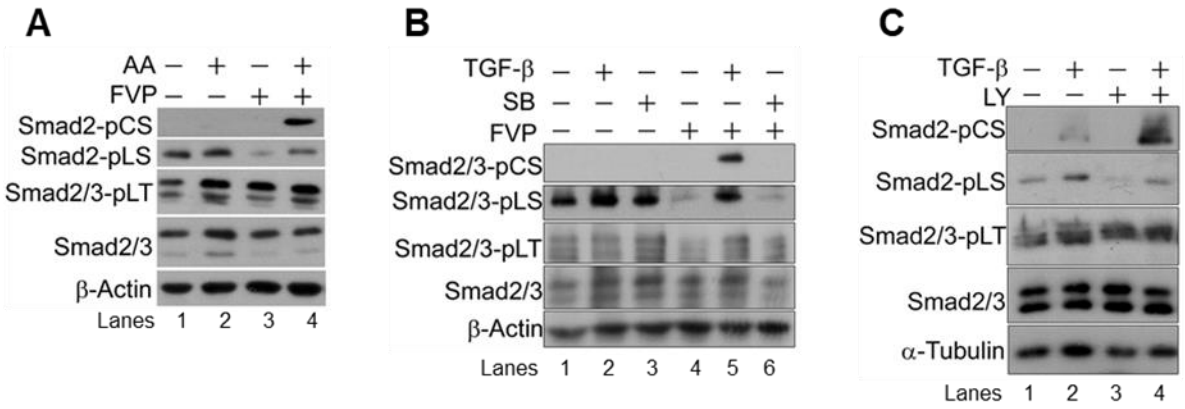

Figure 3.2: Effect of prolonged flavopiridol and LY2857785 treatment on Smad2-pLS and Smad2 activation

A) Representative immunoblot of H1 hESCs treated with activin A and flavopiridol for 6 hours in RPMI/B27 medium after washing off MEF-CM, with antibodies against the indicated proteins (n=5). **B)** Representative immunoblot of serum-starved PC3 cells treated with TGF-β, SB431542, and flavopiridol for 6 hours, with antibodies against indicated proteins (n=9). **C)** Representative immunoblot of serum-starved PC3 cells treated with TGF-β, SB431542, and LY2857785 for 6 hours, with antibodies against indicated proteins (n=5).

3.2.3 FVP extends the duration of Smad2 activation in the nucleus

Next, I asked whether this prolonged Smad2-pCS signals by FVP are localised in the nucleus as it is known that agonist stimulation results in the formation of functional oligomeric complexes of Smad2/3-Smad4 and their accumulation in the nucleus (Schmierer and Hill, 2005, Schmierer et al., 2008). Therefore, I stimulated hESCs and PC3 cells with AA and TGF-β, respectively, in the presence or absence of FVP for 1 and 6 hours. The cells were then fixed for immunostaining with antibody against Smad2/3. At 1-hour post-treatment, there were clear nuclear Smad2/3 signals in cells with agonist-stimulation and FVP treatment did not appear to make any difference (*Fig 3.3A and B*). However, at 6-hours post-agonist stimulation, cells scarcely showed any nuclear Smad2/3 signal in the absence of FVP. In contrast, in the presence of FVP, agonist-stimulated cells still exhibited strong nuclear Smad2/3 signals (*Fig 3.3C and D*). Nonetheless, without agonist-stimulation, FVP did not induce any nuclear localisation of Smad2/3 at both 1- and 6-hours post-treatments, rather showing similar staining patterns as DMSO-treated controls (*Fig 3.3 A-D*). These results indicate that FVP enhances nuclear accumulation of Smad2, in agreement with the activated status of Smad2 by FVP seen earlier (*Fig 3.2*). Note that, the antibody that I have used for Smad2-pCS and Smad2-pLS selectively detects only Smad2, but the antibody for total protein Smad2/3 and Smad2/3-pLT can detect both Smad2 and Smad3. Therefore, in all my future experiments, the focus of my work is on Smad2.

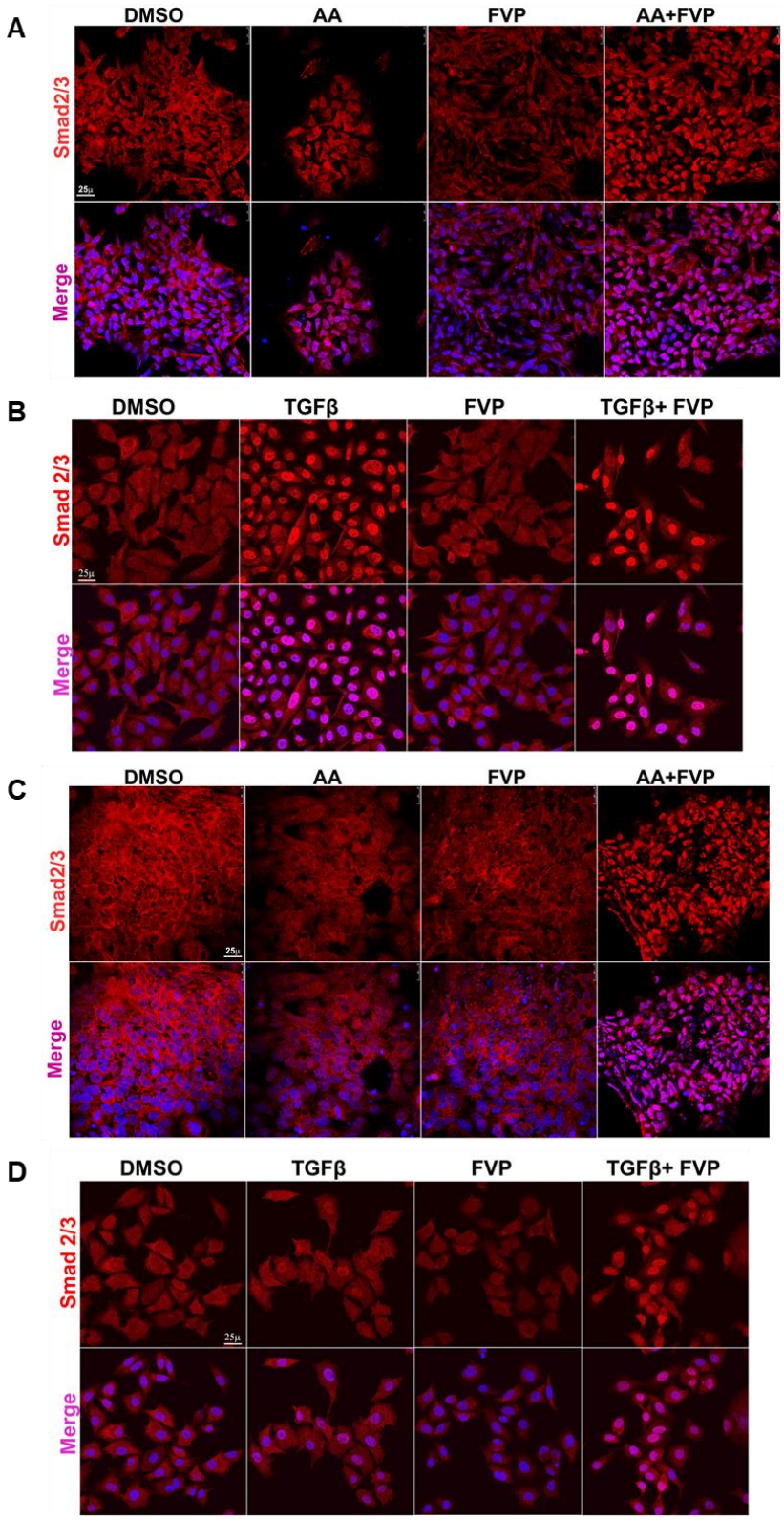

Figure 3.3: Subcellular localisation of activated Smad2 upon flavopiridol treatment and Smad2-pLS inhibition

A) H1 hESCs and **B)** PC3 cells treated with activin A/TGF-β and flavopiridol or dmso (control) for 1 hour, as indicated, in their respective serum-starvation conditions before fixing and analysing by immunofluorescence (IF) with anti-Smad2/3 and DAPI for nuclei staining. **C)** H1 hESCs and **D)** PC3 cells treated the same as A and B, but for 6 hours, as indicated, before fixing and analysing by IF with anti-Smad2/3 and DAPI for nuclei staining. Scale bar- 25μm.

3.3 Discussion and conclusion

In this chapter, I have shown that Smad2-pLS and -pLT exhibit different levels of phosphorylation upon treatment with FVP or LY (FVP/LY) (*Fig 3.1*) and that prolonged treatment with FVP or LY maintains Smad2-pLS suppression and extends the duration of agonist-mediated Smad2 activation without clear changes in the turnover of total Smad2/3 proteins (*Fig 3.2 and 3.3*). Since FVP/LY are both inhibitors of CDK8/9 (Shapiro et al, 2004, Chen et al., 2005, Yin et al., 2014) and application of FVP/LY suppressed pLS regardless of agonist stimulation (*Fig 3.1*), it is plausible that CDK8/9 may be responsible for both agonist-induced and steady state Smad2-pLS. On the contrary, CDK8/9 phosphorylated Smad2 LT only slightly in response to agonist stimulation and had no contribution towards its baseline phosphorylation (*Fig 3.1*). CDK8/9 are transcriptional CDKs, which are components of the mediator complex and are involved in the regulation of RNA polymerase II (RNAPII)-mediated transcription (Malumbres, 2014). Furthermore, Smad2/3 are both effectors in the TGF-β pathway and function as transcription factors (TFs) upon translocation into the nucleus after ligand stimulation, where they interact with other TFs in a cell-context-dependent manner to form transcription complexes of which CDK8/9 are also essential components (Hill, 2016, Morikawa et al., 2013, Massagué et al., 2005, Li et al., 2020, Alarcon et al., 2009). Inhibiting CDK8/9 by FVP/LY, therefore, could presumably, also inhibit Smad2-pLS while in close contact with each other in the transcription complex.

Moreover, similar effects of FVP on Smad2-pLS were observed in various cell lines, in human embryonic stem cells (hESCs) as well as in PC3 cells and HEK293T cells, suggesting it is not a cell type-specific phenomenon. Preferential phosphorylation of LS and LT by the CDKs has not been previously reported, presumably because of cell line differences as most studies are done using HaCat cells, which are derived from primary epidermal keratinocytes, and may have distinct signalling to hESCs and PC3 cells (Matsuura et al., 2004, Alarcon et al., 2009). Linker phosphorylation- whether pLS or pLT, is considered to antagonise canonical TGF-β signalling, however, previous studies do support the notion that pLS might have more

crucial role in Smad2/3 transcriptional activity while pLT may play a more important role in Smad2/3 degradation. Notably, Erk- and CDK-induced pLS attenuates Smad2/3 transcription (Hough et al., 2012, Matsuura et al., 2004, Alarcon et al., 2009) whereas removal of pLS, and not pLT, by the SCPs1/2/3 augments Smad2/3 transcriptional activity (Wrighton et al., 2006, Sapkota et al., 2006). At the same time, pLT relayed by the activation of mTORC2, MAPKs and CDKs enhances the binding of WW domain E3 ubiquitin ligases to Smad2/3 and results in their degradation via the ubiquitin-proteasome system (UPS), and inhibition of pLT prevents Smad2/3 degradation (Aragon et al., 2011, Gao et al., 2009).

Furthermore, in establishing that FVP/LY extend activated Smad2 signal, several mechanisms are posited to induce this effect. It could be attributed to enhanced Smad2 activation due to prolonged receptor kinase activity or sustained stabilisation of the activated Smad2 pool. However, since the availability of activated Smad2/3 is proportional to the receptor activation (Inman et al., 2002), and that identical TGF-β stimulation in both presence and absence of FVP resulted in similar levels of Smad2-pCS (*Fig 3.1, 3.3A, and 3.3B*), it demonstrates that FVP/LY did not affect receptor activation. Actually, the difference in Smad2-pCS signal was observed at 6 hours after ligand-induced receptor activation, which even strongly suggests that it is less likely to be an effect of FVP/LY on receptor kinase activity and higher plausibility that FVP/LY had a direct effect on activated Smad2 itself.

Another mechanism that could promote sustained activated Smad2 in the nucleus in the absence of pLS might be through its increased association with Smad4 in the functional oligomeric complexes or with TAZ thus, keeping the complexes intact in the nucleus for longer than normal (Inman et al., 2002, Schmierer and Hill, 2005, Schmierer et al., 2008, Varelas et al., 2008). Yet another possibility could be that inhibition of Smad2-pLS may affect how activated Smad2 is dephosphorylated by the nuclear phosphatases and therefore, preventing its timely dissociation from the oligomeric complex before enabling their export to the cytoplasm (Schmierer and Hill, 2005, Schmierer et al., 2008, Hill, 2009). As a whole, the results in this chapter suggest that inhibition of Smad2-pLS may act to preserve activated

Smad2 pool, which could enhance the duration of TGF-β signalling. Since I observed a differential regulation of pLS and pLT by CDK8/9 in my cell models, it presents an interesting opportunity to study their separate functions and disentangle their individual roles in regulating TGF-β signalling. It would also be interesting to probe how CDK8/9 differentiate between LS and LT to specifically phosphorylate LS and biological function of this preference regarding TGF-β signalling.

Chapter 4

Results

Inhibition of Smad2-pLS extends the duration of TGF-β signalling and enhances Smad2 activity

4.1 Introduction

In the previous chapter, I showed that the phosphorylation of Smad2-LS and -LT are differentially regulated by CDK8/9. Inhibiting CDK8/9 activities by either flavopiridol (FVP) or LY2857785 (LY) predominantly suppresses Smad2-pLS with little effect on Smad2-pLT. More importantly, application of FVP/LY extended the duration of activated Smad2 signals and their localisation in the nucleus meanwhile, also maintaining inhibition on Smad2-pLS. These findings raise several questions: 1) Does CDK8/9 inhibition extend activated Smad2 signals via suppression of Smad2-pLS? In other words, does Smad2-pLS play a role in regulating the duration of agonist-induced Smad2 activation? 2) If so, does it regulate activated Smad2 through affecting its degradation or dephosphorylation? and 3) Does sustained nuclear presence of activated Smad2 also upregulate its transcriptional activity?

Before making experimental considerations, it is important to understand the dynamics of how activated Smad2/3 are regulated. Activated Smad2/3 make functional oligomeric complexes with Smad4 and accumulate in the nucleus where they also interact with other transcription factors and proteins to drive target gene expression (Massague and Wotton, 2000, Inman et al., 2002, Schmierer and Hill, 2005, Schmierer et al., 2008). During the assembly of the transcription complex, Smad2/3 linker region can be phosphorylated by CDK8/9 (Alarcon et al., 2009). Phosphorylation of the second and third proline-directed linker serine residues (Smad3-S208/213 and likely also of Smad2-S250/255) by CDK8/9 augments binding of Pin1, a peptidyl-prolyl cis-trans-isomerase (PPIase), to the PPxY motif located downstream of phosphorylated Smad2/3-LT (T220/T179), ensuring enhanced activation of Smad transcription (Nakano et al., 2009, Matsuura et al., 2009, Alarcon et al., 2009, Aragon et al., 2011). Next, the two phosphorylated LS residues prime GSK3β-mediated phosphorylation of the first LS (Smad3-S204 and likely also of Smad2-S245), transitioning Smad2/3 activity from transcription to deactivation by promoting binding of the WW domain E3 ubiquitin ligases to the PPxY motif and replacing Pin1 (Tang et al., 2011, Gao et al., 2009, Aragon et al., 2011). Smurf2 and Nedd4L are WW domain E3 ubiquitin ligases implicated in

regulating activated Smad2 turnover through linker phosphorylation (Zhang et al., 2001, Lin et al., 2000, Gao et al., 2009, Aragon et al., 2011). As such, preservation of activated Smad2 in the nucleus upon FVP/LY treatment in my experiments could be attributed to inability of the degradation machinery to deactivate Smad2 in the absence of Smad2-pLS.

Upon cessation of Smad2/3 transcriptional activity, in addition to the action of E3 ubiquitin ligases, activated Smad2/3 can also be dephosphorylated at their SxS motif to trigger their dissociation from the functional oligomeric complex and promote their export back into the cytoplasm (Inman et al., 2002, Pierreux et al., 2000, Schmierer and Hill, 2005, Schmierer et al., 2008). Particularly, phosphatases- PPM1A and PP5 have been found to deactivate Smad2/3 by dephosphorylating them at their SxS motif (Lin et al., 2006, Bruce et al., 2012). Prediction from mathematical model of nucleocytoplasmic shuttling of Smad2/3 suggests involvement of nuclear phosphatases in deactivating activated Smad2/3 (Schmierer et al., 2008). And since PPM1A is an exclusively cytoplasmic phosphatase (Bruce et al., 2012), a nuclear envelope protein, MAN1 may facilitate its binding to Smad2/3 for the dephosphorylation of activated Smad2/3 SxS motif (Bourgeois et al., 2013). However, although this study showed negative regulation of MAN1 on activated Smad2, it only reported *in vitro* binding between MAN1 and PPM1A and their interaction in cells is yet to be shown. Moreover, mediator proteins like chloride intracellular channel 4 (CLIC4) can also bind to Smad2/3 and preserve them in their activated form by preventing their phosphatase-mediated deactivation (Shukla et al., 2009). Loss of C-terminal SxS phosphorylation by the phosphatases improves Smad2/3 affinity to bind with nuclear export machinery and cytoplasmic anchoring proteins such as SARA (Xu et al., 2002, Dai et al., 2009, Hill, 2009). Therefore, FVP/LY-induced nuclear accumulation of activated Smad2 could also be a consequence of hampered phosphatase activity in targeting Smad2 C-terminal SxS phosphorylation (Smad2-pCS). Hence, in this chapter, I have designed and carried out experiments to address the questions raised above.

4.2 Results

4.2.1 FVP extends Smad2-pCS independent of TGF-β type I receptor activity

To explore the molecular mechanisms by which FVP extends Smad2 activation, I first examined the dynamics of FVP-mediated extension of activated Smad2 signals after withdrawal of agonist stimulation. Withdrawal of agonist ensures that further Smad2 activation has ceased, and the Smad2-pCS signal obtained in immunoblot corresponds to the loss of activated Smad2. Serum-starved PC3 cells were transiently stimulated with TGF-β before applying FVP and cells were collected at indicated time points for western blotting analysis (*Fig 4.1A*). Unsurprisingly, TGF-β stimulation induced strong Smad2-pCS signal, which were clearly visible even 1 hour after withdrawal of the stimulation regardless of whether the cells were treated with FVP or not (*Fig 4.1B lanes 1, 2, and 5*). However, 3 hours after agonist withdrawal, Smad2-pCS signal was still clearly visible in FVP-treated cells, whereas it was almost undetectable in the cells without FVP (*Fig 4.1B lanes 3 and 6*). Quantitative analysis of multiple experiments on Smad2-pCS against total Smad2/3 proteins showed a significantly slower rate of decline of Smad2-pCS signals between 3 and 6 hours in FVP-treated cells (*Fig 4.1C*). These observations indicate that FVP extends activated Smad2 half-life, likely, through a mechanism that does not result from enhanced agonist stimulation but rather through decelerating the decline of activated Smad2 signal.

To further eliminate the possibility that the effect of FVP on agonist-induced Smad2 activation is independent of TGF-β receptor kinase activity, similar experiments were carried out but with addition of SB431542 (SB), a TGF-β type I receptor inhibitor, to block the receptor activity. This time the cells were collected and analysed more frequently with shorter intervals and tested up to 1 hour (*Fig 4.1D*). The western blot showed that at 15 and 30 minutes after withdrawing stimulation and inhibiting receptor kinase, both FVP- and control cells exhibited similar levels of Smad2-pCS signals (*Fig 4.1E lanes 2-3 and 6-7*). In contrast, at 45 and 60 minutes, Smad2-pCS signals became undetectable in control cells, whereas they were still present in FVP-treated cells (*Fig 4.1E lanes 4-5 and 8-9*), suggesting that Smad2-pCS signals

decelerated faster in non-FVP treated cells than FVP-treated cells. This was further supported by quantitative analysis on multiple experiments that FVP treatment significantly delayed the disappearance of activated Smad2 (*Fig 4.1F*). These results further show that the effect of FVP on extending agonist-induced activation of Smad2 is independent of agonist-mediated receptor activation and is rather due to extending the half-life of activated Smad2.

It is well known that decline of phosphorylated Smad2/3 signals in the absence of further stimulation is usually controlled by two possible mechanisms: dephosphorylation by nuclear phosphatases and degradation by the proteases. Although there was no visible change in Smad2 protein level, its degradation cannot be completely excluded. Therefore, I thought that FVP might affect Smad2-pCS dephosphorylation. However, the phosphatase(s) responsible for SxS motif dephosphorylation is/are unclear. And also, changes in total Smad2 protein levels due to the degradation of activated Smad2 can be very subtle and not clearly observable (Pierreux et al., 2000). Therefore, I decided to examine the protein degradation in this process. Given that activated Smad2 can be degraded by ubiquitin-mediated proteasome degradation (Lo and Massague, 1999), I blocked the proteasome to compare its effect on Smad2-pCS signal in FVP-treated cells with non-treated control cells. Serum-starved PC3 cells were treated with the proteasome inhibitor MG132 before further stimulation with TGF-β in the presence or absence of FVP for 6 hours (*Fig 4.1G*). As shown in the previous chapter, Smad2-pCS signal became almost undetectable in the absence of FVP, while the signal was clearly visible with FVP treatment (*Fig 4.1H lane 1 vs 3*). Treatment with MG132 to disable proteasome activity considerably increased Smad2-pCS signals in both FVP- and non-FVP-treated cells (*Fig 4.1H lanes 2 and 4*). However, MG132 treatment for 6 hours did not show clear difference in total Smad2/3 proteins in FVP-treated cells (*Fig 4.1H lanes 3 and 4*), which is in contrast with that of non-FVP-treated cells (*Fig 4.1H lanes 1 and 2*). Furthermore, the ratio increase of activated Smad2 by MG132 in FVP-treated cells was not as high as without FVP (*Fig 4.1H lanes 2/1 vs 4/3*). These data suggest that FVP treatment may suppress proteasome-dependent degradation of Smad2. Altogether, FVP prolonged half-life of

activated Smad2 maybe by preventing Smad2 proteasomal degradation while its pLS is inhibited.

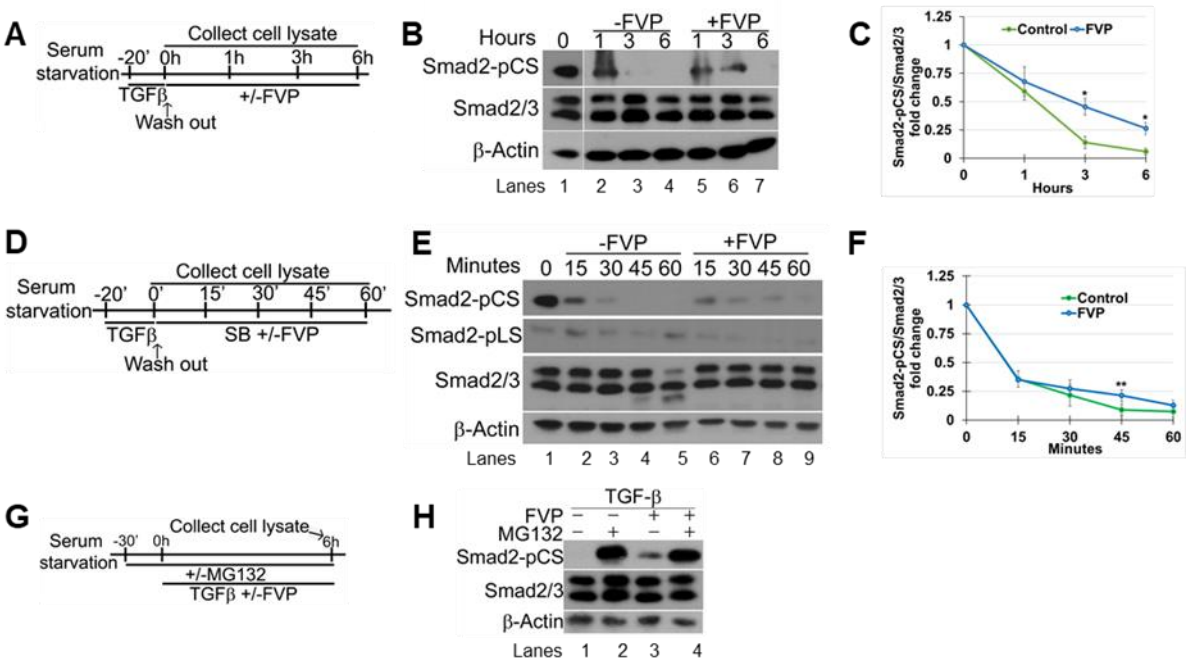

Figure 4.1: Effect of flavopiridol on activated Smad2 (Smad2-pCS)

A) Scheme of treatment for B. **B)** Representative immunoblot of Smad2-pCS in PC3 cells treated as illustrated in A. **C)** Quantification of Smad2-pCS in B, using means±s.d. densitometric measurements, normalised to total Smad2/3 proteins (n=3). **D)** Scheme of treatment for E. **E)** Representative immunoblot of Smad2-pCS and pLS in PC3 cells treated as illustrated in D. **F)** Quantification of Smad2-pCS in E, using means±s.d. densitometric measurements, normalised to total Smad2/3 proteins (n=3). **G)** Scheme of treatment for H. **H)** Representative immunoblot of Smad2-pCS in PC3 cells treated as illustrated in G (n=1). Student t-test was done and '*' and '**' indicate $p<0.05$ and 0.01, respectively.

4.2.2 Smad2-pLS plays a role in FVP-mediated extension of Smad2-pCS

Experiments in the previous section showed that FVP prolongs Smad2 activation possibly by preventing its degradation and that it is independent of TGF-β receptor kinase activity. Since FVP also suppresses Smad2-pLS, it raised the question whether Smad2-pLS may have a function in this process. Given that FVP may exert off-target effects to inhibit other kinases and that CDKs may also phosphorylate other residues in Smad2 besides pLS, they could all possibly result in this increase in half-life of activated Smad2. Therefore, to address the direct role of pLS in activated Smad2 and minimise any effect from other factors, I generated Smad2 expression vectors in which the 3 serine (S) residues (S245/250/255) in the Smad2 linker region were mutated to either non-phosphorylatable amino acid, alanine (A), named Smad2-LSA (*Fig 4.2A*), or to phospho-mimetic amino acid, aspartic acid (D), named Smad2-LSD (*Fig 4.2B*), using site-directed mutagenesis (SDM) from a Smad2 wildtype (Smad2-WT) expression vector. Furthermore, in all these Smad2-expression vectors, Smad2 proteins were also tagged with Flag epitope at their N-terminal.

To test if lack of Smad2-pLS truly prolongs Smad2 activation, Smad2-WT, -LSA, and -LSD were transiently transfected into Smad2-null HEK293T cells (*Fig A-IIIB*). These cells were then serum-starved overnight in 1% serum condition, as 293T cells cannot survive well in complete absence of serum, before stimulating with activin A (AA) for 6 hours (*Fig 4.2C*). Expectedly, AA treatment showed Smad2-pCS signals in all three Smad2 proteins- Smad2-WT, -LSA, and -LSD (*Fig 4.2C lanes 2, 5, and 8*). All three Smad2 proteins seemed to have relatively similar levels of Smad2-pCS signal in response to AA stimulation. However, taking into account the expression levels of Smad2 transgenes represented by Flag expression, it revealed a significantly higher proportion of activated Smad2 in Smad2-LSA proteins than the other two Smad2 proteins (*Fig 4.2D*). The high levels of pLS in Smad2-WT in response to AA stimulation might account for its similar levels of Smad2-pCS as Smad2-LSD. These results are consistent with the effects of FVP where suppression of Smad2-pLS stabilises activated Smad2, supporting the notion that inhibition of pLS in Smad2 prolongs its activation.

Next, to verify if the stabilisation of activated Smad2 is indeed due to slower decline of activated Smad2 in Smad2-LSA, a time course experiment was done to study the dynamic changes in Smad2-pCS signal. Smad2-null HEK293T cells were stably transfected with either Smad2-WT or Smad2-LSA expression vector, which also contained a puromycin selection protein. The stable transfectants were then serum-starved in 1% serum culture condition overnight to minimise interference of serum components in subsequent experiments, followed by a transient stimulation with AA for 20 minutes as shown in the treatment scheme (*Fig 4.2E*). Removal of AA and applying SB in the medium without serum ensured that no new activated Smad2 is generated, and Smad2-pCS signal can be studied at indicated timepoints without upstream interference (*Fig 4.2F*). Both Smad2-WT and -LSA showed Smad2-pCS signal after 20 minutes of AA stimulation (*Fig 4.2F lanes 1 and 5*). However, at latter time points, Smad2-pCS signal was undetectable in Smad2-WT while Smad2-LSA maintained the pCS signal (*Fig 4.2F lanes 2-4 and 6-8*). Furthermore, quantification of Smad2-pCS against total Smad2 proteins as indicated by Flag signal, showed that decline of Smad2-pCS signal in Smad2-LSA was significantly slower than Smad2-WT (*Fig 4.2G*). These results confirm that absence of pLS in Smad2-LSA prolong the half-life of activated Smad2.

Next, to examine the subcellular localisation of these events, Smad2-null HEK293T cells stably transfected with Smad2-WT or -LSA were treated as shown in the treatment scheme (*Fig 4.2E*). The cells were then fixed at 0- and 30-minutes time points and immunostained with anti-Flag antibody to show the subcellular localisation of transgenic Smad2-WT and -LSA (*Fig 4.2H*). These results, as indicated by Flag signal, showed that although both Smad2-WT and -LSA are similarly localised in the nuclear and peri-nuclear region 20 minutes after transient AA stimulation, by 30 minutes of inhibiting receptor activity, Smad2-WT levels diminished in the nucleus while Smad2-LSA still showed robust nuclear Flag staining. Taken together, these results suggest presence of more Smad2 in the nucleus when Smad2-LS is unphosphorylated, after prior agonist stimulation.

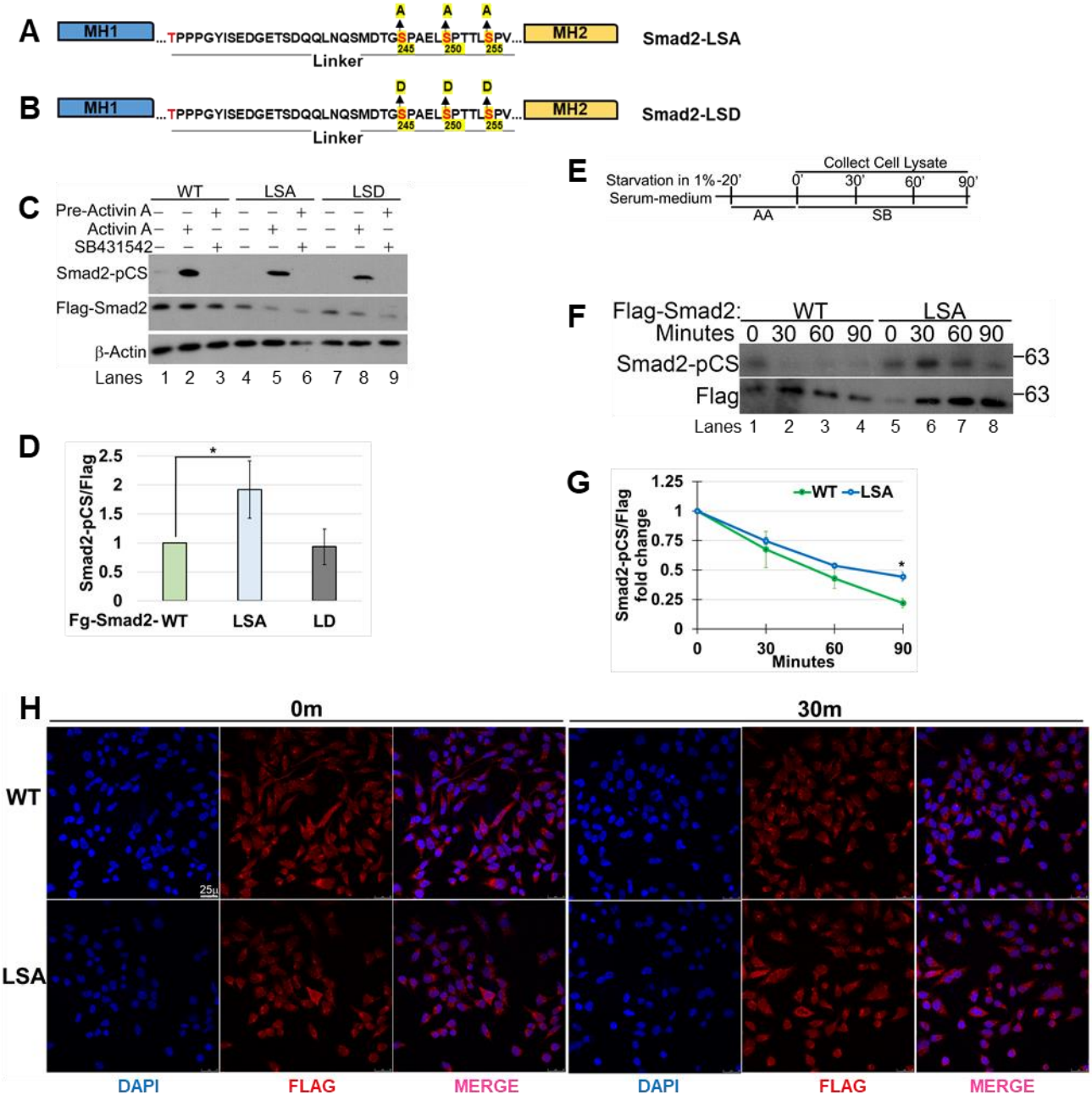

Figure 4.2: Role of Smad2-pLS in activated Smad2 dephosphorylation

A) Schematic depiction of the site-directed mutagenesis (SDM) in Smad2-LSA linker to eliminate the three phosphorylatable serine residues. Position of the residues are indicated. **B)** Schematic depiction of the SDM in Smad2-LSD linker to make the three serine residues constitutively phosphorylated. **C)** Representative immunoblot of Smad2-pCS in Smad2-null HEK293T cells transfected with Flag-Smad2-WT, -LSA, and –LSD cultured in 1% serum-medium overnight and stimulated with activin A for 6 hours. **D)** Quantification of Smad2-pCS in C, using means±s.d. densitometric measurements, normalised to Flag levels (n=4). **E)** Scheme of treatment for F. **F)** Representative immunoblot of Smad2-pCS in Smad2-null HEK293T cells stably expressing Flag-Smad2-WT or -LSA, treated as illustrated in E. **G)** Quantification of Smad2-pCS in F, using means±s.d. densitometric measurements, normalised to Flag levels (n=3). **H)** Smad2-null HEK293T cells stably expressing Flag-Smad2-WT or -LSA, treated as illustrated in E (only 30 minutes representative image shown), were fixed and analysed by immunofluorescence (IF) with anti-Flag and DAPI for nuclei staining. Scale bar- 25µm. For all statistical analysis, student t-test was done and '*' indicates $p<0.05$.

4.2.3 Smad2 has elevated transcriptional activity in the absence of pLS in hESCs

In the previous sections, it was shown that absence of Smad2-pLS significantly increased the duration of TGF-β signalling by limiting the rate of degradation of activated Smad2. I questioned if the sustained nuclear presence of activated Smad2 induced by FVP also improves its transcriptional activity. Since activin/nodal signalling play a crucial role in maintaining hESC pluripotency, *in vivo* specification of definitive endoderm (DE) during early embryonic development, as well as *in vitro* DE differentiation (Vincent et al., 2003, Vallier et al., 2005), I used hESCs to assess whether changes in Smad2 transcriptional activity influenced the mesendodermal markers such as Brachyury, MixL1, Eomes, and Goosecoid (Teo et al., 2011). Therefore, I stimulated H1 hESCs with AA in the presence or absence of FVP for 6 hours and performed an RT-qPCR using cDNA prepared from the samples (*Fig 4.3A*). Analysis of mRNA expression revealed that FVP-treated cells had much lower target gene expression than the non-FVP-treated cells (*Fig 4.3A*), contradictory to my expectation. However, it is not surprising that FVP reduced gene expression as it inhibits all CDKs including the transcription CDKs7/8/9, thereby downregulating global gene expression (Shapiro, 2004, Chen et al., 2005). Therefore, inhibition of transcription machinery by FVP may very likely account for lower mesendodermal gene expression despite AA induction.

To overcome the limitation of using FVP for gene expression analysis, I decided to investigate Smad2 transcription with or without Smad2-pLS by using Smad2 expression vectors-Smad2-LSA and -WT. I used dual luciferase reporter system in which luciferase expression was controlled by twelve repeated CAGA Smad binding elements (SBE) and renilla was used as control to account for variable transfection efficiencies (*Fig 4.3B*). hESCs were transiently transfected with Smad2-WT or -LSA along with luciferase and renilla expression vectors for 24 hours before blocking any TGF-β/activin signalling using receptor blocker, SB for 2 hours. This was followed by stimulation with AA for 20 hours or continued inhibition of receptor kinase using SB as control. The experiment revealed that AA-stimulated hESCs expressing Smad2-LSA had a significantly higher luciferase activity in contrast to both

stimulated Smad2-WT-expressing cells and unstimulated Smad2-LSA-expressing cells (*Fig 4.3B*). Taken together, these results suggest that Smad2-LSA has higher transcriptional activity than Smad2-WT upon stimulation by AA, on account of its sustained nuclear presence. Since CAGA SBE site is more specific to Smad3 activity, a similar experiment with Smad2 activity-specific gene Pitx2 will help in properly ascertaining role of Smad2-pLS in Smad2 transcriptional activity.

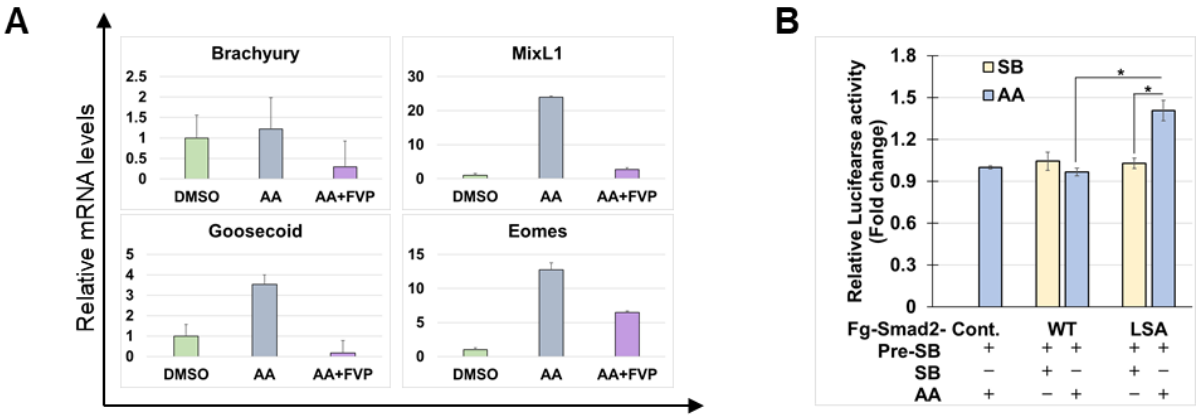

Figure 4.3: Effect of flavopiridol and Smad2-pLS on Smad2 transcriptional activity in H1 hESCs

A) RT-qPCR analysis of mRNA expression of indicated mesendodermal markers in H1 hESCs treated with activin A and flavopiridol or dmso (control) for 6 hours in RPMI/B27 medium after washing off MEF-CM. Data represent means±s.d. of measurements from three independent experiments. **B)** Luciferase assay in H1 hESCs co-transfected with pGL3-$CAGA_{12}$.Luc and renilla constructs along with either Smad2-WT or Smad2-LSA or empty control vector and pre-treated with SB431542 for 2 hours before stimulating with activin A for 20 hours in MEF-CM. Data show means±s.d. of measurements from three independent transfection experiments. Student t-test was done and '*' indicates $p<0.05$.

4.2.4 Smad2 has elevated transcriptional activity without pLS in mESCs

In the previous section, results from luciferase assay in hESCs expressing either Smad2-WT or Smad2-LSA showed upregulated transcriptional activity by the Smad2-LSA protein. In the experiment, H1 hESCs were pre-treated with SB to block activin signalling and Smad2/3 activation before further stimulation with AA. However, activin signalling is essential for maintaining hESC pluripotency factors such as Oct4 and Nanog (Vallier et al., 2004). By contrast, high activin signalling is also required for endoderm differentiation in hESCs (Arnold and Robertson, 2009). So, the experimental setup could easily disrupt hESC self-renewal and their pluripotency. Moreover, endogenous Smad2 activity was intact in these H1 hESCs, which may easily interfere with the activity of transfected Smad2-WT/LSA proteins. Therefore, another similar experiment was done in mESCs in which Smad2 gene was disrupted. Activin signalling is not necessary for self-renewal and maintaining pluripotency in *in vitro* cultures of mESCs (Pauklin and Vallier, 2015, Gaarenstroom and Hill, 2014) and hence, using Smad2-null mESCs presents a better alternative than hESCs to test the transcriptional activity of Smad2-WT and Smad2-LSA proteins without negatively affecting mESC pluripotency.

An immunoblot analysis was performed to check the absence of endogenous Smad2 expression in Smad2-null mESCs (*Fig 4.4A*). Next, Smad2-null mESCs were transiently transfected with either Smad2-WT or Smad2-LSA along with dual luciferase reporter system in which luciferase expression was controlled by twelve repeated CAGA SBE and renilla for 24 hours. The cells were pre-treated with SB to block receptor kinase activity for 2 hours before stimulating with AA for 20 hours or continued inhibition of receptor kinase using SB as control. The experiment showed that AA-stimulated Smad2-null mESCs expressing Smad2-LSA had significantly higher luciferase activity in comparison to both stimulated Smad2-WT-expressing cells and unstimulated Smad2-LSA-expressing cells (*Fig 4.4B*). These results are consistent with the effects of absence of pLS on Smad2 transcription in hESCs and confirm that Smad2-LSA has higher transcriptional activity than Smad2-WT upon stimulation by AA, also in mESCs.

As such, activin/nodal signalling is required for the maintenance of pluripotency in the mouse embryo and in *in vivo* DE specification (Gaarenstroom and Hill, 2014). For *in vitro* mESC cultures, it is required only at a low level to maintain pluripotency but require high activin signalling for mESC differentiation to mesendodermal lineages, similar to hESCs (Gaarenstroom and Hill, 2014, Pauklin and Vallier, 2015). Furthermore, since embryoid bodies (EBs) generated from mESCs present a powerful tool to study lineage specification and offer a model to test gene function in early embryonic development and differentiation, I utilised mESCs-derived EBs in studying the transcriptional activities of Smad2-WT and Smad2-LSA proteins in anterior definitive endoderm (ADE) differentiation. First, both WT mESCs and Smad2-null mESCs were grown in low attachment dish to encourage formation of EBs in the appropriate medium for 48 hours before withdrawing serum and applying high dosage of AA and fibroblast growth factor (FGF) for another 48 hours to promote EB differentiation towards ADE (*Fig 4.4C*). The image shown were taken on the fourth day of EB formation and ADE differentiation protocol in both cell types before collecting them to isolate RNA and prepare cDNA for analysing the expression of ADE markers such as Hex, Cer1, and Sox17 (Morrison et al., 2008). The results showed that EBs derived from Smad2-null cells had little Hex expression and no Cer1 and Sox17 expression in contrast to WT mESCs (*Fig 4.4D*). These results highlight the importance of Smad2-mediated activin signalling in ADE differentiation.

Next, I asked if Smad2-WT and Smad2-LSA proteins could rescue the impaired EB formation and ADE differentiation in Smad2-null mESCs and if there is a difference in their activities given that Smad2-LSA showed higher transcriptional activity in our earlier experiments. Smad2-null mESCs were transfected with either Smad2-WT or Smad2-LSA for 24 hours before subjecting to EB formation and ADE differentiation protocol, same as before. Images were taken on the fourth day of the protocol which showed that expression of Smad2-WT in Smad2-null mESCs could restore their proper EB formation, but Smad2-LSA formed fewer, smaller, and abnormal EBs for which quantification of EBs number and size would be an important data to add here (*Fig 4.4E*). Moreover, analysis of mRNA expression in these

EBs showed higher Smad2-WT transgene expression than Smad2-LSA (*Fig 4.4F left*). On the other hand, ADE marker, Hex expression was similar in both Smad2-WT and -LSA (*Fig 4.4F right*). Altogether, these results indicate the importance of Smad2 in mESC EB formation and ADE differentiation. Also, although Smad2-LSA has relatively lower mRNA expression than Smad2-WT (*Fig 4.4F left* panel), it induces similar Hex expression (*Fig 4.4F right* panel), suggesting that Smad2-LSA protein may have higher transcriptional activity than Smad2-WT protein. However, this experiment needs to be repeated and more ADE target genes need to be analysed before making final conclusions.

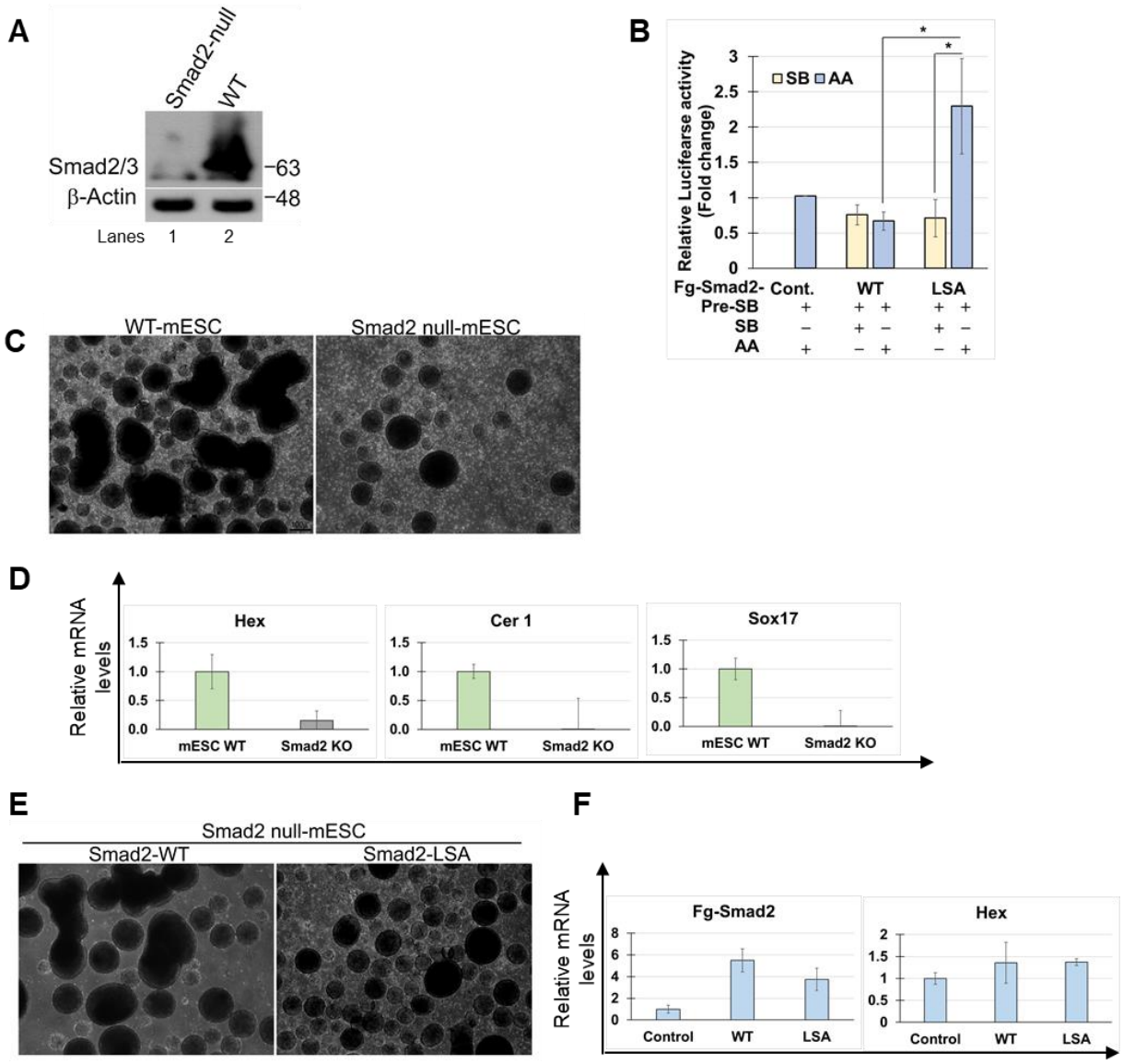

Figure 4.4: Effect of Smad2-pLS on Smad2 transcriptional activity in mESCs

A) Immunoblot analysis of Smad2/3 expression in Smad2-null and WT mESCs. **B)** Luciferase assay in Smad2-null mESCs co-transfected with pGL3-$CAGA_{12}$.Luc and renilla constructs along with either Smad2-WT or Smad2-LSA or empty control vector and pre-treated with SB431542 for 2 hours before stimulating with activin A for 20 hours in normal mESC culture conditions. Data show means±s.d. of nine measurements from three independent transfection experiments. Student t-test was done and '*' indicates $p<0.05$. **C)** Representative phase-contrast images of embryoid bodies (EBs) formed from WT- and Smad2-null mESCs and differentiated to anterior definitive endoderm (ADE) (n=3). **D)** RT-qPCR analysis of mRNA expression of indicated mesendodermal markers in EBs from C. Data represent means±s.d. of nine measurements from three independent experiments. **E)** Representative phase-contrast images of EBs formed from Smad2-null mESCs expressing Smad2-WT or Smad2-LSA and differentiated to ADE (n=3). **F)** RT-qPCR analysis of mRNA expression of Flag-Smad2 transgene and mesendodermal marker Hex, in EBs from E. Data represent means±s.d. of three measurements from one experiment.

4.3 Discussion and conclusion

In this chapter, I have shown that FVP-induced extension of activated Smad2 half-life may occur as a result of Smad2 evading its proteasomal degradation (*Fig 4.1*). Since FVP also inhibited Smad2-pLS, it was hypothesised that Smad2-pLS may interfere with Smad2 deactivation. So, further experiments done utilising Smad2 expression vectors with modified pLS confirmed that absence of pLS does indeed extend the half-life of activated Smad2 by slowing down its deactivation and resulting in its prolonged nuclear presence (*Fig 4.2*). Consequently, it resulted in higher transcriptional activity of Smad2 in the absence of pLS, as shown in both hESCs and mESCs (*Fig 4.3 and 4.4*).

4.3.1 Smad2-pLS plays a role in regulating activated Smad2 signals

Delayed deactivation of activated Smad2 in the absence of pLS could be attributed to various factors such as hindered interaction of Smad2 with the nuclear phosphatase(s) that target its C-terminal SxS motif or its evasion from the degradation mechanism. Previous studies have shown that activated Smad2 are consistently targeted for proteasomal degradation in order to terminate TGF-β signalling (Lo and Massague, 1999). Therefore, it is possible that inhibition of pLS may extend the activated Smad2 signal by avoiding its timely degradation. However, to robustly claim a role of degradation in preserving activated Smad2 in FVP-treated cells in Fig 4.1, a similar time-course experiment must be done in cells with the proteasome inhibited, expecting that both FVP-treated and proteasome-inhibited would show similar patterns of Smad2-pCS signals. Smad2-pLS is not essential in the binding of WW-HECT domain E3 ubiquitin ligases, Nedd4L and Smurf2, to the PPxY domain of activated Smad2/3, however, its presence does enhance Smad2/3 interaction with Nedd4L (Aragon et al., 2011, Gao et al., 2009). Studies show that the various WW domains of Nedd4L bind to PPxY domain located downstream of pLT as well as at the pLS residues (Aragon et al., 2011). Abrogation of pLS does not inhibit Nedd4L-Smad2/3 binding and subsequent Smad2/3 degradation, but as stated earlier, it does slightly diminish their interaction (Aragon et al., 2011, Gao et al., 2009). Furthermore, since Smurf2 functions similar to Nedd4L in ubiquitinating

Smad2 and priming its degradation (Tang et al., 2011, Aragon et al., 2011) and that Smurf2 is a predominantly nuclear protein, unlike Nedd4L (Kavsak et al., 2007, Kuratomi et al., 2005), it is plausible that Smurf2 has a larger involvement in eliminating activated Smad2/3 from the nucleus after their transcription activity ceases. Conversely, cytoplasmic localisation of Nedd4L suggests that it might be more responsible to attenuate TGF-β signalling rather than in terminating it by limiting the number of activated Smad2/3 that can translocate to the nucleus. Taken together, it suggests that if indeed activated Smad2 is degraded, in FVP-treated cells (*Fig 4.1H*), it might be attributable to Smurf2 activity. In addition, given that preventing activated Smad2/3 degradation, if so, clearly prolonged its nuclear presence, it hints towards the possibility that deactivation of activated Smad2/3 through degradation is a much more rapid process than dephosphorylation of their SxS motif.

Furthermore, since Smad2/3 activation maybe prolonged by evading its degradation, but that Smad2 did eventually lose its SxS motif phosphorylation, inhibiting pLS may also lead to additional Smad2 interactions with mediator proteins that may control recruitment of phosphatases such as PPM1A and PP5 to Smad2 SxS motif (Lin et al., 2006, Bruce et al., 2012). Possibly, suppression of pLS may enhance interaction between Smad2/3 and CLIC4, preserving activated Smad2 by protecting it from SxS motif phosphatases (Shukla et al., 2009) or pLS suppression may prevent Smad2 interaction with MAN1 that may further facilitate recruitment of PPM1A to dephosphorylate SxS motif (Bourgeois et al., 2013). Furthermore, preventing MAN1-Smad2 interaction may also result in increased Smad2 transcription because MAN1 competes with a transcription factor, FOXH1 (previously called FAST1) to bind to Smad2 and results in its dissociation from FOXH1, thus, diminishing Smad2 transcription (Attisano et al., 2001, Bourgeois et al., 2013). So, these combined interactions of Smad2 may account for its possible evasion from proteasomal degradation, decline in SxS motif dephosphorylation, and enhanced Smad2 transcription.

4.3.2 Role of Smad2-pLS in regulating functions of TGF-β signalling

Stabilised activation of Smad2 and its delayed deactivation may also augment its interaction with Smad4 within the functional oligomeric complex, thus, promoting its nuclear accumulation and transcription (Schmierer et al., 2008, Massague et al, 2005). In addition, absence of pLS in activated Smad2 may also enhance its interaction with proteins such as TAZ or the components of the transcription machinery (Varelas et al., 2008, Schmierer et al., 2008), further contributing to Smad2 nuclear accumulation and upregulated transcription. Nuclear presence of activated Smad2 is generally synonymous with its active transcription function, so, it is not surprising that pLS inhibition-mediated nuclear accumulation of activated Smad2 also improved its transcriptional activity in hESCs and mESCs (*Fig 4.3 and 4.4*). It also highlights the important role of Smad2-pLS in controlling its agonist-induced transcriptional activity. Further experiments are required to determine Smad2 interaction with Smad4 and other nuclear proteins in the absence of pLS by applying techniques such as proximate ligation assay (PLA), immunostaining, and co-immunoprecipitation that can identify the underpinnings of precisely how activated Smad2 degradation is prevented in the absence of Smad2-pLS.

In addition, the results in this chapter showing increased agonist-induced Smad2 transcriptional activity upon inhibition of pLS by mutating LS to LA are consistent with the earlier studies that inhibiting pLS by overexpressing small c-terminal phosphatases (SCPs) maximises Smad2 transcriptional activation (Sapkota et al., 2006, Wrighton et al., 2006). Moreover, given that pLS is important in regulating timing and competency to respond to activin signalling during *Xenopus* development (Grimm and Gurdon, 2002), demonstration of similar effect of pLS mutation in hESCs and mESCs indicates the importance of non-canonical Smad signalling in regulating canonical TGF-β signalling in mammalian systems as well.

Also, as described before, there is a specific sequence of linker phosphorylation in Smad3 (and likely similar in Smad2) that occurs upon TGF-β activation, i.e., firstly, threonine and the second and third serine residues are phosphorylated by various kinases like MAPKs and CDK8/9 to allow binding with Pin1 and permit maximum transcription, followed by

phosphorylation of the first linker serine by GSK3β, ceasing Smad2/3-Pin1 binding and switching its action from transcription to deactivation via binding to WW domain E3 ubiquitin ligases which eventually, prime it for degradation (Aragon et al., 2011, Massague, 2012). At the same time, SCPs remove Smad2-pLS, but not pLT, to ensure peak transcriptional activation of Smad2/3 (Wrighton et al., 2006, Sapkota et al., 2006). Combining the findings from these two studies, it appears that inhibiting the phosphorylation of the first linker serine must play a much more crucial role in enhancing Smad2 transcription and warrants further investigation.

Moreover, while investigating the effects of absence of pLS in mESC EBs ADE differentiation, cells overexpressing Smad2-LSA could only generate smaller EBs. It could be explained by prolonged Smad2-LSA activity upon agonist stimulation (*Fig 4.1 and 4.2*), which extends the duration and intensity of activin signalling (*Fig 4.3B and 4.4A*). TGF-β/activin signalling generally have an anti-proliferative effect in normal cells which may account for the limited size of EBs in Smad2-LSA transfected cells. Although, in these Smad2-null mESCs, endogenous Smad3 could also respond to AA stimulation, I believe that it has not interfered with my results and affected data interpretation as Smad2/3 have distinct roles in gene expression regulation and also, Smad3 is unable to rescue developmental phenotype of mice lacking Smad2 expression (Tremblay et al., 2008, Aragon et al., 2019, Liu et al., 2016). Moreover, since EB differentiation to ADE in Smad2-LSA expressing Smad2-null mESCs were impaired despite similar Hex expression as in Smad2-WT-expressing cells, these results suggest that it may be necessary to maintain the right balance of linker phosphorylation during the events of early embryonic development in the absence of which mesendoderm differentiation may be impaired, highlighting the importance of non-canonical Smad signalling in embryonic development.

Chapter 5

Results

Role of Smad2-pLS in maintaining Smad2 stability and turnover

5.1 Introduction

Activation of TGF-β signalling initiates multiple negative feedback mechanisms to regulate its signal intensity, duration, and specificity. It could be regulated through feedback from gene products of Smad transcription or via post-translational modifications (PTMs) that could operate at levels of ligands, receptors, Smads, as well as their transcription (Xu et al., 2016, Tzavlaki and Moustakas, 2020). Given that, Smad2/3 proteins are downstream signal transducers of TGF-β signalling, regulating their activity would effectively modulate TGF-β signalling. Smad2/3 are subjected to extensive PTMs such as phosphorylation, ubiquitylation, sumoylation, acetylation, etc. that stringently control their activity by altering their protein interactions, transcriptional activity, protein stabilisation, and degradation (Xu et al., 2016). Smad2/3 linker region is a hotspot for such PTMs, especially phosphorylation as it is enriched with several phosphorylatable threonine and serine amino acids that are substrates of a wide range of kinases such as PI3K/mTORC2, GSK3β, Erk1/2, JNK, p38, CDKs, NLK, CaMKII, ROCK etc. Increasing studies highlight the importance of linker phosphorylation in regulating TGF-β signalling (Kretzschmar et al., 1999, Wicks et al., 2000, Funaba et al., 2002, Mori et al., 2004, Matsuura et al., 2004, Kamaraju and Roberts, 2005, Yoshida et al., 2005, Matsuura et al., 2005, Millet et al., 2009, Alarcon et al., 2009, Burch et al., 2010, Hough et al., 2012, Yu et al., 2015, Liang et al., 2021).

Smad2/3 linker phosphorylation via Erk1/2 and CDK8/9 prevent their nuclear translocation and transcriptional activity upon TGF-β activation (Kretzschmar et al., 1999, Hough et al., 2012, Matsuura et al., 2005, Alarcon et al., 2009, Chapter 4). In addition, GSK3β- and CDK8/9-induced linker serine phosphorylation (pLS) promotes binding of WW-HECT domain-containing E3 ubiquitin ligases such as Nedd4L and Smurf2, that recognise linker threonine phosphorylation (pLT) and bind to the PPxY motif downstream of pLT and eventually, prime Smad2/3 for proteasomal degradation (Millet et al., 2009, Aragon et al, 2011). These findings have established firm association between linker phosphorylation events and Smad2/3 ubiquitination-mediated proteasomal degradation. As yet, Nedd4L and Smurf2 are the only

known E3 ubiquitin ligases that degrade Smad2/3 by acting on Smad2/3 agonist-induced linker phosphorylation (ALP) (Gao et al., 2009, Lin et al., 2000, Zhang et al., 2001, Aragon et al., 2011). However, Smad2/3 degradation by Nedd4L and Smurf2 appear to be quite limited and only acts on activated Smad2/3 and does not exhibit much difference in total Smad2/3 protein levels. Additionally, there are several RING domain E3 ubiquitin ligases as well that negatively regulate TGF-β signalling by mediating activated Smad2/3 degradation. Instead of acting on Smad2/3-ALP, RING E3 ubiquitin ligases degrade activated Smad2/3 via their associations with other negative regulators of TGF-β signalling. For example, Tiul1 associates with Smad7 (Seo et al., 2004), Arkadia with co-repressors SKI/SKIL (Mavrakis et al., 2007), and ROC1-SCF^{Fbw1a} with the co-activator p300 (Fukuchi et al., 2017), to degrade activated Smad2/3. CHIP is another RING E3 ubiquitin ligase that can promote ubiquitin-mediated Smad3 degradation even in its inactivated form (Xin et al., 2005).

Interestingly, our laboratory previously showed that prolonged inhibition of CDKs by FVP in AA-pre-stimulated hESCs not only suppressed Smad2 linker serine phosphorylation (Smad2-pLS) but also caused considerable decrease in total Smad2 protein levels several hours after disappearance of activated Smad2 (*Fig 1.9B*) (Yu et al., 2015). However, the underlying mechanisms remain largely unknown. In this chapter, I sought to verify whether prolonged FVP treatment indeed reduced Smad2 protein level in hESCs (Yu et al., 2015) and if this observation holds true for other cell types as well. I also asked if this reduction in Smad2 protein is attributable to its degradation, and if there is a link between Smad2-pLS and Smad2 stability and turnover.

5.2 Results

5.2.1 Prolonged FVP or LY treatment following pre-activation of Smad2/3 diminishes their protein levels

H1 hESCs were stimulated with AA for 20 minutes after washing out MEF-CM with PBS and applying RPMI/B27 medium, then, AA was removed and washed out by PBS followed by application of SB431542 (SB) to block receptor activity (hereafter simply referred to as 'transient stimulation or pre-stimulation' unless otherwise stated). The cells were then collected at indicated time points for further analysis (*Fig 5.1A*). As shown before, Smad2/3 activation signal (Smad2-pCS) was undetectable 1 hour after removal of agonist and application of SB regardless of FVP application (*Fig 5.1B*). While pLT was mostly unaffected, Smad2-pLS signal exhibited clear reduction in FVP-treated cells compared with controls at 1-hour of FVP treatment (*Fig 5.1B lanes 3, 4, and 6*). FVP treatment might also have induced slight reduction in total Smad2/3 proteins (*Fig 5.1B lanes 3 and 6*). By 6 hours of FVP treatment, Smad2-pLS was still suppressed in FVP-treated cells, while pLT was rather high in FVP-treated cells than the controls (*Fig 5.1B lane 12*). More interestingly, FVP-treated cells exhibited considerably lower expression of total Smad2/3 proteins than the control (*Fig 5.1B lane 12*), which is statistically significant reduction in multiple repeat experiments (*Fig 5.1C*). In fact, application of FVP to hESCs that were not pre-stimulated by the agonist also resulted in small but significant decrease in the total Smad2/3 proteins (*Fig 5.1B lane 9 and 5.1C*). When additional SB was applied to block endogenous ligand stimulation, FVP resulted in even more considerable reduction in total Smad2/3 protein levels (*Fig 5.1C*). Nonetheless, combined FVP and SB treatment on pre-stimulated hESCs induced the maximum reduction of Smad2/3 proteins (*Fig 5.1B lane 12 and 5.1C*). These results indicate that the mechanism involved in reducing Smad2/3 protein levels by FVP may be influenced by agonist stimulation and requires further investigation.

To verify whether FVP-mediated reduction in Smad2/3 proteins is not cell type-specific, PC3 cells were treated the same as hESCs after overnight serum-starvation and as shown in

the treatment scheme (*Fig 5.1A*). The results were similar to that in hESCs and treatment with FVP not only maintained Smad2-pLS suppression throughout (*Fig 5.1D lanes 3, 6, 9, and 12*) but also dramatically reduced both Smad2 and Smad3 expression after 6 hours (*Fig 5.1D lanes 9 and 12*). Moreover, FVP had similar effect on PC3 cells to hESCs in slightly elevating Smad2-pLT levels after agonist pre-stimulation (*Fig 5.1D lane 12*). Furthermore, quantification of total Smad2/3 proteins against the loading control also showed a significantly lowered Smad2/3 expression upon prolonged application of FVP (*Fig 5.1E*). Also, FVP induced variable degree of reduction in Smad2/3 levels depending on Smad2/3 activation status as dictated by ligand availability and receptor activation, similar to hESCs (*Fig 5.1E*). Since closely associated Smad4 protein as well as loading control β-actin expression did not change on FVP treatment, it appears to be an effect specifically on Smad2/3 proteins (*Fig 5.1D and E*). Similar effect of FVP treatment on total Smad2/3 proteins was also observed in HEK293T cells (*Fig A-II lane 6*). Altogether, these results indicate that prolonged FVP treatment in agonist-pre-stimulated cells specifically, significantly diminishes Smad2/3 protein expression.

Next, I addressed whether the reduction in the Smad2 proteins is indeed associated with the inhibition of CDKs by FVP. For this, I used the CDK8/9 inhibitor, LY2857785 (LY) in PC3 cells as I did with FVP to study its effects on Smad2 protein (*Fig 5.1F*) (Yin et al., 2014). 1 hour of LY treatment on cells that were pre-stimulated by TGF-β showed slight reduction in Smad2-pLS compared with controls while Smad2-pLT as well as total Smad2 protein was clearly not affected (*Fig 5.1F lanes 3 and 6*). On the contrary, 6 hours of LY treatment almost completely abolished Smad2-pLS signals while pLT was still not much affected (*Fig 5.1F lane 12*). However, the total Smad2/3 proteins showed considerably lower expression in LY-treated cells than the non-treated controls (*Fig 5.1F lane 12*), similar to that detected in cells with FVP treatment. These results show that prolonged application of LY to the pre-agonist stimulated cells reduces Smad2/3 protein expression and that this reduction is likely attributable to the inhibition of CDK8/9, which suppress Smad2-pLS and also likely Smad3-pLS.

Finally, I asked how FVP induced changes in Smad2/3 protein expression in the subcellular compartments. To address this, cytoplasmic and nuclear fractions were separated from the PC3 cells that were treated for 6 hours as shown in the treatment scheme (*Fig 5.1A*). In the cytosol, application of FVP for 6 hours resulted in undetectable Smad2-pLS signal compared with the control cells (*Fig 5.1G lanes 1-3*), while there was almost no detectable Smad2-pLS signal in the nucleus regardless of FVP application (*Fig 5.1G lanes 4-6*). The Smad2/3-pLT signals revealed only subtle reduction with FVP treatment in the cytosol or the nucleus, which might be due to reduced total Smad2/3 protein levels (*Fig 5.1G lanes 3 and 6*). Notably, FVP treatment reduced the Smad3 protein levels in both cytosol and nucleus (*Fig 5.1G lanes 3 and 6*). Interestingly, Smad2 protein could be detected only in the cytoplasmic fraction, while Smad3 protein could be visible in both the cell fractions (*Fig 5.1G*). Together, these results suggest that FVP-induced reduction in Smad2/3 proteins may occur in both cytoplasm and nucleus. More importantly, since FVP suppressed Smad2-pLS and also negatively affected Smad2 levels, it also suggests a possible link between Smad2-pLS and Smad2 activity. Also, of note, in the absence of agonist stimulation, Smad2 is more strictly localised in the cytoplasm whereas, Smad3 is nearly equally distributed in both cytoplasm and nucleus.

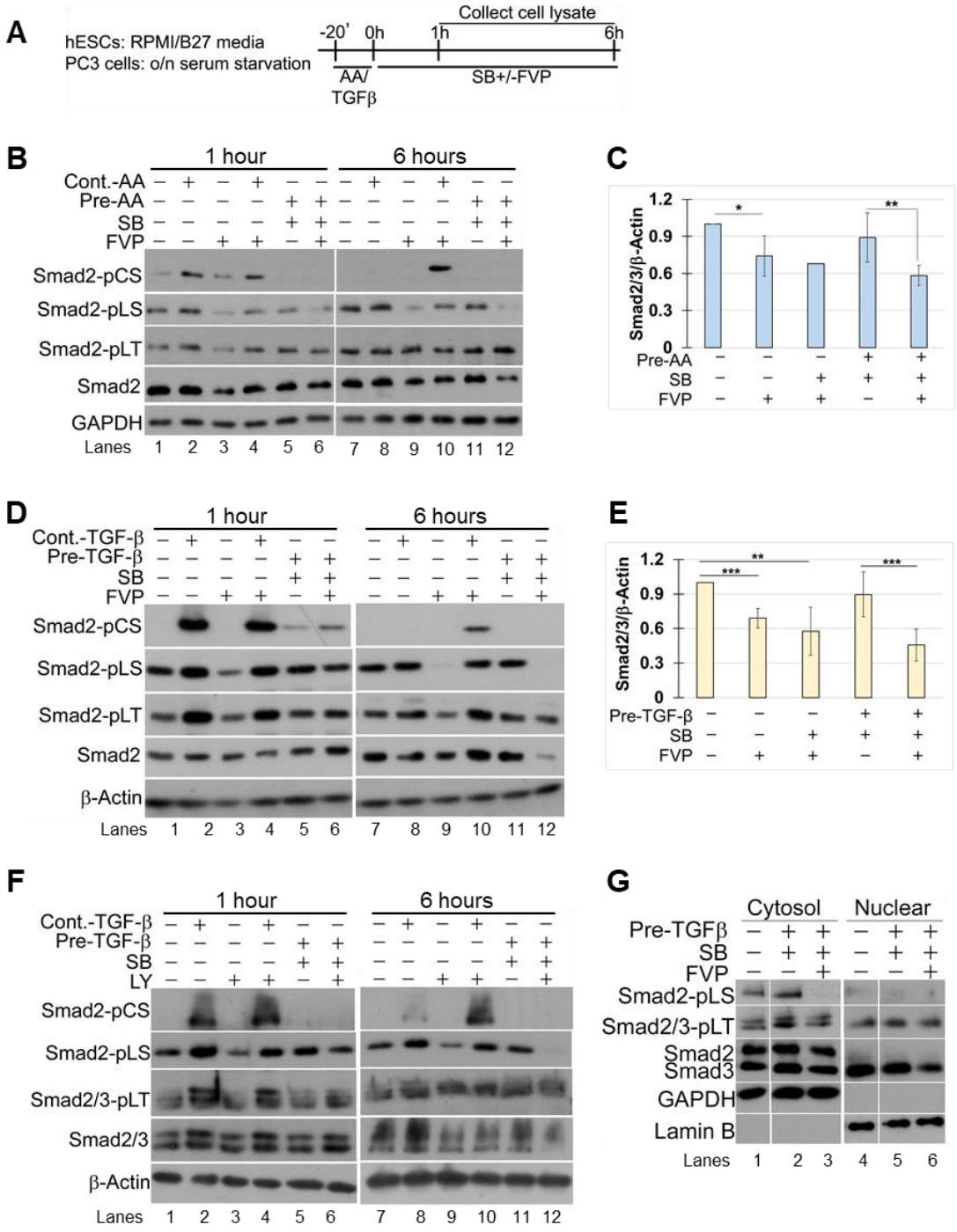

Figure 5.1: Flavopiridol or LY2857785 treatments result in reduced Smad2/3 proteins
A) Scheme of treatment for B, D, F, and G. **B)** Representative immunoblot of H1 hESCs treated as illustrated in A, with antibodies against the indicated proteins. **C)** Quantification of Smad2/3 at 6 hours of FVP treatment as indicated in H1 hESCs, using means±s.d. densitometric measurements, normalised to loading control (n=5). **D)** Representative immunoblot of PC3 cells treated as illustrated in A, with antibodies against the indicated proteins. **E)** Quantification of Smad2/3 at 6 hours of FVP treatment as indicated in PC3 cells, using means±s.d. densitometric measurements, normalised to loading control (n=7). **F)** Representative immunoblot of PC3 cells treated as illustrated in A but with LY2857785 (LY) instead of flavopiridol (FVP), with antibodies against the indicated proteins. **G)** Representative immunoblot of cytoplasmic and nuclear fractions of PC3 cells treated as illustrated in A for 6 hours, with antibodies against the indicated proteins. All experiments in F and G have been done at least 3 times. Targets of inhibitors used are: Flavopiridol- CDK2/4/6/7/8/9, LY2857785- CDK8/9, SB431542-ALK4/5/7. Student t-test was done and '*', '**', and '***' indicate $p<0.05$, 0.01, and 0.001, respectively.

5.2.2 Proteasome-degradation pathway accounts for FVP-mediated reduction in Smad2/3 proteins

Experiments in the previous section established that prolonged application of CDK8/9 inhibitors, FVP and LY results in reduction in Smad2/3 proteins. CDK8/9 are known to be involved in the RNA-polymerase II (RNAP-II) transcriptome activity and their inhibition could hinder the transcription machinery, and then subsequently reduce the protein levels (Shapiro, 2004, Chen et al., 2005). However, our data also showed that FVP treatment reduced only Smad2/3 expression without affecting other proteins like Smad4, β-Actin, GAPDH, and Lamin B (*Fig 5.1*). Therefore, it is unlikely that it is due to the effects of FVP/LY on the transcriptome. Alternatively, FVP/LY treatment in cells could result in Smad2/3 protein degradation and therefore, the decrease in Smad2/3 levels. To check if FVP diminishes Smad2/3 proteins by affecting its protein stability, serum-starved PC3 cells were pre-stimulated with TGF-β, followed by treatment with FVP in conjunction with 26S proteasome inhibitor MG132 or lysosome inhibitor chloroquine (CQ) as shown in the treatment scheme (*Fig 5.2A*). Consistent with the previous observations, FVP-treatment resulted in reduction of Smad2/3 protein levels (*Fig 5.2B lane 2*). This reduction could be abolished in the presence of MG132 (*Fig 5.2B lane 3*) whereas CQ failed to rescue Smad2/3 proteins (*Fig 5.2B lane 4*). This indicates that FVP-induced Smad2/3 reduction is attributed to their proteasomal degradation.

Next, to eliminate possible interference from synthesis of new proteins, a potent protein biosynthesis inhibitor- cycloheximide (Chx) was used in combination with MG132 and cells were treated as shown in the treatment scheme (*Fig 5.2C*). Like before, FVP treatment showed reduced Smad2/3 expression (*Fig 5.2D lane 3*) and as expected, MG132 recovered Smad2/3 expression whether the cells were treated with FVP or not (*Fig 5.2D lanes 2 and 4*). Furthermore, quantification of total Smad2/3 proteins against β-Actin also showed significant reduction in Smad2/3 expression upon FVP treatment as well as a significant increase in their levels upon inhibiting the proteasome (*Fig 5.1D*), showing that MG132 rescued Smad2/3 degradation in FVP-treated cells and that this recovery is not influenced by synthesis of new

proteins. To further investigate whether reduction of Smad2/3 in hESCs (*Fig 5.1B and C*) is also because of their proteasomal degradation, similar experiment was done in H1 hESCs (*Fig 5.2E*). hESCs were treated as shown in the treatment scheme (*Fig 5.2C*). In hESCs as well, applying FVP reduced Smad2/3 proteins (*Fig 5.2E lane 3*), and their expression was clearly recovered on inhibiting the proteasome by MG132 (*Fig 5.2E lane 4*). Overall, these results show that FVP-mediated reduction in Smad2/3 proteins may occur as a result of their proteasomal degradation. However, additional experiments are needed to study the time-course changes in Smad2/3 protein levels while synthesis of new proteins is inhibited. This will enable us to distinguish between Smad2/3 degradation caused by FVP treatment and normal constitutive Smad2/3 turnover in the cells.

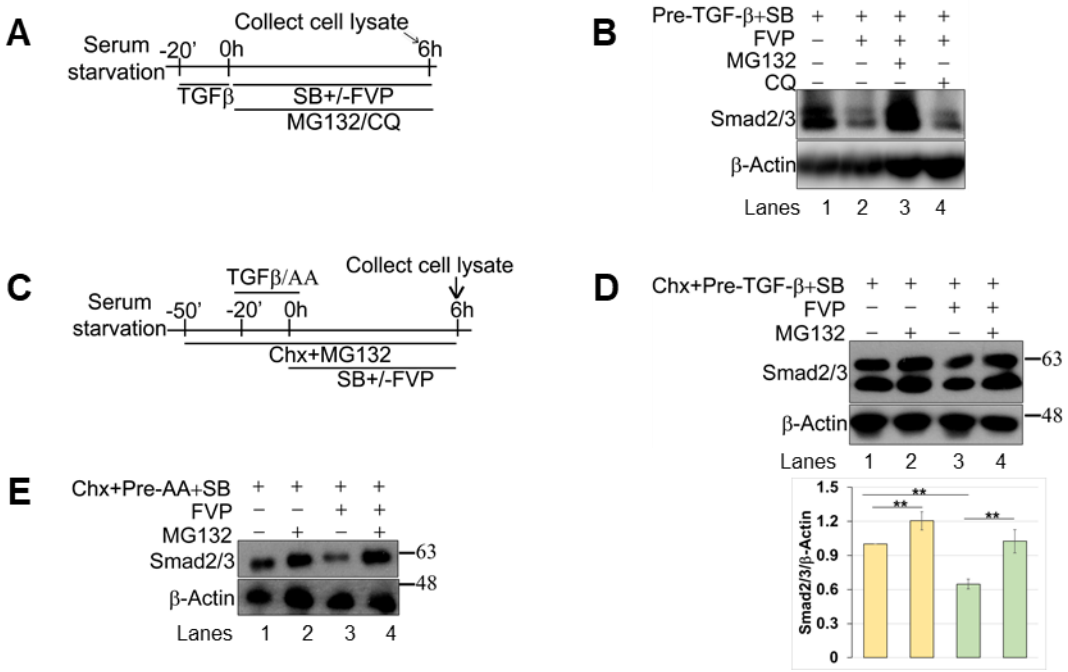

Figure 5.2: Proteasomal degradation results in flavopiridol-induced reduction of Smad2/3 proteins

A) Scheme of treatment for B. **B)** Representative immunoblot of PC3 cells treated as illustrated in A, with anti-Smad2/3 (n=1). **C)** Scheme of treatment for D and E. **D)** Representative immunoblot of PC3 cells treated as illustrated in C, with anti-Smad2/3 (top). Quantification of Smad2/3, using means±s.d. densitometric measurements, normalised to β-Actin (n=3). Student t-test was done and '**' and '***' indicate p<0.01 and 0.001, respectively (bottom). **E)** Representative immunoblot of H1 hESCs treated as illustrated in C, with anti-Smad2/3 (n=1).

5.2.3 FVP-induced Smad2/3 degradation is independent of Nedd4L

Experiments in the earlier section established the role of proteasome in mediating Smad2/3 degradation upon prolonged FVP treatment. Furthermore, FVP also maintained Smad2-pLS suppression, indicating the possibility of Smad2-pLS in affecting Smad2 stability and protein degradation. Since Nedd4L has been reported to act as an E3 ubiquitin ligase in mediating Smad2/3 degradation via the ubiquitin-proteasome system (UPS) and its function is regulated by the phosphorylation status of the linker region of Smad2/3 (Gao et al., 2009, Aragon et al., 2011), I sought to ask if Nedd4L is involved in FVP-induced Smad2/3 degradation. Since Nedd4L is a cytosolic protein (Gao et al., 2009, Emanuelli et al., 2019), I thought that by studying the subcellular localisation of Smad2/3 degradation, it may be possible to discern if Nedd4L might be involved in this process.

Cytoplasmic and nuclear fractions were separated in PC3 cells that were treated the same as shown in the treatment scheme (*Fig 5.2C*). In the cytosol, FVP treatment reduced Smad2-pLS but did not affect Smad2-pLT as also shown before (*Fig 5.3A lane 3*) and this reduction in Smad2-pLS was recovered by MG132 (*Fig 5.3A lane 4*). Similarly, total Smad2/3 proteins were also recovered by MG132 in FVP-treated and non-treated cells (*Fig 5.3A lanes 2 and 4*), albeit relatively higher recovery occurred in FVP-treated cells. These data correspond with the results shown in Fig 5.2, indicating that FVP-induced reduction of Smad2 may result from proteosome-mediated degradation. Furthermore, in the nucleus, Smad2-pLS and -pLT were almost undetectable but Smad3-pLT was sufficiently recovered upon MG132 treatment, in both FVP-treated and non-treated cells (*Fig 5.3A lanes 6 and 8*). More importantly, FVP treatment showed reduced nuclear Smad3 protein (*Fig 5.3A lane 8*), while application of MG132 recovered it in both FVP-treated and non-treated cells (*Fig 5.3A lanes 6 and 8*), although to a lower extent in FVP-treated cells. Taken together the higher degree of recovery of Smad2/3 proteins from FVP-induced degradation by applying MG132 in the cytoplasm, hints towards cytoplasmic degradation of Smad2/3 upon FVP treatment, and possibly involvement of a cytoplasmic E3 ubiquitin ligase such as, Nedd4L.

To investigate whether Nedd4L is involved in FVP-induced Smad2/3 degradation, I used PC3 cells previously generated in our lab, in which Nedd4L expression is inhibited by stably expressing shRNA-Nedd4L resulting in Nedd4L knockdown (Nedd4L-KD). Also, stably expressing shRNA-GFP PC3 cells were used as control. Both control and Nedd4L-KD cells were serum-starved and subjected to FVP treatment for 6 hours after transient TGF-β treatment as indicated in the treatment scheme (*Fig 5.1A*). As expected, Nedd4L expression was considerably lower in Nedd4L-KD cells than in controls (*Fig 5.3B lanes 1-3 vs 4-6*) and FVP treatment inhibited Smad2-pLS in both control and KD cells (*Fig 5.3B lanes 3 and 6*). Notably, Smad2/3 protein levels also decreased in Nedd4L-KD cells when subjected to FVP (*Fig 5.3B lane 6*), contrary to my expectation that absence of Nedd4L would rescue Smad2/3 degradation. Moreover, the extent of Smad2/3 reduction in Nedd4L-KD cells was slightly higher than in the control cells (*Fig 5.3C*). These results demonstrate that FVP-mediated Smad2/3 degradation is unlikely to be carried out through Nedd4L and indicate that other E3 ubiquitin ligases may be involved, requiring further investigation in the future.

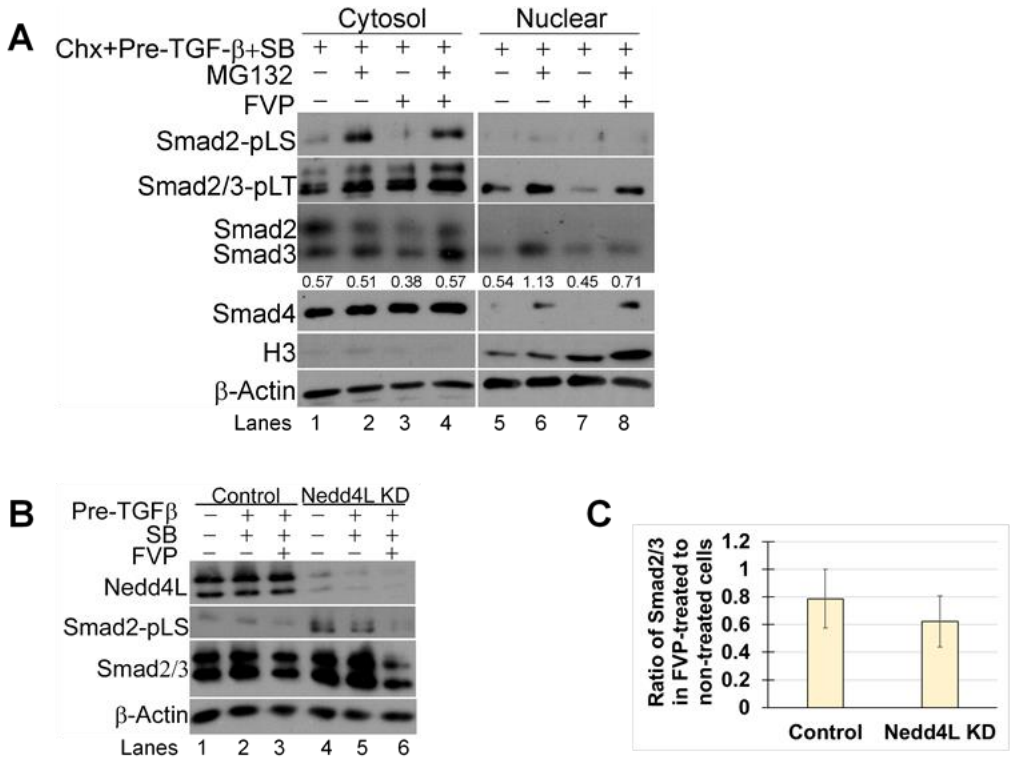

Figure 5.3: Role of Nedd4L in regulating Smad2/3 degradation

A) Representative immunoblot of cytoplasmic and nuclear fractions of PC3 cells treated as illustrated in 5.2C, with antibodies against the indicated proteins. Numbers indicate densitometric measurements of Smad2/3 normalised to β-Actin (n=1). **B)** Representative immunoblot of PC3 cells with stable shRNA for GFP as control (left panel) and for Nedd4L (right panel), both treated as illustrated in 5.1A, with antibodies against the indicated proteins. **C)** Analysis of ratio of total Smad2/3 protein levels in flavopiridol-treated cells versus non-treated cells in control and Nedd4L-KD cells in B. Quantification of Smad2/3 was done using means±s.d. densitometric measurements, normalised to β-Actin (n=4).

5.2.4 Role of pLS in Smad2 stability

Given that prolonged exposure to FVP/LY results in Smad2 degradation in PC3 cells, HEK293T cells, and H1 hESCs and that FVP/LY suppress CDK8/9-mediated Smad2-pLS, it raises the question whether Smad2-pLS plays any role in regulating Smad2 protein stability. To address this question, I used Smad2 expression vectors described in chapter 4, in which Smad2-LS were either mutated to non-phosphorylatable Smad2-LSA or phospho-mimetic Smad2-LSD (*Fig 4.2, section 4.2.2*). In addition, I also used another Smad2 expression vector-Smad2-LVA, in which all S/T-P linker sites are unphosphorylatable (*Fig 5.4A*). To test if absence of Smad2-pLS destabilises Smad2 protein, Smad2-WT, -LSA, and -LSD were transiently transfected into PC3 cells for 24 hours, followed by overnight serum-starvation (*Fig 5.4B*). Immunoblot analysis showed that Smad2-LSA expression, as indicated by Flag signal, was lowest in comparison to Smad2-WT and -LSD (*Fig 5.4B*). Diminished Smad2-LSA expression suggests that absence of pLS does negatively affect Smad2 stability and turnover, consistent with the effects of FVP-mediated pLS inhibition. However, on close observation of PC3 cells transfected with Smad2-LSA construct, they exhibited a markedly high number of floating cells (*Fig 5.4C*). Trypan blue staining confirmed that those floating cells were not dead (data not shown). Likely, the cells were floating due to poor cell attachment caused by greater TGF-β activation, as I showed higher transcriptional activity of Smad2-LSA in the previous chapter. These observations made it difficult to distinguish if low Smad2-LSA expression is due to altered Smad2 stability or collection of cells with lower transfection rate for analysis. Moreover, presence of endogenous Smad2 in PC3 cells could interfere with the experimental setup. Therefore, I chose to change my cell model to Smad2-null HEK293T cells.

Smad2-null HEK293T cells were transiently transfected with Smad2-WT, -LSA, -LSD, and -LVA for 24 hours before collecting samples for both RNA isolation and cell lysate preparation, since variation in Smad2 proteins can also be due to difference in their mRNA expression. cDNA prepared from the transfected cells were analysed by RT-qPCR using a pair of primers that bind to flag sequence and a few nucleotides downstream in Smad2 MH1 domain, thus,

selectively detecting Flag-Smad2 tagged transgene proteins (*Fig 5.4D*). The results showed unequal mRNA levels of Smad2 linker constructs, highest in Smad2-LSD, followed by -LSA, -LVA and then -WT, despite transfecting the cells with identical plasmid DNA concentration (*Fig 5.4D*). This variation is not surprising as transfection efficiency of each experiment could differ depending on variety of factors such as cell density, culture conditions etc., but is useful to know to properly interpret any variation in subsequent protein expression analysis. Next, immunoblot analysis of Smad2 protein expression revealed lower Smad2-LSA and -LVA levels than Smad2-WT and -LSD (*Fig 5.4E lanes 2 and 4*). Quantification of Flag, representing Smad2 proteins, normalised against β-Actin, also showed significant reduction in both Smad2-LSA and -LVA in comparison to Smad2-WT and -LSD (*Fig 5.4F*). These results show that Smad2-pLS does play a crucial role in maintaining Smad2 stability and that pLS-mediated Smad2 stability may not be dependent on Smad2-pLT. These results are consistent with the effects of FVP-mediated Smad2/3 degradation seen in the earlier experiments.

In the previous experiments, FVP could induce maximum Smad2/3 degradation after transient agonist stimulation. Therefore, I sought to determine next if Smad2-LSA expression is further reduced after transient AA stimulation and whether MG132 could recover them. Smad2-null HEK293T cells were transiently transfected with Smad2-WT, -LSA, and -LSD for 24 hours before serum-starving them overnight in 1% serum medium and treating them with AA, SB, and MG132, as shown in the treatment scheme (*Fig 5.4G*). Immunoblot analysis of Flag expression showed higher Flag expression in MG132-treated cells in Smad2-WT and Smad2-LSA proteins (*Fig 5.4H lanes 2 and 4*), indicating rescue of Smad2 protein from degradation upon proteasome inhibition. However, transient AA stimulation resulted in much lower Smad2-LSD expression than previously observed (*Fig 5.4H lane 5*) and also MG132 could not generate any change in Smad2-LSD protein level (*Fig 5.4H lanes 5 and 6*), indicating that its reduced expression is not accounted by proteasomal degradation but may occur through some other mechanism. Furthermore, quantification of the ratio of Flag signals in MG132-treated cells versus non-treated cells, normalised against β-Actin, showed highest

recovery in Smad2-LSA protein on proteasome inhibition, followed by Smad2-WT and none in Smad2-LSD (*Fig 5.4I*). However, it must be noted that proteasome inhibition recovered Flag-tagged Smad2 proteins in both WT and LSA proteins which makes it unclear if Smad2 protein instability is indeed a consequence of loss of Smad2-pLS. To address this, it would be necessary to perform a time-course experiment in the presence of proteasome and protein translation inhibitors to observe changes in Smad2 (WT or LSA) protein expression.

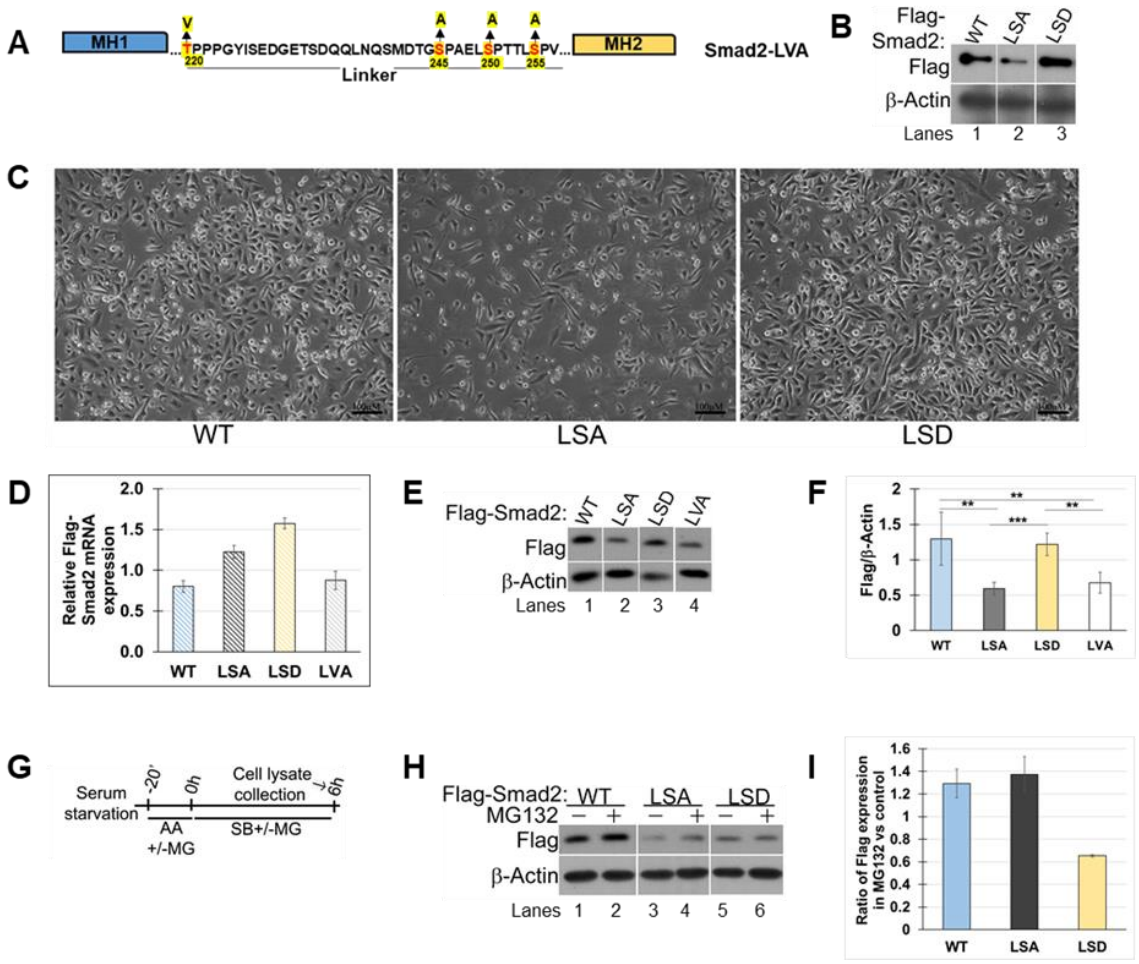

Figure 5.4: Effect of pLS on Smad2 stability
A) Schematic depiction of the site-directed mutagenesis in Smad2-LVA linker region to eliminate phosphorylatable serine and threonine residues. Position of the residues are indicated. **B)** Representative immunoblot of Flag in PC3 cells 24 hours after transfection with Flag-Smad2-WT, -LSA, and -LSD in serum-free culture. **C)** Representative phase-contrast images of PC3 cells expressing Smad2-WT, -LSA and -LSD. Scale bar- 100 µM. **D)** RT-qPCR analysis of mRNA expression of Flag-Smad2-WT, -LSA, -LSD, and -LVA against β-Actin in Smad2-null HEK293T cells cultured in 1% serum-medium overnight, 24 hours after transfection. Data represent means±s.d. of three measurements from one experiment. **E)** Representative immunoblot of Flag in Smad2-null HEK293T cells 24 hours after transfection with Flag-Smad2-WT, -LSA, -LSD, and -LVA in 1% serum medium. **F)** Quantification of Flag signals in E, using means±s.d. densitometric measurements, normalised to β-Actin (n=6). Student t-test was done and '**' and '***' indicate p<0.01 and 0.001, respectively. **G)** Scheme of treatment for H. **H)** Representative immunoblot of Flag in Smad2-null HEK293T cells transiently expressing Flag-Smad2-WT, -LSA, and –LSD and treated as illustrated in G (n=3). **I)** Analysis of ratio of Flag-Smad2 recovered by MG132 in H. Quantification of Flag was done using means±s.d. densitometric measurements, normalised to β-Actin (n=3).

5.3 Discussion and conclusion

The experiments described in this chapter show a novel function of Smad2-pLS in maintaining Smad2 protein expression and turnover. It shows that Smad2-pLS have a protective effect on inactivated Smad2 protein stability, in the absence of which, it is readily targeted by the UPS (*Fig 5.2 and 5.4*). Interestingly, the results also show that inhibition of CDK8/9 can have distinct effects on Smad2/3 protein levels, depending on the activation status of Smad2/3 as determined by ligand availability and receptor activity (*Fig 5.1C and E*). In hESCs as well as in PC3 cells, application of FVP alone after their serum-starvation resulted in slight but significant decrease in Smad2/3 proteins. However, when all autocrine TGF-β/activin signalling was inhibited with SB, FVP caused even more significant reduction in total Smad2/3 whereas, transient agonist stimulation induced maximum reduction of Smad2/3 proteins (*Fig 5.1*). These results suggest that the mechanism involved in the degradation of Smad2/3 proteins is dependent on TGF-β activation and its effects can be observed once the receptor activity is blocked, and Smad2/3 no longer in their activated states. There could be two possibilities as to why transient agonist stimulation may show maximal Smad2/3 degradation. First, transient agonist stimulation can result activation of non-canonical TGF-β signalling which can further induce PTMs on Smad2/3, while CDK8/9 inhibition suppresses their pLS, increasing Smad2/3 affinity to be targeted by the UPS. Second, it may be related to nuclear accumulation of Smad2/3 on transient agonist stimulation which may impart them with features that make Smad2/3 more susceptible to proteasomal degradation. Previous studies do show that Smad2/3 are heavily ubiquitinated solely as a consequence of their nuclear localisation (Lo and Massague, 1999), which may affect Smad2/3 stability in the absence of their pLS.

However, the physiological relevance of why Smad2 that is already deactivated, would further be degraded, is unclear. One explanation could be the need to limit total Smad2 protein availability to enhance its transcriptional response during subsequent TGF-β activation because cells exhibit a boost in Smad2/3 transcriptional activity depending on fold change in

the amount of nuclear Smad2/3 proteins relative to the background, in response to TGF-β activation (Frick et al., 2017). This relative sensing of TGF-β signalling may have implications in both during embryonic development as well as in any disease in which TGF-β signalling is dysregulated. Moreover, cell fractionation experiments showed that although Smad3 can localise in both nucleus and cytoplasm, regardless of agonist stimulation, Smad2 localisation is more tightly controlled and has very little to no nuclear presence without agonist stimulation (*Fig 5.1G and 5.3A, Fig A-IA and A-IB*). These results are well supported by earlier studies which found that Smad3 can localise in the nucleus and bind to FoxH1 independent of agonist stimulation, while it is mainly Smad2 that is sensitive to agonist stimulation and effects downstream signalling by rapidly translocating to the nucleus (Liu et al., 2016, Aragon et al., 2019).

Furthermore, my results in this chapter also showed that FVP-mediated Smad2/3 degradation is not rescued in Nedd4L-deficient cells, suggesting that this degradation is independent of Nedd4L activity (*Fig 5.3B and C*). Although activated Smad2/3 degradation through Nedd4L effectively requires pLT and can occur without pLS, absence of pLS somewhat curtails Nedd4L-Smad3 interaction, and likely Nedd4L-Smad2 interaction as well (Fig S3, Gao et al., 2009, Aragon et al., 2011). This is evidently because WW2 domain of Nedd4L binds to the PPxY motif whereas its WW3 domain requires binding with the first two LS residues to induce maximal Smad2/3 degradation (Aragon et al., 2011). More importantly, Nedd4L-mediated degradation requires Smad2/3 to be in the activated form (Gao et al., 2009, Yu et al., 2015), while the degradation identified in my results occurs predominantly in inactivated Smad2/3, which further supports my finding that Nedd4L is not the factor involved in pLS-related Smad2/3 degradation. Moreover, another experiment from the same study, showed that co-transfection of SCP2 that is reported to be responsible for dephosphorylation of Smad2/3-pLS, with Nedd4L, ubiquitin, and Smad3-WT in HEK293T cells, abolished Nedd4L-mediated poly-ubiquitination of Smad3 whereas mutated SCP2 could not (*Fig 4D*, Gao et al., 2009, Sapkota et al., 2006, Wrighton et al., 2006), further suggesting that Nedd4L

requires both pLT and pLS to effectively bind with Smad3 and prime it for degradation. Hence, it is unlikely that Nedd4L causes such large Smad2 degradation in the absence of its pLS.

Furthermore, although both Nedd4L and Smurf2 induce activated Smad2/3 degradation through similar mechanisms (Aragon et al., 2011, Tang et al, 2011, Gao et al., 2009), Smurf2 can also negatively affect inactivated Smad2 protein expression (Lin et al., 2000) and therefore, role of Smurf2 in FVP-mediated Smad2/3 degradation must be further investigated. Another RING E3 ubiquitin ligase called CHIP can also degrade inactivated Smad3 (Xin et al., 2005), but its mechanism of action has not been studied yet. It would be interesting to see if CHIP could regulate Smad2/3 via its interactions with their pLS and induce their degradation. Moreover, a time course analysis of Smad2 expression via immunostaining or live cell imaging can be a better technique to study where its degradation localisation instead of single time point analysis of Smad2 signal using cell fractionation-immunoblotting as it may lead to data misinterpretation because it fails to take Smad2 nucleocytoplasmic shuttling in consideration. For example, on signal termination, Smad2/3 may get degraded in the nucleus (Lin et al., 2000) or translocate back to the cytoplasm and be degraded there (Gao et al., 2009, Yu et al., 2015). But their nuclear degradation would cause fewer Smad2/3 to be exported out to the cytoplasm and hence, lower cytoplasmic Smad2/3 signal on an immunoblot or vice versa. Studying the localisation of Smad2/3 degradation would help to gain better insights into regulation and termination of TGF-β signalling.

Yet another mechanism that could result in proteasomal degradation of pLS-deficient Smad2 could be that phosphorylation of LS confers Smad2 protection from degradation through the N-end rule pathway. Most proteins are acetylated at their N-terminal during their translation, endowing them with an inherent ubiquitin-mediated degradation signal to maintain their *in vivo* half-lives (Varshavsky, 2011). Additionally, recent publications suggest that phosphorylation of a protein can inhibit its proteasomal degradation initiated via the N-end rule pathway (Eldeeb and Fahlman, 2016), hinting that pLS may prevent Smad2 degradation by inhibiting the activation of N-end rule pathway, and warrants further investigation. Exploring

these possibilities present an interesting avenue of research in identifying novel mechanisms of Smad2/3 degradation and regulation of TGF-β signalling. Moreover, it would also be interesting to uncover the role of other CDK8/9-induced Smad2/3 phosphorylation of linker and non-linker residues on Smad2/3 protein stability and turnover, as earlier studies show T8 and T388 as targets of CDK8/9 (Matsuura et al., 2004, Qu et al., 2014).

Chapter 6

General Discussion

6.1 Overview

Transforming growth factor-β (TGF-β)/activin/nodal signalling pathway play a critical role in many physiological processes such as in embryogenesis, cell proliferation, differentiation, and adult tissue homeostasis. As such, perturbations in their signalling lead to disease onset and progression (Morikawa et al., 2016, David and Massague, 2018). Evidently, TGF-β signalling is tightly regulated at multiple levels to maintain its normal functions. Regulation of its mediators, Smad2 and Smad3 (Smad2/3) presents an effective mode of regulating TGF-β signalling. Activity of Smad2/3 can be controlled by numerous post-translational modifications such as phosphorylation and ubiquitination (Xu et al., 2016). Phosphorylation of Smad2/3 linker region has emerged to be an important regulatory mechanism in TGF-β signalling, particularly, the four proline-directed linker threonine and serine (S/T-P) residues which can be phosphorylated by numerous kinases such as CDKs, PI3K/mTORC2, MAPKs etc (Kamato et al., 2013, Matsuzaki, 2013). Since the activity of linker threonine (LT) and linker serine residues (LS) are closely related, they have been considered to be indistinctly regulated and to have similar functions in TGF-β signalling in most of the studies in the field. However, a previous study in our lab showed that LS and LT phosphorylation could be differentially regulated by the CDKs (Yu et al., 2015).

In this thesis, I have further verified the finding that Smad2-LS and -LT are differentially phosphorylated by CDK8/9 in which CDK8/9 mainly regulate Smad2-pLS (*Chapter 3*). Furthermore, I have revealed that inhibition or removal of Smad2-pLS leads to prolonged half-life of activated Smad2 in the nucleus and as a consequence, enhances its agonist-induced transcriptional activity (*Chapter 4*). In contrast, absence of Smad2-pLS makes inactivated Smad2 protein unstable and results in its proteasomal degradation upon withdrawing agonist stimulation (*Chapter 5*). These findings emphasise the important role of Smad2 linker serine phosphorylation in regulating TGF-β signalling and more importantly, distinguishes between the function of linker threonine and linker serine phosphorylation, which may be exploited for therapeutical purposes to modulate TGF-β signalling that is dysregulated in diseases.

6.2 Differential regulation and function of pLS and pLT

In this study, it was clearly demonstrated that Smad2-pLS and -pLT can be differentially regulated by CDK8/9. Application of either a pan-CDK inhibitor, flavopiridol (FVP) or a more specific CDK8/9 inhibitor, LY2857785 (LY), considerably inhibited Smad2-pLS but did not have much effect on Smad2-pLT (*Fig 3.1*). Moreover, it appears that CDK8/9 regulate majority of steady-state Smad2-pLS and only phosphorylate Smad2-LT upon agonist activation (*Fig 3.1*). Regardless, Smad2-pLT level is relatively higher than pLS in the two cell models I used, hESCs and PC3 cells, even after overnight serum starvation (PC3 cells). This is likely to be attributed to high PI3K/Akt/mTOR signalling in both the cell lines which has been shown to positively regulate Smad2-pLT (Zoumaro-Djayoon et al., 2011, Dubrovska et al., 2009, Yu et al., 2015). Nevertheless, it would be interesting to discern how CDK8/9 may exert differential propensities to two such closely located phosphorylation sites in Smad2 linker region in the future studies, although all CDKs preferentially recognise S/T-P sequences (Malumbres, 2004).

In non-malignant cells, canonical TGF-β signalling has anti-proliferative effects and non-canonical signalling-induced Smad2/3 linker phosphorylation functions to antagonise the canonical TGF-β signalling, thus, maintaining the fine balance of Smad2/3 activities to regulate TGF-β signalling (Kamato et al., 2013, Matsuzaki, 2013, Xu et al., 2016). Though, both Smad2/3-pLS and -pLT negatively influence TGF-β signalling, it has not been reported before if they have distinct functions in doing so. Nonetheless, previous studies do indicate differences in their role in TGF-β signalling regulation. Studies indicate that Smad2/3-pLS may have more crucial role in regulating their transcriptional activities whereas, Smad2/3-pLT may function more in their deactivation via proteasomal degradation. In support, pLS induced by Erk1/2 and CDK8/9 weaken Smad2/3 transcription (Hough et al., 2012, Matsuura et al., 2004, Alarcon et al., 2009) while pLT augments Smad2/3 recognition by the WW E3 ubiquitin ligases which primes them for proteasomal degradation (Aragon et al., 2011, Gao et al., 2009). In addition, there are also mechanisms in place to reverse the effects of linker phosphorylation

such as, small C-terminal phosphatases1/2/3 (SCP1/2/3), which preferentially target pLS over pLT to maximise Smad2/3-mediated transcription and augment the intensity of TGF-β signalling (Wrighton et al., 2006, Sapkota et al., 2006). On the other hand, there are deubiquitinating enzymes (DUBs) that can remove ubiquitin molecules from Smad2/3 and reverse its priming for degradation initiated by their pLT (Kim and Baek, 2018). Overall, it can be concluded that although both Smad2/3-pLS and -pLT antagonise canonical TGF-β signalling, they can be differentially regulated by upstream kinases and can exert their effects on TGF-β signalling via distinct mechanisms.

6.3 Dual role of Smad2-pLS in regulating TGF-β signalling

In this study, it was also found that Smad2-pLS can have distinct effects on activated and inactivated Smad2 protein. For activated Smad2, inhibiting Smad2-pLS resulted in prolonged Smad2 activation due to delayed deactivation of activated Smad2, which consequently led to higher transcription and amplified TGF-β signalling (*Chapter 4*). Conversely, inhibiting Smad2-pLS destabilised inactivated Smad2 protein and resulted in its proteasomal degradation and this phenomenon was particularly enhanced after transient agonist stimulation and blocking the receptor kinase activity (*Chapter 5*). Thus, the dual role of Smad2-pLS in regulating Smad2 protein appears to be dependent on Smad2-activation status.

This dual role of Smad2-pLS on Smad2 proteins is interesting even though the exact underlying mechanisms remain to be elucidated. First, agonist stimulation activates Smad2/3 (SxS motif phosphorylation), leading to its translocation and accumulation in the nucleus. At the same time, non-canonical TGF-β signalling is also activated, leading to the activation of MAPK pathway, which further induces phosphorylation of Smad2/3 linker S/T-P residues. In the nucleus, SCPs specifically remove Smad2-pLS for maximal transcription of activated Smad2/3 and CDK8/9 are able to re-phosphorylate Smad2-pLS to facilitate their subsequent proteasomal degradation and cease transcription (Wrighton et al., 2006, Sapkota et al., 2006, Alarcon et al., 2009). The function of this re-phosphorylation on Smad2-LS could be a negative feedback mechanism for activated Smad2 as inhibition of CDK8/9 or mutating Smad2-LS to -

LA prolongs activated Smad2 signals and enhances its transcription (*Fig 3.2, 3.3, 4.1 and 4.2*). It was shown that inhibition of Smad2-pLS reduces the degradation of activated Smad2 (*Fig 4.1H*), indicating that Smad2-pLS may suppress ubiquitin-proteosome degradation of activated Smad2 (Tang et al., 2011, Gao et al., 2009, Aragon et al., 2011). Therefore, inhibiting Smad2-pLS by using CDK8/9 inhibitors such as FVP/LY or mutating Smad2-LS to non-phosphorylatable residues, limits Smad2 degradation, stabilises their activation and nuclear accumulation and hence, upregulates Smad2 transcription (*Fig 4.3 and 4.4*, Bae et al., 2014, Cohen-Solal et al., 2011, Matsuura et al., 2005, Kretzschmar et al., 1999). However, nuclear phosphatases-mediated dephosphorylation that may target Smad2/3 SxS motif and deactivate Smad2/3 cannot be completely excluded by our experiments (Inman et al., 2002, Schmierer et al, 2008, Lin et al., 2006, Bruce et al., 2012). Since the identity of nuclear phosphatase(s) responsible for SxS motif dephosphorylation remains debated, it is currently not feasible for me to investigate this possibility.

Second, inhibiting CDK8/9-mediated Smad2/3-pLS in inactivated Smad2/3 after withdrawing agonist or altogether mutating Smad2-LS to -LA, results in degradation of Smad2/3 proteins (*Fig 5.1 and 5.4*). Note that, transient agonist stimulation also activates non-canonical TGF-β signalling and presents a Smad2/3 phospho-isoform in which SxS motif becomes non-phosphorylated but non-canonical signalling-induced phosphorylation on other residues may still be present (e.g., pLT). In addition, transient agonist stimulation also results in a wave of nuclear translocation of Smad2/3, which are readily ubiquitinated simply as a consequence of their nuclear presence (Lo and Massague, 1999). Furthermore, it is interesting to note in my results that inactivated Smad2 are exclusively cytoplasmic while inactivated Smad3 can still exist in the nucleus (*Fig 5.1G, 5.3A, A-I*). This differential localisation of inactivated Smad2 and Smad3 is consistent with various studies (Liu et al., 2016, Aragon et al., 2019). Given the predominantly cytoplasmic localisation of inactivated Smad2 and the fact that Smad2/3 degradation occurs gradually overtime (visible after 3 hours and continues to degrade at least up to 6 hours), it is more likely that inactivated Smad2

phospho-isoform that lacks its pLS, might be degraded in the cytoplasm. As such, it can be postulated that high pLT induced by non-canonical TGF-β signalling might have a role in enhancing Smad2/3 degradation in the absence of phosphorylation of their SxS motif and LS. However, I observed similar significant reduction in both Smad2-LSA and Smad2-LVA proteins (*Fig 5.4E and F*) in which only LS and both LT/LS are mutated, respectively, to non-phosphorylatable residues. This demonstrates that pLT does not have any role in mediating degradation of inactivated Smad2/3 proteins. Next, the possibility of role of high ubiquitination conferred to transiently activated Smad2/3 due to their nuclear localisation in prompting such large degradation of Smad2/3, can also be excluded as Smad2/3 were degraded gradually over time. If high ubiquitination were to be solely responsible for degradation in pLS-deficient Smad2/3, it would likely have occurred much more rapidly, given the nuclear localisation of both ubiquitinated Smad2/3 and proteasomes (Marshall and Vierstra, 2019). Nevertheless, non-canonical TGF-β signalling also induces phosphorylation on other Smad2/3 amino acid residues in addition to LT (Smad2/3-T220/179), such as T8, S110, T197, S240, S253, S260, and S417 in Smad2 and T8, T66, S309, T388, and S418 in Smad3 (summarised in Xu et al., 2016, Qu et al., 2014). This suggests that such large degradation of pLS-deficient Smad2/3 is very likely attributable to non-LT phosphorylation. It may also be due to other PTMs that may occur on Smad2/3 structure as a consequence of non-canonical TGF-β signalling. Furthermore, E3 ubiquitin ligases, Smurf2 and CHIP can target inactivated Smad2 (Lin et al., 2000, Xin et al., 2005) and it would be interesting to study if they are involved in promoting this significantly large Smad2/3 degradation, in the future.

In addition, this theory can also explain how FVP induces variable degree of Smad2/3 degradation depending on Smad2 activation status as dictated by ligand availability and receptor activity (*Fig 5.1C and E*). Reduction in Smad2/3 levels is highest in FVP treated cells that are pre-stimulated, but least in FVP-treated cells that are only previously serum-starved. As described above, non-pLT PTMs that occur as a result of non-canonical TGF-β signalling by transiently applying agonist, results in high amount of Smad2/3 degradation in the absence

of their pLS. Nonetheless, steady-state non-pLT PTMs on Smad2/3 may also exist and contribute to Smad2/3 degradation in the absence of their pLS, as shown by small but significant reduction in Smad2/3 levels in cells treated with just FVP (*Fig 5.1C and E*). However, presence of autocrine TGF-β signalling in these cells may also contribute to SxS motif phosphorylation to a miniscule degree which would instead result in prolonged activation of Smad2/3 in the absence of their pLS, thus, preventing their degradation (*Fig 4.1 and 4.2*). Conversely, FVP treatment along with blocked receptor activity with SB, results in complete inhibition of autocrine TGF-β signalling as well as inhibition of CDK8/9-induced pLS. This would prevent any extension of Smad2/3 activation and at the same time facilitate Smad2/3 degradation mediated by non-pLT PTMs in the absence of their pLS, as shown from the medium level of Smad2/3 reduction in cells treated with SB+FVP which is higher than FVP only treatment but smaller than transient activation (*Fig 5.1C and E*). A summary of this mechanism is shown (*Fig 6.1*).

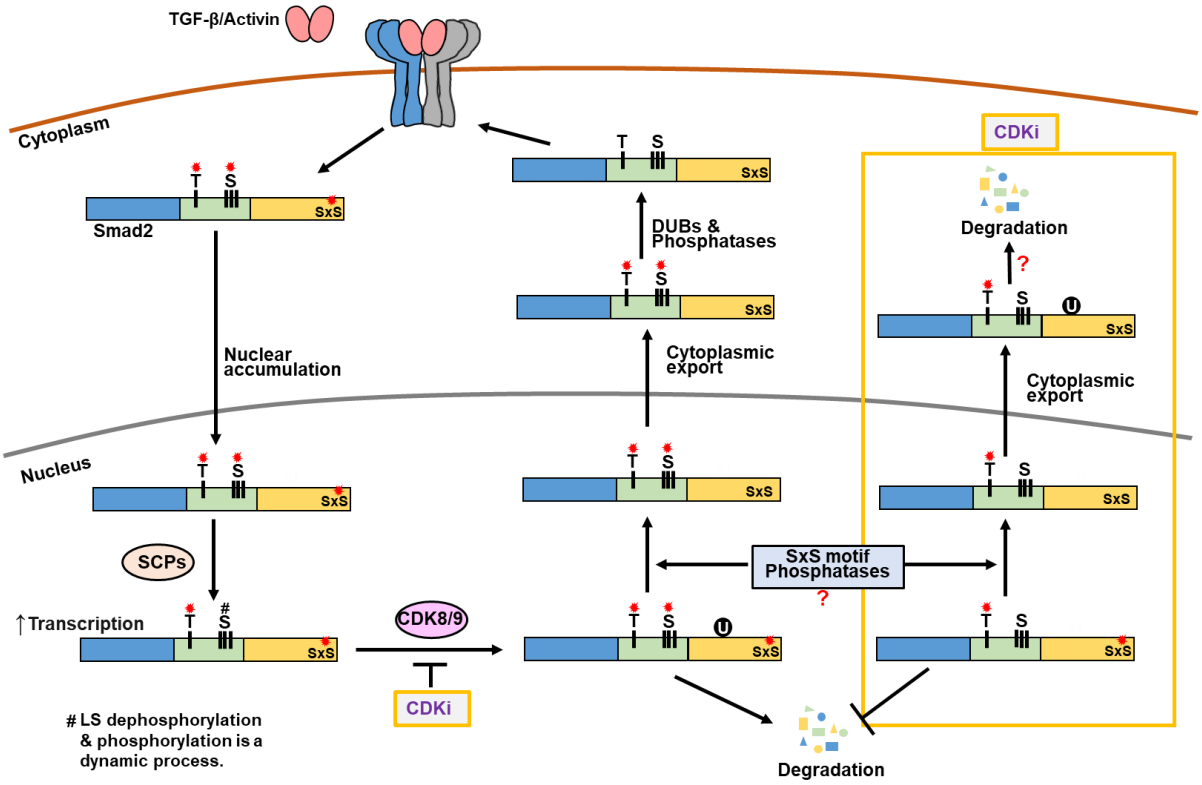

Figure 6.1: Dual role of Smad2-pLS in its activity

Activated Smad2 in the nucleus are targeted by SCPs to remove its pLS to enhance transcription, and CDK8/9 re-phosphorylate pLS to promote ubiquitination and degradation of activated Smad2. Inhibiting CDK8/9 (yellow box) impedes Smad2-pLS re-phosphorylation and inhibits activated Smad2 degradation. However, inhibiting CDK-mediated Smad2-pLS accelerates inactivated Smad2 degradation in the cytoplasm by unknown mechanisms. '✸' represents phosphorylation.

6.5 Future work

Whilst my current work clearly describes a dual role of Smad2-pLS in regulating TGF-β signalling depending on the status of Smad2 activation, several questions remain open for investigation. Firstly, what is the molecular mechanism responsible for extending the activated Smad2 upon inhibiting pLS? Our data suggests that it might be due to activated Smad2/3 escaping proteasomal degradation, however, E3 ubiquitin ligase(s) involved in this process and how pLS regulates its affinity to the activated Smad2 remain to be identified. Secondly, what is the underlying molecular mechanism that targets inactivated Smad2 for degradation without pLS and what E3 ubiquitin ligase(s) is/are accountable for it? Smurf2 and CHIP are two previously identified E3 ubiquitin ligase (Lin et al., 2000, Xin et al., 2005) and knockdown and overexpression of them in cells to study their effects on Smad2/3 protein levels might reveal the identity of the E3 ubiquitin ligase(s) involved. Alternatively, siRNA screening with siRNA library of E3 ubiquitin ligase may aid to identify candidates, which could be verified by knockdown and overexpression of identified E3 ubiquitin ligase candidates.

Moreover, my study focused mainly on Smad2 activity by mutating its LS to unphosphorylatable alanine. It would be interesting to check if Smad3 activity is similarly affected upon doing similar mutation. Also, it can be useful to extend the study to BMP R-Smads, Smad1/5/8, and check if their pLS and pLT can also be differentially regulated. Furthermore, I mutated all three linker serine residues of Smad2 in my experiments, studying them as a single unit. However, although individual linker serine residues have not been studied for their differential functions in Smad2 activity, preliminary evidence suggests that there might be variation in the function of each linker serine residue (Smad2-S245/250/255 and Smad3-S204/208/213), with last two serines having a more crucial role in mediating Smad2/3 transcription and the first serine mediating the switch from transcription to deactivation (Aragon et al., 2011, Gao et al., 2009, Millet et al., 2009, Wrighton et al., 2006, Sapkota et al., 2006). Therefore, it would be useful to delineate the role of each linker serine residue to specifically target them for therapeutic interventions.

Whilst this study has clearly shown the importance of Smad2/3-pLS in regulating TGF-β activity in hESCs, mESCs, and PC3 cells, it remains unknown how linker phosphorylation might modulate canonical TGF-β signalling during embryonic development. Specially, given that mutation of pLS is important for the regulation of timing and competency in responding to activin signalling during *Xenopus* development (Grimm and Gurdon, 2002), demonstration of similar effect of pLS mutation in hESCs and mESCs indicates the importance of non-canonical Smad signalling in regulating canonical TGF-β signalling in mammalian systems as well. However, as discussed before, it would be necessary to perform Smad2 linker mutation studies in human and mouse ESCs to study the effect of pLS on Smad2 transcriptional activity by utilising a more Smad2-specific systems such as using Pitx2-luciferase system instead of CAGA. In addition, phenotypic effects of Smad2-pLS mutation in EBs formed from mESCs such as difference in the size and structure needs to be further quantified and investigated. Furthermore, studying the phenotypic effects of linker serine phosphorylation in hESCs might help us in understanding their role in embryonic development. However, since it is difficult to perform Smad2/3 knockout experiments without compromising hESC pluripotency, in the future, genome editing technology such as clustered regularly interspaced short palindromic repeat (CRISPR)-Cas9 may help in generating desirable mutations directly on endogenous Smad2/3 genes and generate phospho-null (Smad2-LSA) or phospho-mimetic (Smad2-LSD) linker serine mutants of Smad2/3 in order to interrogate their importance in regulating Smad2/3 activities. Moreover, such editing methods can also be employed to generate mice model that presents desirable Smad2/3 linker serine mutation, hence, allowing the study of its phenotypic effects during the course of mice development.

It must also be noted that since there are multiple phospho-isoforms of Smad2 that can exist and they may have different effects on cell metabolism and physiology, it would be interesting to study the implication of different phospho-isoform pools of Smad2 in development and disease. Although, distinguishing these separate pools from each other may be a complicated process, techniques such as immunoprecipitation and mass

spectrophotometry can be employed to study various binding partners of a specific Smad2 phospho-isoform which may help to understand specific roles of different phosphorylation or other PTMs on Smad2 protein. Depending on the Smad2 binding partners identified, function of that phospho-isoform may be further investigated.

6.6 Implications on development and disease

Signalling crosstalk is an important mechanism which determines downstream activity of a signalling pathway. In TGF-β signalling, linker region phosphorylation forms a key hub to integrate other signalling pathways, thus, fine-modulating the response of canonical TGF-β signalling. As described above, I showed a dual role of linker serine phosphorylation where it limits the duration of Smad2 activity upon TGF-β activation, and in contrast, confers protection on inactivated Smad2 from degradation. As these findings appear to be applicable to both hESC and mESC as well as in HEK293T cells and cancer cell line PC3 cells, it represents the general relevance of this mechanism in regulating TGF-β signalling. It also emphasises the important role that Smad2/3 linker phosphorylation may play during embryonic development and mesendoderm differentiation in regulating activin/nodal signalling and its crosstalk with other signalling pathways. Moreover, BMP R-Smads, Smad1/5/8, also have linker region comprised of similar S/T-P sites but with different configuration, and such differential regulation of pLS and pLT may be applicable to BMP signalling as well. Moreover, if inhibiting Smad2/3-pLS augments their transcriptional activity and extends the intensity of TGF-β/activin A signalling, they can be useful targets to develop small molecule inhibitors that specifically inhibit pLS. This can help in improving protocols for *in vitro* differentiation of pluripotent stem cells to definitive endoderm (DE) and subsequently to cells of associated organs such as liver, lungs, pancreas, thyroid, and thymus (Zorn et al., 2009), which may have applications in disease modelling as well as in regenerative medicine.

Furthermore, TGF-β signalling is usually dysregulated in many diseases and Smad2/3 linker phosphorylation specially, has been implicated in numerous conditions such as cancer, fibrosis, cardiovascular diseases, immune conditions, polycystic kidney disease, and diabetes

(Matsuzaki et al., 2013, Batlle and Massague, 2019, Ooshima et al., 2019, Derynck et al., 2021, Hachimine et al., 2008, Rostam et al., 2016, Cohen-Solal et al., 2011, Kamato et al., 2013, Hama et al., 2017, Pan et al., 2021, Yoshida et al., 2018, Sun et al., 2015, Murata et al., 2009, Suwa et al., 2020, Li et al., 2021, Suzuki et al., 2015). Specially, in some cancer and fibrosis diseases, TGF-β signalling is inhibited and therefore, it no longer can function to suppress cell proliferation. In addition, Smad2/3 linker phosphorylation (that opposes the effects of canonical TGF-β signalling) has been associated with more aggressive forms of diseases and in causing epithelial to mesenchymal transition (EMT) and uncontrolled cell proliferation (Wang et al., 2009, Matsuzaki et al., 2013, Millet et al., 2009, Bae et al., 2012). It has also been implicated in promoting cancer stem cell development (Bae et al., 2014, Suzuki et al., 2015). On the other hand, some cancers may have hyperactive TGF-β signalling driving tumour growth, EMT, and metastases (Derynck and Budi, 2019). Therefore, drugs targeting Smad2/3 linker phosphorylation to either enhance or abrogate TGF-β signalling depending on the disease mechanism can be a therapeutically beneficial approach.

References

Akiyoshi, S., Inoue, H., Hanai, J.-I., Kusanagi, K., Nemoto, N., Miyazono, K. & Kawabata, M. 1999. c-Ski Acts as a Transcriptional Co-repressor in Transforming Growth Factor-β Signaling through Interaction with Smads. J Biol Chem., 274, 35269-35277.

Alarcon, C., Zaromytidou, A. I., Xi, Q., Gao, S., Yu, J., Fujisawa, S., Barlas, A., Miller, A. N., Manova-Todorova, K., Macias, M. J., Sapkota, G., Pan, D. & Massague, J. 2009. Nuclear CDKs drive Smad transcriptional activation and turnover in BMP and TGF-Beta Pathways. Cell, 139, 757-69.

Alliston, T., Choy, L., Ducy, P., Karsenty, G. & Derynck, R. 2001. TGF-beta-induced repression of CBFA1 by Smad3 decreases cbfa1 and osteocalcin expression and inhibits osteoblast differentiation. EMBO, 20, 2254-2272.

Aluwihare, P., Mu, Z., Zhao, Z., Yu, D., Weinreb, P. H., Horan, G. S., Violette, S. M., Munger, and J. S. 2009. Mice that lack activity of alphavbeta6- and alphavbeta8-integrins reproduce the abnormalities of Tgfb1- and Tgfb3-null mice. J Cell Sci. 122(Pt 2):227-32.

Annes, J. P., Chen, Y., Munger, J. S., & Rifkin, D. B. 2004. Integrin alphaVbeta6-mediated activation of latent TGF-beta requires the latent TGF-beta binding protein-1. J Cell Biol.l., *165*(5), 723–734.

Anzano, M. A., Roberts, A. B., Meyers, C. A., Komoriya, A., Lamb, L. C., Smith, J. M. & Sporn, M. B. 1982. Synergistic Interaction of Two Classes of Transforming Growth Factors from Murine Sarcoma Cells. Cancer Res., 42, 4776.

Aragon, E., Goerner, N., Zaromytidou, A. I., Xi, Q., Escobedo, A., Massague, J. & Macias, M. J. 2011. A Smad action turnover switch operated by WW domain readers of a phosphoserine code. Genes Dev.., 25, 1275-88.

Aragon, E., Wang, Q., Zou, Y., Morgani, S. M., Ruiz, L., Kaczmarska, Z., Su, J., Torner, C., Tian, L., Hu, J., Shu, W., Agrawal, S., Gomes, T., Marquez, J. A., Hadjantonakis, A. K., Macias, M. J. & Massague, J. 2019. Structural Basis for Distinct Roles of Smad2 and Smad3 in Foxh1 Pioneer-Directed Tgf-Beta Signaling. Genes Dev.., 33, 1506-1524.

Arnold, S. J. and Robertson, E. J. 2009. Making a commitment: cell lineage allocation and axis patterning in the early mouse embryo. Nat Rev Mol Cell Biol., 10, 91-103.

Aspalter, I. M., Gordon, E., Dubrac, A., Ragab, A., Narloch, J., Vizán, P., Geudens, I., Collins, R. T., Franco, C. A., Abrahams, C. L., Thurston, G., Fruttiger, M., Rosewell, I., Eichmann, A. & Gerhardt, H. 2015. Alk1 and Alk5 inhibition by Nrp1 controls vascular sprouting downstream of Notch. Nat Commun., 6, 7264.

Assoian, R. K., Komoriya, A., Meyers, C. A., Miller, D. M. & Sporn, M. B. 1983. Transforming growth factor-beta in human platelets. Identification of a major storage site, purification, and characterization. J Biol Chem., 258, 7155-7160.

Attisano, L., Silvestri, C., Izzi, L., and Labbé, E. 2001. The transcriptional role of Smads and FAST (FoxH1) in TGFb and activin signalling. Mol Cell Endocrinol., 180, 3–11.

Bae E, Kim S-J, Hong S, Liu F, Ooshima A. 2012. Smad3 linker phosphorylation attenuates Smad3 transcriptional activity and TGF-b1/Smad3- induced epithelial–mesenchymal transition in renal epithelial cells. Biochem. Biophys. Res. Commun., 427, 593–99.

Bae, E., Sato, M., Kim, R. J., Kwak, M. K., Naka, K., Gim, J., Kadota, M., Tang, B., Flanders, K. C., Kim, T. A., Leem, S. H., Park, T., Liu, F., Wakefield, L. M., Kim, S. J., Ooshima, A. 2014. Definition of smad3 phosphorylation events that affect malignant and metastatic behaviors in breast cancer cells. Cancer Res., 1, 74, 21, 6139-49.

Bai, Y., Yang, C., Hu, K., Elly, C. & Liu, Y. C. 2004. Itch E3 ligase-mediated regulation of TGF-beta signaling by modulating smad2 phosphorylation. Mol Cell, 15, 825-31.

Barbara, N. P., Wrana, J. L. & Letarte, M. 1999. Endoglin Is an Accessory Protein That Interacts with the Signaling Receptor Complex of Multiple Members of the Transforming Growth Factor-β Superfamily. J Biol Chem., 274, 584-594.

Batlle, E. & Massagué, J. 2019. Transforming Growth Factor-beta Signaling in Immunity and Cancer. Immunity, 50, 924-940.

Beyer, T. A., Narimatsu, M., Weiss, A., David, L. & Wrana, J. L. 2013a. The TGFβ superfamily in stem cell biology and early mammalian embryonic development. Biochim Biophys Acta., 1830, 2268-2279.

Beyer, Tobias A., Weiss, A., Khomchuk, Y., Huang, K., Ogunjimi, Abiodun A., Varelas, X. & Wrana, Jeffrey L. 2013b. Switch Enhancers Interpret TGF-β and Hippo Signaling to Control Cell Fate in Human Embryonic Stem Cells. Cell Reports, 5, 1611-1624.

Bizet, A. A., Liu, K., Tran-Khanh, N., Saksena, A., Vorstenbosch, J., Finnson, K. W., Buschmann, M. D. & Philip, A. 2011. The TGF-β co-receptor, CD109, promotes internalization and degradation of TGF-β receptors. Biochim Biophys Acta., 1813, 742-753.

Blahna, M. T. & Hata, A. 2012. Smad-mediated regulation of microRNA biosynthesis. FEBS Letters, 586, 1906-12.

Bonni, S., Wang, H. R., Causing, C. G., Kavsak, P., Stroschein, S. L., Luo, K. & Wrana, J. L. 2001. TGF-beta induces assembly of a Smad2-Smurf2 ubiquitin ligase complex that targets SnoN for degradation. Nat Cell Biol.l., 3, 587-95.

Bourgeois B, Gilquin B, Tellier-Lebègue C, Östlund C, Wu W, Pérez J, El Hage P, Lallemand F, Worman HJ, Zinn-Justin S. 2013. Inhibition of TGF-β signaling at the nuclear envelope: characterization of interactions between MAN1, Smad2 and Smad3, and PPM1A. Sci Signal., 18, 6, 280.

Brown, K. A., Pietenpol, J. A. & Moses, H. L. 2007. A tale of two proteins: differential roles and regulation of Smad2 and Smad3 in TGF-beta signaling. J Cell Biol.chem., 101, 9-33.

Bruce, D.L., Macartney, T., Yong, W., Shou, W. and Sapkota, G.P. 2012. Protein phosphatase 5 modulates SMAD3 function in the transforming growth factor-beta pathway. Cell Signal, 24, 11, 1999–2006.

Bruce, D. L., and Sapkota, G. P. 2012. Phosphatases in Smad Regulation. FEBS Letters, 586.

Budi, E. H., Schaub, J. R., Decaris, M., Turner, S. & Derynck, R. 2021. TGF-β as a driver of fibrosis: physiological roles and therapeutic opportunities. J Pathol., 254, 4, 358-373.

Burch, M. L., Yang, S. N. Y., Ballinger, M. L., Getachew, R., Osman, N. & Little, P. J. 2010. TGF-β stimulates biglycan synthesis via p38 and Erk phosphorylation of the linker region of Smad2. Cell Mol Life Sci., 67, 2077-2090.

Camus, A., Perea-Gomez, A., Moreau, A., and Collingnon, J. 2006. Absence of nodal signalling promotes precocious neural differentiation in the mouse embryo. Development Biol. 295, 743-755.

Cao, Y., Szabolcs, A., Dutta, S. K., Yaqoob, U., Jagavelu, K., Wang, L., Leof, E. B., Urrutia, R. A., Shah, V. H. & Mukhopadhyay, D. 2010. Neuropilin-1 Mediates Divergent R-Smad Signaling and the Myofibroblast Phenotype. J Biol Chem., 285, 31840-31848.

Chacko, B. M., Qin, B., Correia, J. J., Lam, S. S., De Caestecker, M. P. & Lin, K. 2001. The L3 loop and C-terminal phosphorylation jointly define Smad protein trimerization. Nat Struct Biol., 8, 248-53.

Chaikuad, A. & Bullock, A. N. 2016. Structural basis of intracellular TGF-β Signaling: Receptors and Smads. Cold Spring Harb Perspect Biol., 8.

Chen, R., Keating, M. J., Gandhi, V., Plunkett, W. 2005. Transcription inhibition by flavopiridol: mechanism of chronic lymphocytic leukemia cell death. Blood, 106, 7, 2513–2519.

Chen, C. & Shen, M. M. 2004. Two Modes by which Lefty Proteins Inhibit Nodal Signaling. Curr Biol., 14, 618-624.

Chen, X., Rubock, M. J. & Whitman, M. 1996. A transcriptional partner for MAD proteins in TGF-β signalling. Nature, 383, 691-696.

Chen, X., Weisberg, E., Fridmacher, V., Watanabe, M., Naco, G. & Whitman, M. 1997a. Smad4 and FAST-1 in the assembly of activin-responsive factor. Nature, 389, 85-89.

Chen, Y. G., Liu, F. & Massagué, J. 1997b. Mechanism of TGFbeta receptor inhibition by FKBP12. EMBO, 16, 3866-3876.

Chen, Y. G. & Meng, A. M. 2004. Negative regulation of TGF-β signaling in development. Cell Res., 14, 441-449.

Chng, Z., Vallier, L. & Pedersen, R. 2011. Chapter Three - Activin/Nodal Signaling and Pluripotency. In: LITWACK, G. (ed.) Vitam. Horm., Academic Press.

Cohen-Solal, K. A., Merrigan, K. T., Chan, J. L., Goydos, J. S., Chen, W., Foran, D. J., Liu, F., Lasfar, A., Reiss, M. 2011. Constitutive Smad linker phosphorylation in melanoma: a mechanism of resistance to transforming growth factor-β-mediated growth inhibition. Pigment Cell Melanoma Res., 24, 3, 512-24.

Cui, W., Fowlis, D. J., Bryson, S., Duffie, E., Ireland, H., Balmain, A. & Akhurst, R. J. 1996. TGFβ1 Inhibits the Formation of Benign Skin Tumors,but Enhances Progression to Invasive Spindle Carcinomas in Transgenic Mice. Cell, 86, 531-542.

Dai, F., Lin, X., Chang, C. & Feng, X. H. 2009. Nuclear export of Smad2 and Smad3 by RanBP3 facilitates termination of TGF-β Signalling. Development Cell, 16, 345-57.

David, C. J. & Massagué, J. 2018. Contextual determinants of TGFbeta action in development, immunity and cancer. Nat Rev Mol Cell Biol., 19, 419-435.

de Larco, J. E. & Todaro, G. J. 1978. Growth factors from murine sarcoma virus-transformed cells. Proc Natl Acad Sci U S A, 75, 4001.

Deheuninck, J. & Luo, K. 2009. Ski and SnoN, potent negative regulators of TGF-beta signaling. Cell Res., 19, 47-57.

Derynck, R. & Budi, E. H. 2019. Specificity, versatility, and control of TGF-beta family signaling. Sci Signal., 12.

Derynck, R., Jarrett, J. A., Chen, E. Y., Eaton, D. H., Bell, J. R., Assoian, R. K., Roberts, A. B., Sporn, M. B. & Goeddel, D. V. 1985. Human transforming growth factor-β complementary DNA sequence and expression in normal and transformed cells. Nature, 316, 701-705.

Derynck, R., Turley, S.J., and Akhurst, R.J. 2021. TGFβ biology in cancer progression and immunotherapy. Nat Rev Clin. Oncol., 18, 9–34.

Di Guglielmo, G. M., Le Roy, C., Goodfellow, A. F. & Wrana, J. L. 2003. Distinct endocytic pathways regulate TGF-β receptor signalling and turnover. Nat Cell Biol.l., 5, 410-421.

Doré, J. J. E., Yao, D., Edens, M., Garamszegi, N., Sholl, E. L. & Leof, E. B. 2001. Mechanisms of Transforming Growth Factor-β Receptor Endocytosis and Intracellular Sorting Differ between Fibroblasts and Epithelial Cells. Mol Biol Cell, 12, 675-684.

Doyle, J. J., Gerber, E. E. & Dietz, H. C. 2012. Matrix-dependent perturbation of TGFβ signaling and disease. FEBS Letters, 586, 2003-2015.

Du, D., Katsuno, Y., Meyer, D., Budi, E. H., Chen, S.-H., Koeppen, H., Wang, H., Akhurst, R. J. & Derynck, R. 2018. Smad3-mediated recruitment of the methyltransferase SETDB1/ESET controls Snail1 expression and epithelial–mesenchymal transition. EMBO, 19, 135-155.

Dubois, C. M., Laprise, M.-H., Blanchette, F., Gentry, L. E. & Leduc, R. 1995. Processing of Transforming Growth Factor β1 Precursor by Human Furin Convertase. J Biol Chem., 270, 10618-10624.

Dubrovska, A., Kim, S., Salamone, R. J., Walker, J. R., Maira, S. M., García-Echeverría, C., Schultz, P. G., Reddy, V. A. 2009. The role of PTEN/Akt/PI3K signaling in the maintenance and viability of prostate cancer stem-like cell populations. Proc Natl Acad Sci U S A, 106, 1, 268-273.

Dupont, S., Zacchigna, L., Cordenonsi, M., Soligo, S., Adorno, M., Rugge, M. & Piccolo, S. 2005. Germ-Layer Specification and Control of Cell Growth by Ectodermin, a Smad4 Ubiquitin Ligase. Cell, 121, 87-99.

Ehrlich, M., Gutman, O., Knaus, P. & Henis, Y. I. 2012. Oligomeric interactions of TGF-β and BMP receptors. FEBS Letters, 586, 1885-1896.

Eldeeb, M. A., and Fahlman, R. P. 2016. Phosphorylation Impacts N-end Rule Degradation of the Proteolytically Activated Form of BMX Kinase. J Biol Chem., 291, 43, 22757-22768.

Emanuelli A, Manikoth Ayyathan D, Koganti P, Shah PA, Apel-Sarid L, Paolini B, Detroja R, Frenkel-Morgenstern M, Blank M. 2019. Altered Expression and Localization of Tumor Suppressive E3 Ubiquitin Ligase SMURF2 in Human Prostate and Breast Cancer. Cancers, 11, 4, 556.

Feng, X. H. & Derynck, R. 2005. Specificity and versatility in tgf-beta signaling through Smads. Annu Rev Cell Development Biol., 21, 659-93.

Finger, E. C., Lee, N. Y., You, H.-J. & Blobe, G. C. 2008. Endocytosis of the type III transforming growth factor-beta (TGF-beta) receptor through the clathrin-independent/lipid raft pathway regulates TGF-beta signaling and receptor down-regulation. J Biol Chem., 283, 34808-34818.

Finnson, K. W., Tam, B. Y., Liu, K., Marcoux, A., Lepage, P., Roy, S., Bizet, A. A., Philip, A. 2006. Identification of CD109 as part of the TGF-beta receptor system in human keratinocytes. FASEB J, 20, 9, 1525-7.

Fowlis, D., Cui, W., Johnson, S., Balmain, A. & Akhurst, R. 1996. Altered epidermal cell growth control in vivo by inducible expression of transforming growth factor beta 1 in the skin of transgenic mice. Cell Growth Differ., 7, 679-687.

Frick, C. L., Yarka, C., Nunns, H., and Goentoro, L. 2017. Sensing relative signal in the Tgf-β/Smad pathway. Proc Natl Acad Sci U S A, 114, 14, E2975-E2982.

Frolik, C. A., Dart, L. L., Meyers, C. A., Smith, D. M. & Sporn, M. B. 1983. Purification and initial characterization of a type beta transforming growth factor from human placenta. Proc Natl Acad Sci U S A, 80, 3676.

Fukuchi, M., Imamura, T., Chiba, T., Ebisawa, T., Kawabata, M., Tanaka, K. & Miyazono, K. 2001. Ligand-dependent degradation of Smad3 by a ubiquitin ligase complex of ROC1 and associated proteins. Mol Biol Cell*,* 12**,** 1431-1443.

Funaba, M. & Mathews, L. S. 2000. Identification and Characterization of Constitutively Active Smad2 Mutants: Evaluation of Formation of Smad Complex and Subcellular Distribution. Mol Endocrinol., 14, 1583-1591.

Funaba, M., Zimmerman, C. M. & Mathews, L. S. 2002. Modulation of Smad2-mediated signaling by extracellular signal-regulated kinase. J Biol Chem., 277, 41361-8.

Gao, S., Alarcon, C., Sapkota, G., Rahman, S., Chen, P. Y., Goerner, N., Macias, M. J., Erdjument-Bromage, H., Tempst, P. & Massague, J. 2009. Ubiquitin Ligase Nedd4L Targets Activated Smad2/3 to Limit TGF-β Signaling. Mol Cell, 36, 6, 457-68.

Gaarenstroom T, Hill CS. 2014. TGF-β signaling to chromatin: how Smads regulate transcription during self-renewal and differentiation. Semin Cell Development Biol. 32, 107, 18.

Gentry, L. E., Lioubin, M. N., Purchio, A. F. & Marquardt, H. 1988. Molecular events in the processing of recombinant type 1 pre-pro-transforming growth factor beta to the mature polypeptide. Mol Cell Biol., 8, 4162-4168.

Gleizes, P.-E., Beavis, R. C., Mazzieri, R., Shen, B. & Rifkin, D. B. 1996. Identification and Characterization of an Eight-cysteine Repeat of the Latent Transforming Growth Factor-β Binding Protein-1 that Mediates Bonding to the Latent Transforming Growth Factor-β1. J Biol Chem., 271, 29891-29896.

Glinka, Y. And Prud'homme, G. J. 2008. Neuropilin-1 is a receptor for latent and active TGFβ-1and is involved in suppression by regulatory T cells. J Leukoc Biol., 22, 664.4-664.4.

Glinka, Y., Stoilova, S., Mohammed, N. & Prud'homme, G. J. 2010. Neuropilin-1 exerts co-receptor function for TGF-beta-1 on the membrane of cancer cells and enhances responses to both latent and active TGF-beta. Carcinogenesis, 32, 613-621.

Gomis, R. R., Alarcon, C., He, W., Wang, Q., Seoane, J., Lash, A. & Massagué, J. 2006a. A FoxO-Smad synexpression group in human keratinocytes. Proc Natl Acad Sci USA, 103, 12747-52.

Gomis, R. R., Alarcon, C., Nadal, C., Van Poznak, C. & Massagué, J. 2006b. C/EBPbeta at the core of the TGFbeta cytostatic response and its evasion in metastatic breast cancer cells. Cancer Cell, 10, 203-14.

Gori, I., George, R., Purkiss, A. G., Strohbuecker, S., Randall, R. A., Ogrodowicz, R., Carmignac, V., Faivre, L., Joshi, D., Kjær, S., Hill, C.S. 2021. Mutations in SKI in Shprintzen-Goldberg syndrome lead to attenuated TGF-β responses through SKI stabilization. Elife, 10, e63545.

Goumans, M.-J. & ten Dijke, P. 2018. TGF-β Signaling in Control of Cardiovascular Function. Cold Spring Harb Perspect Biol., 10.

Gray, A. M. & Mason, A. J. 1990. Requirement for activin A and transforming growth factor--beta 1 pro-regions in homodimer assembly. Science, 247, 1328.

Gray, P. C., Shani, G., Aung, K., Kelber, J. & Vale, W. 2006. Cripto binds transforming growth factor beta (TGF-beta) and inhibits TGF-beta signaling. Mol cell Biol., 26, 9268-9278.

Grimm and Gurdon. 2002. Nuclear Exclusion of Smad2 Is a Mechanism Leading to Loss of Competence. Nat Cell Biol., Vol. 4, 7.

Gronroos, E., Hellman, U., Heldin, C. H. & Ericsson, J. 2002. Control of Smad7 stability by competition between acetylation and ubiquitination. Mol Cell, 10, 483-93.

Groppe, J., Hinck, C. S., Samavarchi-Tehrani, P., Zubieta, C., Schuermann, J. P., Taylor, A. B., Schwarz, P. M., Wrana, J. L. & Hinck, A. P. 2008. Cooperative Assembly of TGF-β Superfamily Signaling Complexes Is Mediated by Two Disparate Mechanisms and Distinct Modes of Receptor Binding. Mol Cell, 29, 157-168.

Grotewold, L., Plum, M., Dildrop, R., Peters, T. & Rüther, U. 2001. Bambi is coexpressed with Bmp-4 during mouse embryogenesis. Mech Development., 100, 327-330.

Guerrero-Esteo, M., Sánchez-Elsner, T., Letamendia, A. & Bernabéu, C. 2002. Extracellular and Cytoplasmic Domains of Endoglin Interact with the Transforming Growth Factor-β Receptors I and II. J Biol Chem., 277, 29197-29209.

Guo, X., Ramirez, A., Waddell, D. S., Li, Z., Liu, X. & Wang, X.-F. 2008a. Axin and GSK3-control Smad3 protein stability and modulate TGF- signaling. Genes Dev.., 22, 106-120.

Guo, X., Waddell, D. S., Wang, W., Wang, Z., Liberati, N. T., Yong, S., Liu, X. & Wang, X. F. 2008b. Ligand-dependent ubiquitination of Smad3 is regulated by casein kinase 1 gamma 2, an inhibitor of TGF-β signaling. Oncogene, 27, 7235-7247.

Hachimine, D., Uchida, K., Asada, M., Nishio, A., Kawamata, S., Sekimoto, G., Murata, M., Yamagata, H., Yoshida, K., Mori, S., Tahashi, Y., Matsuzaki, K., Okazaki, K. 2008.

Involvement of Smad3 phosphoisoform-mediated signaling in the development of colonic cancer in IL-10-deficient mice. Int J Oncol., 32, 6, 1221-6.

Haider, S., Kunihs, V., Fiala, C., Pollheimer, J., Knöfler, M. 2017. Expression pattern and phosphorylation status of Smad2/3 in different subtypes of human first trimester trophoblast. Placenta, 57, 17-25.

Hama, T., Nakanishi, K., Sato, M., Mukaiyama, H., Togawa, H., Shima, Y., Miyajima, M., Nozu, K., Nagao, S., Takahash,i H., Sako, M., Iijima, K., Yoshikawa, N., Suzuki, H. 2017. Aberrant Smad3 phosphoisoforms in cyst-lining epithelial cells in the *cpk* mouse, a model of autosomal recessive polycystic kidney disease. Am J Physiol Renal Physiol., 1, 313, 6, F1223-F1231.

Hammond, T. R., Marsh, S. E. & Stevens, B. 2019. Immune Signaling in Neurodegeneration. Immunity, 50, 955-974.

Hanyu, A., Ishidou, Y., Ebisawa, T., Shimanuki, T., Imamura, T. & Miyazono, K. 2001. The N domain of Smad7 is essential for specific inhibition of transforming growth factor-β signaling. J Cell Biol., 155, 1017-1028.

Hart, P. J., Deep, S., Taylor, A. B., Shu, Z., Hinck, C. S. & Hinck, A. P. 2002. Crystal structure of the human TβR2 ectodomain–TGF-β3 complex. Nat Struct Biol., 9, 203-208.

Hashimoto, H., Rebagliati, M., Ahmad, N., Muraoka, O., Kurokawa, T., Hibi, M. & Suzuki, T. 2004. The Cerberus/Dan-family protein Charon is a negative regulator of Nodal signaling during left-right patterning in zebrafish. Development, 131, 1741-1753.

Hayes, S., Chawla, A. & Corvera, S. 2002. TGF beta receptor internalization into EEA1-enriched early endosomes: role in signaling to Smad2. J Cell Biol.l., 158, 1239-1249.

Heldin, C.-H. & Moustakas, A. 2012. Role of Smads in TGFβ signaling. Cell Tissue Res., 347, 21-36.

Heldin, C.-H. & Moustakas, A. 2016. Signaling Receptors for TGF-β Family Members. Cold Spring Harb Perspect Biol., 8.

Heldin, C. H., Landstrom, M. & Moustakas, A. 2009. Mechanism of TGF-beta signaling to growth arrest, apoptosis, and epithelial-mesenchymal transition. Curr Opin Cell Biol., 21, 166-76.

Hill, C. S. 2009. Nucleocytoplasmic Shuttling of Smad Proteins. Cell Res., 19, 36-46.

Hill, C. S. 2016. Transcriptional control by the Smads. Cold Spring Harb Perspect Biol., 8, A022079.

Hill, C. S. 2018. Spatial and temporal control of Nodal signaling. Curr Opin Cell Biol., 51, 50-57.

Hinck, A. P., Mueller, T. D. & Springer, T. A. 2016. Structural Biology and Evolution of the TGF-β Family. Cold Spring Harb Perspect Biol., 8.

Hocevar, B. A., Smine, A., Xu, X.-X. & Howe, P. H. 2001. The adaptor molecule Disabled-2 links the transforming growth factor β receptors to the Smad pathway. EMBO, 20, 2789-2801.

Hough, C., Radu, M. & Dore, J. J. 2012. TGF-β-induced Erk phosphorylation of Smad linker region regulates Smad signaling. Plos One, 7, E42513.

Huang, T., David, L., Mendoza, V., Yang, Y., Villarreal, M., De, K., Sun, L., Fang, X., López-Casillas, F., Wrana, J. L. & Hinck, A. P. 2011. TGF-β signalling is mediated by two autonomously functioning TβRI:TβRII pairs. EMBO, 30, 1263-1276.

Huminiecki, L., Goldovsky, L., Freilich, S., Moustakas, A., Ouzounis, C. & Heldin, C.-H. 2009. Emergence, development and diversification of the TGF-βsignalling pathway within the animal kingdom. BMC Evol. Biol., 9, 28.

Huse, M., Chen, Y.-G., Massagué, J. & Kuriyan, J. 1999. Crystal Structure of the Cytoplasmic Domain of the Type I TGF β Receptor in Complex with FKBP12. Cell, 96, 425-436.

Huse, M., Muir, T. W., Xu, L., Chen, Y.-G., Kuriyan, J. & Massagué, J. 2001. The TGFβ Receptor Activation Process: An Inhibitor- to Substrate-Binding Switch. Mol Cell, 8, 671-682.

Iemura, S.-I., Yamamoto, T. S., Takagi, C., Uchiyama, H., Natsume, T., Shimasaki, S., Sugino, H. & Ueno, N. 1998. Direct binding of follistatin to a complex of bone-morphogenetic protein and its receptor inhibits ventral and epidermal cell fates in early *Xenopus* embryo. Proc Natl Acad Sci U S A, 95, 9337.

Inman, G. J., Nicolás, F. J. & Hill, C. S. 2002. Nucleocytoplasmic shuttling of Smads 2, 3, and 4 permits sensing of TGF-β receptor activity. Mol Cell, 10, 283-294.

Itoh, S., Landström, M., Hermansson, A., Itoh, F., Heldin, C.-H., Heldin, N.-E. & Ten Dijke, P. 1998. Transforming Growth Factor β1 Induces Nuclear Export of Inhibitory Smad7. J Biol Chem., 273, 29195-29201.

Janakiraman, H., House, R. P., Gangaraju, V. K., Diehl, J. A., Howe, P. H. & Palanisamy, V. 2018. The Long (lncRNA) and Short (miRNA) of It: TGFβ-Mediated Control of RNA-Binding Proteins and Noncoding RNAs. Mol Can Res, 16, 567.

Jhappan, C., Geiser, A. G., Kordon, E. C., Bagheri, D., Hennighausen, L., Roberts, A. B., Smith, G. H. & Merlino, G. 1993. Targeting expression of a transforming growth factor beta 1 transgene to the pregnant mammary gland inhibits alveolar development and lactation. EMBO, 12, 1835-1845.

Jia, S. & Meng, A. 2021. TGFβ family signaling and development. Development., 148.

Kamaraju, A. K. & Roberts, A. B. 2005. Role of Rho/Rock and p38 Map kinase pathways in Transforming Growth Factor-Beta-mediated Smad-dependent growth inhibition of human breast carcinoma cells *in vivo*. J Biol Chem., 280, 1024-36.

Kamato, D., Burch, M. L., Piva, T. J., Rezaei, H. B., Rostam, M. A., Xu, S., Zheng, W., Little, P. J. & Osman, N. 2013. Transforming Growth Factor-Beta signalling: Role and consequences of smad linker region phosphorylation. Cell Signal, 25, 2017-24.

Kang, J. S., Alliston, T., Delston, R. & Derynck, R. 2005. Repression of Runx2 function by TGF-β through recruitment of class II histone deacetylases by Smad3. EMBO, 24, 2543-2555.

Kang, Y., Chen, C.-R. & Massagué, J. 2003. A Self-Enabling TGFβ Response Coupled to Stress Signaling: Smad Engages Stress Response Factor ATF3 for Id1 Repression in Epithelial Cells. Mol Cell, 11, 915-926.

Kashima, R. & Hata, A. 2017. The role of TGF-β superfamily signaling in neurological disorders. Acta Biochim. Biophys. Sin., 50, 106-120.

Katsuno, Y., Qin, J., Oses-Prieto, J., Wang, H., Jackson-Weaver, O., Zhang, T., Lamouille, S., Wu, J., Burlingame, A., Xu, J. & Derynck, R. 2018. Arginine methylation of SMAD7 by PRMT1 in TGF-β–induced epithelial–mesenchymal transition and epithelial stem-cell generation. J Biol Chem., 293, 13059-13072.

Kavsak, P., Rasmussen, R. K., Causing, C. G., Bonni, S., Zhu, H., Thomsen, G. H. & Wrana, J. L. 2000. Smad7 binds to Smurf2 to form an E3 ubiquitin ligase that targets the TGF beta receptor for degradation. Mol Cell, 6, 1365-75.

Kawabata, M., Inoue, H., Hanyu, A., Imamura, T. & Miyazono, K. 1998. Smad proteins exist as monomers in vivo and undergo homo- and hetero-oligomerization upon activation by serine/threonine kinase receptors. EMBO, 17, 4056-4065.

Kim, S-Kim, S-Y., and Baek, K-H. 2019, TGF-β signaling pathway mediated by deubiquitinating enzymes. Cell Mol Lif Sci., 76, 653-665.

Knelson, E. H., Gaviglio, A. L., Tewari, A. K., Armstrong, M. B., Mythreye, K. & Blobe, G. C. 2013. Type III TGF-β receptor promotes FGF2-mediated neuronal differentiation in neuroblastoma. J Clinic. Invest., 123, 4786-4798.

Koinuma, D., Shinozaki, M., Komuro, A., Goto, K., Saitoh, M., Hanyu, A., Ebina, M., Nukiwa, T., Miyazawa, K., Imamura, T. & Miyazono, K. 2003. Arkadia amplifies TGF-beta superfamily signalling through degradation of Smad7. EMBO, 22, 6458-70.

Komuro, A., Imamura, T., Saitoh, M., Yoshida, Y., Yamori, T., Miyazono, K., and Miyazawa, K. 2004. Negative regulation of transforming growth factor-β (TGF-β) signaling by WW domain-containing protein 1 (WWP1). Oncogene, 23, 6914–6923.

Kramer, E. L. & Clancy, J. P. 2018. TGFβ as a therapeutic target in cystic fibrosis. Expert Opin. Ther. Targets, 22, 177-189.

Kretzschmar, M., Doody, J., Timokhina, I. & Massague, J. 1999. A mechanism of repression of TGF-β/ Smad signalling by oncogenic Ras. Genes Dev.., 13, 804-16.

Kume, S., Haneda, M., Kanasaki, K., Sugimoto, T., Araki, S.-I., Isshiki, K., Isono, M., Uzu, T., Guarente, L., Kashiwagi, A. & Koya, D. 2007. SIRT1 Inhibits Transforming Growth Factor β-Induced Apoptosis in Glomerular Mesangial Cells via Smad7 Deacetylation. J Biol Chem., 282, 151-158.

Kuratomi, G., Komuro, A., Goto, K., Shinozaki, M., Miyazawa, K., Miyazono, K., Imamura, T. 2005. Nedd4-2 (Neural Precursor Cell Expressed, Developmentelopmentally Down-Regulated 4-2) Negatively Regulates TGF-β (Transforming Growth Factor-B) Signalling by Inducing Ubiquitin-Mediated Degradation of Smad2 and TGF-β Type I Receptor. Biochem J., 386, 3, 461–470.

Kurisaki, A., Kose, S., Yoneda, Y., Heldin, C.-H. & Moustakas, A. 2001. Transforming Growth Factor-β Induces Nuclear Import of Smad3 in an Importin-β1 and Ran-dependent Manner. Mol Biol Cell, 12, 1079-1091.

Lawler, S., Feng, X.-H., Chen, R.-H., Maruoka, E. M., Turck, C. W., Griswold-Prenner, I. & Derynck, R. 1997. The Type II Transforming Growth Factor-β Receptor Autophosphorylates Not Only on Serine and Threonine but Also on Tyrosine Residues. J Biol Chem., 272, 14850-14859.

Lebrin, F., Goumans, M.-J., Jonker, L., Carvalho, R. L. C., Valdimarsdottir, G., Thorikay, M., Mummery, C., Arthur, H. M. & Dijke, P. T. 2004. Endoglin promotes endothelial cell proliferation and TGF-β/ALK1 signal transduction. EMBO, 23, 4018-4028.

Leclerc, S., Garnier, M., Hoessel, R., Marko, D., Bibb, J. A., Snyder, G. L., Greengard, P., Biernat, J., Wu, Y.-Z., Mandelkow, E.-M., Eisenbrand, G. & Meijer, L. 2001. Indirubins inhibit Glycogen Synthase Kinase-3β and Cdk5/P25, two protein kinases involved in abnormal tau phosphorylation in Alzheimer's disease: a property common to most cyclin-dependent kinase inhibitors. J Biol Chem., 276, 251-260.

Lederer, D. J. & Martinez, F. J. 2018. Idiopathic Pulmonary Fibrosis. NEJM, 378, 1811-1823.

Lee, M. K., Pardoux, C., Hall, M. C., Lee, P. S., Warburton, D., Qing, J., Smith, S. M. & Derynck, R. 2007. TGF-β activates Erk MAP kinase signalling through direct phosphorylation of ShcA. EMBO, 26, 3957-3967.

Lee, N. Y., Kirkbride, K. C., Sheu, R. D. & Blobe, G. C. 2009. The Transforming Growth Factor-β Type III Receptor Mediates Distinct Subcellular Trafficking and Downstream Signaling of Activin-like Kinase (ALK)3 and ALK6 Receptors. Mol Biol Cell, 20, 4362-4370.

Lewis, K. A., Gray, P. C., Blount, A. L., Macconell, L. A., Wiater, E., Bilezikjian, L. M. & Vale, W. 2000. Betaglycan binds inhibin and can mediate functional antagonism of activin signalling. Nature, 404, 411-414.

Li, X., Liu, M., Ren, X., Loncle, N., Wang, Q., Hemba-Waduge, R. U. S., Yu, S. H., Boube, M., Bourbon, H. M. G., Ni, J. Q., and Ji, J. Y. 2020. The Mediator CDK8-Cyclin C complex modulates Dpp signaling in *Drosophila* by stimulating Mad-dependent transcription. PLoS Genet, 16(5), e1008832.

Li, Y., Li, L., Qin, J., Wu, J., Dai, X., and Xu, J. 2021. OSR1 phosphorylates the Smad2/3 linker region and induces TGF-β1 autocrine to promote EMT and metastasis in breast cancer. Oncogene**,** 40**,** 68–84.

Liang, J., Zhou, Y., Zhang, N., Wang, D., Cheng, X., Li, K., Huang, R., Lu, Y., Wang, H., Han, D., Wu, W., Han, M., Miao, S., Wang, L., Zhao, H. & Song, W. 2021. The phosphorylation of the Smad2/3 linker region by Nemo-Like Kinase regulates TGF-β Signalling. J Biol Chem., 296, 100512.

Liénart, S., Merceron, R., Vanderaa, C., Lambert, F., Colau, D., Stockis, J., Van Der Woning, B., De Haard, H., Saunders, M., Coulie, P. G., Savvides, S. N. & Lucas, S. 2018. Structural basis of latent TGF-β1 presentation and activation by GARP on human regulatory T cells. Science, 362, 952-956.

Lin, H.-K., Bergmann, S. & Pandolfi, P. P. 2004. Cytoplasmic PML function in TGF-β signalling. Nature, 431, 205-211.

Lin, M., Sutherland, D. R., Horsfall, W., Totty, N., Yeo, E., Nayar, R., Wu, X.-F. & Schuh, A. C. 2002. Cell surface antigen CD109 is a novel member of the α2 macroglobulin/C3, C4, C5 family of thioester-containing proteins. Blood, 99, 1683-1691.

Lin, X., Liang, M. and Feng, X.H. 2000. Smurf2 is a ubiquitin E3 ligase mediating proteasome-dependent degradation of Smad2 in transforming growth factor-beta signaling. J Biol Chem., 275, 47, 36818–36822.

Lin, X., Duan, X., Liang, Y.-Y., Su, Y., Wrighton, K.H., Long, J., Hu, M., Davis, C.M., Wang, J., Brunicardi, F.C., et al. 2006. PPM1A Functions as a Smad Phosphatase to Terminate TGFβ Signaling. Cell. 125, 5, 915–928.

Liu, L., Liu, X., Ren, X., Tian, Y., Chen, Z., Xu, X., Du, Y., Jiang, C., Fang, Y., Liu, Z., Fan, B., Zhang, Q., Jin, G., Yang, X. & Zhang, X. 2016. Smad2 and Smad3 Have Differential Sensitivity in Relaying Tgf-beta Signaling and inversely Regulate Early Lineage Specification. Sci Rep, 6, 21602.

Liu, X., Xiong, C., Jia, S., Zhang, Y., Chen, Y.-G., Wang, Q. & Meng, A. 2013. Araf kinase antagonizes Nodal-Smad2 activity in mesendoderm development by directly phosphorylating the Smad2 linker region. Nat Commun., 4, 1728.

Lo, R. S., and Massagué, J. 1999. Ubiquitin-dependent degradation of TGF-beta-activated smad2. Nat Cell Biol., 1, 8, 472-478.

Lo, R. S., Chen, Y. G., Shi, Y., Pavletich, N. P. & Massagué, J. 1998. The L3 loop: a structural motif determining specific interactions between SMAD proteins and TGF-beta receptors. EMBO, 17, 996-1005.

Lodyga, M. & Hinz, B. 2019. TGF-beta1 - A truly transforming growth factor in fibrosis and immunity. Semin Cell Development Biol., 101, 123-139.

López-Casillas, F., Cheifetz, S., Doody, J., Andres, J. L., Lane, W. S. & Massagué, J. 1991. Structure and expression of the membrane proteoglycan betaglycan, a component of the TGF-β receptor system. Cell, 67, 785-795.

López-Casillas, F., Payne, H. M., Andres, J. L. & Massagué, J. 1994. Betaglycan can act as a dual modulator of TGF-beta access to signaling receptors: mapping of ligand binding and GAG attachment sites. J Cell Biol., 124, 557-568.

López-Casillas, F., Wrana, J. L. & Massagué, J. 1993. Betaglycan presents ligand to the TGFβ signaling receptor. Cell, 73, 1435-1444.

Lucarelli, P., Schilling, M., Kreutz, C., Vlasov, A., Boehm, M. E., Iwamoto, N., Steiert, B., Lattermann, S., Wäsch, M., Stepath, M., Matter, M. S., Heikenwälder, M., Hoffmann, K., Deharde, D., Damm, G., Seehofer, D., Muciek, M., Gretz, N., Lehmann, W. D., Timmer, J. & Klingmüller, U. 2018. Resolving the Combinatorial Complexity of Smad Protein Complex Formation and Its Link to Gene Expression. Cell Sys., 6, 75-89, e11.

Luo, K. & Lodish, H. F. 1997. Positive and negative regulation of type II TGF-beta receptor signal transduction by autophosphorylation on multiple serine residues. EMBO, 16, 1970-1981.

Luo, K., Stroschein, S. L., Wang, W., Chen, D., Martens, E., Zhou, S. & Zhou, Q. 1999. The Ski oncoprotein interacts with the Smad proteins to repress TGF-beta signaling. Genes Dev.., 13, 2196-206.

Macias, M. J., Martin-Malpartida, P. & Massagué, J. 2015. Structural determinants of Smad function in TGF-beta signaling. Trends Biochem Sci, 40, 296-308.

Malhotra, R., Paskin-Flerlage, S., Zamanian, R. T., Zimmerman, P., Schmidt, J. W., Deng, D. Y., Southwood, M., Spencer, R., Lai, C. S., Parker, W., Channick, R. N., Morrell, N. W., Elliott,

C. G. & Yu, P. B. 2013. Circulating Angiogenic Modulatory Factors Predict Survival and Functional Class in Pulmonary Arterial Hypertension. Pulm. Circ., 3, 369-380.

Malumbres, M. 2014. Cyclin-Dependent Kinases. Gen. Biol., 15, 122.

Manning, G., Whyte, D. B., Martinez, R., Hunter, T. & Sudarsanam, S. 2002. The Protein Kinase Complement of the Human Genome. Science, 298, 1912.

Marquez, R. T., Bandyopadhyay, S., Wendlandt, E. B., Keck, K., Hoffer, B. A., Icardi, M. S., Christensen, R. N., Schmidt, W. N. & Mccaffrey, A. P. 2010. Correlation between microRNA expression levels and clinical parameters associated with chronic hepatitis C viral infection in humans. Lab. Invest., 90, 1727-1736.

Marshall, R. S., and Vierstra, R. D. 2019. Dynamic Regulation of the 26S Proteasome: From Synthesis to Degradation. Front. Mol. Biosci., 6, 40.

Martin-Malpartida, P., Batet, M., Kaczmarska, Z., Freier, R., Gomes, T., Aragon, E., Zou, Y., Wang, Q., Xi, Q., Ruiz, L., Vea, A., Marquez, J. A., Massagué, J. & Macias, M. J. 2017. Structural basis for genome wide recognition of 5-bp GC motifs by SMAD transcription factors. Nat Commun., 8, 2070.

Massagué, J. and Wotton, D. 2000. Transcriptional control by the TGF-β/Smad signaling system. EMBO, 19, 1745–1754.

Massagué, J. 2003, Integration of Smad and MAPK pathways: a link and a linker revisited. Genes Dev.., 17, 2993-3997.

Massagué, J., Seoane, J., Wotton, D. 2005. Smad transcription factors. Genes Dev., 19, 2783-2810.

Massagué, J. 2012. TGFβ signalling in context. Nat Rev Mol Cell Biol., 13, 616–630.

Matsuura, I., Chiang, K. N., Lai, C. Y., He, D., Wang, G., Ramkumar, R., Uchida, T., Ryo, A., Lu, K., Liu, F. 2009. Pin1 promotes transforming growth factor-b-induced migration and invasion. J Biol Chem., 285, 1754–1764.

Matsuura, I., Denissova, N. G., Wang, G., He, D., Long, J. & Liu, F. 2004. Cyclin-Dependent Kinases regulate the antiproliferative function of Smads. Nature, 430, 226-231.

Matsuura, I., Wang, G., He, D. & Liu, F. 2005. Identification and characterization of Erk/Map Kinase phosphorylation sites in Smad3. Biochemistry, 44, 12546-53.

Matsuzaki K, Kitano C, Murata M, Sekimoto G, Yoshida K, Uemura Y, Seki, T., Taketani, S., Fujisawa, J-I., Okazaki, K. 2009. Smad2 and Smad3 phosphorylated at both linker and COOH terminal regions transmit malignant TGF-b signal in later stages of human colorectal cancer. Cancer Res., 69, 5321–30.

Mavrakis, K. J., Andrew, R. L., Lee, K. L., Petropoulou, C., Dixon, J. E., Navaratnam, N., Norris, D. P. & Episkopou, V. 2007. Arkadia enhances Nodal/TGF-beta signaling by coupling phospho-Smad2/3 activity and turnover. PLoS Biol., 5, e67.

Mendoza, V., Vilchis-Landeros, M. M., Mendoza-Hernández, G., Huang, T., Villarreal, M. M., Hinck, A. P., López-Casillas, F. & Montiel, J.-L. 2009. Betaglycan has Two Independent Domains Required for High Affinity TGF-β Binding: Proteolytic Cleavage Separates the

Domains and Inactivates the Neutralizing Activity of the Soluble Receptor. Biochemistry, 48, 11755-11765.

Mesnard, D., Guzman-Ayala, M. and Constam, D. B. 2006. Nodal specifies embryonic visceral endoderm and sustains pluripotent cells in the epiblast before overt axial patterning. Development. 133, 2497-2505.

Millet, C., Yamashita, M., Heller, M., Yu, L. R., Veenstra, T. D. & Zhang, Y. E. 2009. A negative feedback control of Transforming Growth Factor-Beta signalling by Glycogen Synthase Kinase 3-mediated Smad3 linker phosphorylation at ser-204. J Biol Chem., 284, 19808-16.

Mitchell, H., Choudhury, A., Pagano, R. E. & Leof, E. B. 2004. Ligand-dependent and -independent Transforming Growth Factor-β Receptor Recycling Regulated by Clathrin-mediated Endocytosis and Rab11. Mol Biol Cell, 15, 4166-4178.

Miyazono, K., Olofsson, A., Colosetti, P. & Heldin, C. H. 1991. A role of the latent TGF-beta 1-binding protein in the assembly and secretion of TGF-beta 1. EMBO, 10, 1091-1101.

Mori, S., Matsuzaki, K., Yoshida, K., Furukawa, F., Tahashi, Y., Yamagata, H., Sekimoto, G., Seki, T., Matsui, H., Nishizawa, M., Fujisawa, J. & Okazaki, K. 2004. TGF-β And HGF transmit the signals through JNK-dependent Smad2/3 phosphorylation at the linker regions. Oncogene, 23, 7416-29.

Morikawa, M., Derynck, R. & Miyazono, K. 2016. TGF-β and the TGF-β Family: Context-Dependent Roles in Cell and Tissue Physiology. Cold Spring Harb Perspect Biol., 8.

Morikawa, M., Koinuma, D., Miyazono, K. & Heldin, C. H. 2013. Genome-wide mechanisms of Smad binding. Oncogene, 32, 1609-1615.

Morrison GM, Oikonomopoulou I, Migueles RP, Soneji S, Livigni A, Enver T, Brickman JM. 2008. Anterior definitive endoderm from ESCs reveals a role for FGF signaling. Cell Stem Cell. 3, 4, 402-15.

Mossahebi-Mohammadi, M., Quan, M., Zhang, J.-S. & LI, X. 2020. FGF Signaling Pathway: A Key Regulator of Stem Cell Pluripotency. Front. Cell Development Biol., 8.

Mu, D., Cambier, S., Fjellbirkeland, L., Baron, J. L., Munger, J. S., Kawakatsu, H., Sheppard, D., Broaddus, V. C., and Nishimura, S. L. 2002. The integrin alpha(v)beta8 mediates epithelial homeostasis through MT1-MMP-dependent activation of TGF-beta1. J Cell Biol., l,157(3):493-507.

Mullen, A. C., Orlando, D. A., Newman, J. J., Loven, J., Kumar, R. M., Bilodeau, S., Reddy, J., Guenther, M. G., Dekoter, R. P. & Young, R. A. 2011. Master transcription factors determine cell-type-specific responses to TGF-beta signaling. Cell, 147, 565-76.

Munger, J. S., Huang, X., Kawakatsu, H., Griffiths, M.J., Dalton, S.L., Wu, J., Pittet, J.F., Kaminski, N., Garat, C., Matthay, M.A., Rifkin, D. B., and Sheppard, D. 1999. The integrin alpha v beta 6 binds and activates latent TGF beta 1: a mechanism for regulating pulmonary inflammation and fibrosis. Cell, 96(3):319-28.

Murata, M., Matsuzaki, K., Yoshida, K., Sekimoto, G., Tahashi, Y., Mori, S., Uemura, Y., Sakaida, N., Fujisawa, J., Seki, T., Kobayashi, K., Yokote, K., Koike, K., Okazaki, K. 2009. Hepatitis B virus X protein shifts human hepatic transforming growth factor (TGF)-beta

signaling from tumor suppression to oncogenesis in early chronic hepatitis B. Hepatology, 49, 4, 1203-17.

Murayama, K., Kato-Murayama, M., Itoh, Y., Miyazono, K., Miyazawa, K. & Shirouzu, M. 2020. Structural basis for inhibitory effects of Smad7 on TGF-β family signaling. J Struc. Biol., 212, 107661.

Nagano, Y., Mavrakis, K. J., Lee, K. L., Fujii, T., Koinuma, D., Sase, H., Yuki, K., Isogaya, K., Saitoh, M., Imamura, T., Episkopou, V., Miyazono, K. & Miyazawa, K. 2007. Arkadia induces degradation of SnoN and c-Ski to enhance transforming growth factor-beta signaling. J Biol Chem., 282, 20492-501.

Nagaoka, T., Karasawa, H., Castro, N. P., Rangel, M. C., Salomon, D. S. & Bianco, C. 2012. An evolving web of signaling networks regulated by Cripto-1. Growth Factors, 30, 13-21.

Nakano, A., Koinuma, D., Miyazawa, K., Uchida, T., Saitoh, M., Kawabata, M., Hanai, J., Akiyama, H., Abe, M., Miyazono, K., Matsumoto, T., Imamura, T. 2009. Pin1 down-regulates transforming growth factor-beta (TGF-beta) signaling by inducing degradation of Smad proteins. J Biol Chem., 284, 10, 6109-15.

Nakao, A., Afrakhte, M., Morn, A., Nakayama, T., Christian, J. L., Heuchel, R., Itoh, S., Kawabata, M., Heldin, N.-E., Heldin, C.-H. & Dijke, P. T. 1997b. Identification of Smad7, a TGFβ-inducible antagonist of TGF-β signalling. Nature, 389, 631-635.

Ohtsuka, S., Nakai-Futatsugi, Y. & Niwa, H. 2015. LIF signal in mouse embryonic stem cells. JAKSTAT, 4, e1086520-e1086520.

Onichtchouk, D., Chen, Y.-G., Dosch, R., Gawantka, V., Delius, H., Massagué´, J. & Niehrs, C. 1999. Silencing of TGF-β signalling by the pseudoreceptor BAMBI. Nature, 401, 480-485.

Ooshima, A., Park, J. & Kim, S. J. 2019. Phosphorylation status at Smad3 linker region modulates transforming growth factor-beta-induced epithelial-mesenchymal transition and cancer progression. Cancer Sci*,* 110**,** 481-488.

Pais, H., Nicolas, F. E., Soond, S. M., Swingler, T. E., Clark, I. M., Chantry, A., Moulton, V. & Dalmay, T. 2010. Analyzing mRNA expression identifies Smad3 as a microRNA-140 target regulated only at protein level. RNA, 16, 489-494.

Pan, X., Phanish, M. K., Baines, D. L., Dockrell, M. E. C. 2021. High glucose-induced Smad3 linker phosphorylation and CCN2 expression are inhibited by dapagliflozin in a diabetic tubule epithelial cell model. Biosci Rep., 25, 41, 6, BSR20203947.

Pauklin, S. and Vallier, L. 2015. Activin/Nodal signalling in stem cells. Development., 142, 607-619.

Penheiter, S. G., Mitchell, H., Garamszegi, N., Edens, M., Jules J. E. Doré & Leof, E. B. 2002. Internalization-Dependent and -Independent Requirements for Transforming Growth Factor β Receptor Signaling via the Smad Pathway. Mol Cell Biol., 22, 4750-4759.

Penheiter, S. G., Singh, R. D., Repellin, C. E., Wilkes, M. C., Edens, M., Howe, P. H., Pagano, R. E. & Leof, E. B. 2010. Type II transforming growth factor-beta receptor recycling is dependent upon the clathrin adaptor protein Dab2. Mol Biol Cell, 21, 4009-4019.

Piccolo, S., Agius, E., Leyns, L., Bhattacharyya, S., Grunz, H., Bouwmeester, T. & Robertis, E. M. D. 1999. The head inducer Cerberus is a multifunctional antagonist of Nodal, BMP and Wnt signals. Nature, 397, 707-710.

Pierce, D. F., Johnson, M. D., Matsui, Y., Robinson, S. D., Gold, L. I., Purchio, A. F., Daniel, C. W., Hogan, B. L. & Moses, H. L. 1993. Inhibition of mammary duct development but not alveolar outgrowth during pregnancy in transgenic mice expressing active TGF-beta 1. Genes Dev., 7, 2308-2317.

Pierreux, C. E., Nicolás, F. J., Hill, C. S. 2000. Transforming growth factor beta-independent shuttling of Smad4 between the cytoplasm and nucleus. Mol Cell Biol, 20, 23, 9041-54.

Qu, X., Li, X., Zheng, Y., Ren, Y., Puelles, V. G., Caruana, G., Nikolic-Paterson, D. J., Li, J. 2014. Regulation of Renal Fibrosis by Smad3 Thr388 Phosphorylation. Am J Pathol., 184, 4, 944-952.

Radaev, S., Zou, Z., Huang, T., Lafer, E. M., Hinck, A. P. & Sun, P. D. 2010. Ternary Complex of Transforming Growth Factor-β1 Reveals Isoform-specific Ligand Recognition and Receptor Recruitment in the Superfamily. J Biol Chem., 285, 14806-14814.

Ray, B. N., Lee, N. Y., How, T. & Blobe, G. C. 2010. ALK5 phosphorylation of the endoglin cytoplasmic domain regulates Smad1/5/8 signaling and endothelial cell migration. Carcinogenesis, 31, 435-441.

Razani, B., Zhang, X. L., Bitzer, M., Von Gersdorff, G., Böttinger, E. P. & Lisanti, M. P. 2001. Caveolin-1 Regulates Transforming Growth Factor (TGF)-β/SMAD Signaling through an Interaction with the TGF-β Type I Receptor. J Biol Chem., 276, 6727-6738.

Roberts, A. B., Anzano, M. A., Lamb, L. C., Smith, J. M. & Sporn, M. B. 1981. New class of transforming growth factors potentiated by epidermal growth factor: isolation from non-neoplastic tissues. Proc Natl Acad Sci U S A, 78, 5339.

Roberts, A. B., Anzano, M. A., Meyers, C. A., Wideman, J., Blacher, R., Pan, Y. C. E., Stein, S., Lehrman, S. R. & Smith, J. M. 1983. Purification and properties of a type beta. transforming growth factor from bovine kidney. Biochemistry, 22, 5692-5698.

Roberts, A. B., Anzano, M. A., Wakefield, L. M., Roche, N. S., Stern, D. F. & Sporn, M. B. 1985. Type beta transforming growth factor: a bifunctional regulator of cellular growth. Proc Natl Acad Sci U S A, 82, 119.

Roberts, A. B., Lamb, L. C., Newton, D. L., Sporn, M. B., De Larco, J. E. & Todaro, G. J. 1980. Transforming Growth Factors: Isolation of Polypeptides from Virally and Chemically Transformed Cells by Acid / Ethanol Extraction. Proc Natl Acad Sci U S A, 77, 3494-3498.

Robertson, E. J. 1987. Embryo-derived stem cell lines. In Teratocarcinomas and Embryonic Stem Cells: A Practical Approach (ed. E. J. Robertson), pp. 72-112.Oxford, IRL Press.

Robertson, E. J. 2014. Dose-dependent Nodal/Smad signals pattern the early mouse embryo. Semin. Cell Development. Biol., 32, 73-79.

Robertson, I. B. & Rifkin, D. B. 2016. Regulation of the Bioavailability of TGF-β and TGF-β-Related Proteins. Cold Spring Harb Perspect Biol., 8.

Ross, S., Cheung, E., Petrakis, T. G., Howell, M., Kraus, W. L. & Hill, C. S. 2006. Smads orchestrate specific histone modifications and chromatin remodeling to activate transcription. EMBO, 25, 4490-4502.

Ross, S. & Hill, C. S. 2008. How the Smads regulate transcription. Int J Biochem Cell Biol, 40, 383-408.

Rostam, M. A., Kamato, D., Piva, T. J., Zheng, W., Little, P. J., Osman, N. 2016. The role of specific Smad linker region phosphorylation in TGF-β mediated expression of glycosaminoglycan synthesizing enzymes in vascular smooth muscle. Cell Signal, 28, 8, 956-66.

Saharinen, J., Taipale, J. & Keski-Oja, J. 1996. Association of the small latent transforming growth factor-beta with an eight cysteine repeat of its binding protein LTBP-1. EMBO, 15, 245-253.

Sapkota, G., Knockaert, M., Alarcon, C., Montalvo, E., Brivanlou, A. H. & Massague, J. 2006. Dephosphorylation of the linker regions of Smad1 and Smad2/3 by Small C-Terminal domain phosphatases has distinct outcomes for Bone Morphogenetic Protein and Transforming Growth Factor-Beta pathways. J Biol Chem., 281, 40412-9.

Saura, M., Zaragoza, C., Herranz, B., Griera, M., Diez-Marqués, L., Rodriguez-Puyol, D. & Rodriguez-Puyol, M. 2005. Nitric Oxide Regulates Transforming Growth Factor-β; Signaling in Endothelial Cells. Circ Res., 97, 1115-1123.

Scherner, O., Meurer, S. K., Tihaa, L., Gressner, A. M. & Weiskirchen, R. 2007. Endoglin Differentially Modulates Antagonistic Transforming Growth Factor-β1 and BMP-7 Signaling. J Biol Chem., 282, 13934-13943.

Schmierer, B. & Hill, C. S. 2005. Kinetic analysis of Smad nucleocytoplasmic shuttling reveals a mechanism for Transforming Growth Factor Beta-dependent nuclear accumulation of smads. Mol Cell Biol, 25, 9845-58.

Schmierer, B., Tournier, A. L., Bates, P. A. & Hill, C. S. 2008. Mathematical modeling identifies Smad nucleocytoplasmic shuttling as a dynamic signal-interpreting system. Proc Natl Acad Sci, 105, 6608-13.

Sekiya, T., Oda, T., Matsuura, K. & Akiyama, T. 2004. Transcriptional regulation of the TGF-β pseudoreceptor BAMBI by TGF-β signaling. Biochem Bioph Res Co, 320, 680-684.

Seo, S. R., Lallemand, F., Ferrand, N., Pessah, M., L'hoste, S., Camonis, J. & Atfi, A. 2004. The novel E3 ubiquitin ligase Tiul1 associates with TGIF to target Smad2 for degradation. EMBO, 23**,** 3780-3792.

Seoane, J., Le, H.-V., Shen, L., Anderson, S. A. & Massagué, J. 2004. Integration of Smad and Forkhead Pathways in the Control of Neuroepithelial and Glioblastoma Cell Proliferation. Cell, 117, 211-223.

Shapiro, G. I. 2004. Preclinical and clinical development of the Cyclin-Dependent kinase inhibitor flavopiridol. Clin Cancer Res. 10, 12, 4270s-4275s.

Shi, Y. and Massague, J. 2003. Mechanisms of TGFb signalling from cell membrane to the nucleus. Cell, 113, 685-700.

Shi, M., Zhu, J., Wang, R., Chen, X., Mi, L., Walz, T. & Springer, T. A. 2011. Latent TGF-β structure and activation. Nature, 474, 343-349.

Shi, Y. 2001. Structural insights on Smad function in TGFβ signaling. BioEssays, 23, 223-232.

Shi, Y., Hata, A., Lo, R. S., Massagué, J. & Pavletich, N. P. 1997. A structural basis for mutational inactivation of the tumour suppressor Smad4. Nature, 388, 87-93.

Shi, Y., Wang, Y.-F., Jayaraman, L., Yang, H., Massagué, J. & Pavletich, N. P. 1998. Crystal Structure of a Smad MH1 Domain Bound to DNA: Insights on DNA Binding in TGF-β Signaling. Cell, 94, 585-594.

Shukla, A., Malik, M., Cataisson, C., Ho, Y., Friesen, T., Suh, K.S. and Yuspa, S.H. 2009. TGFβ signalling is regulated by Schnurri-2-dependent nuclear translocation of CLIC4 and consequent stabilization of phospho-Smad2 and 3. Nat Cell Biol, 11, 6, 777–784.

Silberstein, G. B. & Daniel, C. W. 1987. Reversible inhibition of mammary gland growth by transforming growth factor-beta. Science, 237, 291.

Simonsson, M., Heldin, C.-H., Ericsson, J. & Grönroos, E. 2005. The Balance between Acetylation and Deacetylation Controls Smad7 Stability. J Biol Chem., 280, 21797-21803.

Sorrentino, A., Thakur, N., Grimsby, S., Marcusson, A., Von Bulow, V., Schuster, N., Zhang, S., Heldin, C.-H. & Landström, M. 2008. The type I TGF-β receptor engages TRAF6 to activate TAK1 in a receptor kinase-independent manner. Nat Cell Biol., 10, 1199-1207.

Stroschein, S. L., Wang, W., Zhou, S., Zhou, Q. & Luo, K. 1999. Negative feedback regulation of TGF-beta signaling by the SnoN oncoprotein. Science, 286, 771-4.

Sun, Y., Liu, X., Ng-Eaton, E., Lodish, H. F. & Weinberg, R. A. 1999. SnoN and Ski protooncoproteins are rapidly degraded in response to transforming growth factor β signaling. Proc Natl Acad Sci U S A, 96, 12442.

Sun, Y. B., Qu, X., Howard, V., Dai, L., Jiang, X., Ren, Y., Fu, P., Puelles, V. G., Nikolic-Paterson, D. J., Caruana, G., Bertram, J. F., Sleeman, M. W., Li, J. 2015. Smad3 deficiency protects mice from obesity-induced podocyte injury that precedes insulin resistance. Kidney Int., 88, 2, 286-98.

Suwa, K., Yamaguchi, T., Yoshida, K., Murata, M., Ichimura, M., Tsuneyama, K., Seki, T., Okazaki, K. 2020. Smad Phospho-Isoforms for Hepatocellular Carcinoma Risk Assessment in Patients with Nonalcoholic Steatohepatitis. Cancers (Basel), 24, 12, 2, 286.

Suzuki, H., Yagi, K., Kondo, M., Kato, M., Miyazono, K. & Miyazawa, K. 2004. c-Ski inhibits the TGF-β signaling pathway through stabilisation of inactive Smad complexes on Smad-binding elements. Oncogene, 23, 5068-5076.

Suzuki, R., Fukui, T., Kishimoto, M., Miyamoto, S., Takahashi, Y., Takeo, M., Mitsuyama, T., Sakaguchi, Y., Uchida, K., Nishio, A., Okazaki, K. 2015. Smad2/3 Linker Phosphorylation Is a Possible Marker of Cancer Stem Cells and Correlates with Carcinogenesis in a Mouse Model of Colitis-Associated Colorectal Cancer. J Crohn's & Colitis, 9, 7, 565–574.

Tang, L.-Y., Yamashita, M., Coussens, N.P., Tang, Y., Wang, X., Li, C., Deng, C.-X., Cheng, S.Y. and Zhang, Y.E. 2011. Ablation of Smurf2 reveals an inhibition in TGF-β signalling through multiple mono-ubiquitination of Smad3. EMBO, 30, 4777-4789.

ten Dijke, P. & Arthur, H. M. 2007. Extracellular control of TGFβ signalling in vascular development and disease. Nat Rev Mol Cell Biol., 8, 857-869.

Teo, A.K.K., Valdez, I.A., Dirice, E. and Kulkarni, R.N. 2014. Comparable Generation of Activin-Induced Definitive Endoderm via Additive Wnt or BMP Signaling in Absence of Serum. Stem Cell Rep., 3, 1.

Thomson, J. A., Itskovitz-Eldor, J., Shapiro, S. S., Waknitz, M. A., Swiergiel, J. J., Marshall, V. S., and Jones, J. M. 1998. Embryonic stem cell lines derived from human blastocysts. Sci., 282, 5391, 1145-1147.

Thuault, S., Tan, E. J., Peinado, H., Cano, A., Heldin, C.-H. & Moustakas, A. 2008. HMGA2 and Smads Co-regulate SNAIL1 Expression during Induction of Epithelial-to-Mesenchymal Transition. J Biol Chem., 283, 33437-33446.

Tominaga, K. & Suzuki, H. I. 2019. TGF-β Signaling in Cellular Senescence and Aging-Related Pathology. Int J Mol. Sci., 20, 5002.

Tremblay K.D., Hoodless, P.A., Bikoff, E.K., and Robertson, E.J. 2000. Formation of the definitive endoderm in mouse is a Smad2-dependent process. Development., 127**,** 3079–3090.

Tsukazaki, T., Chiang, T. A., Davison, A. F., Attisano, L. & Wrana, J. L. 1998. SARA, a FYVE Domain Protein that Recruits Smad2 to the TGFβ Receptor. Cell, 95, 779-791.

Tucker, R. F., Shipley, G. D., Moses, H. L. & Holley, R. W. 1984. Growth inhibitor from BSC-1 cells closely related to platelet type beta transforming growth factor. Science, 226, 705.

Tzavlaki, K. & Moustakas, A. 2020. TGF-β Signaling. Biomolecules, 10.

Vale, W., Hsueh, A., Rivier, C. & Yu, J. 1990. The Inhibin/Activin Family of Hormones and Growth Factors. Peptide Growth Factors and their receptors II. Berlin, Heidelberg, Springer Berlin Heidelberg.

Vallier, L., Reynolds, D., and Pederson, R. A. 2004. Nodal inhibits differentiation of human embryonic stem cells along the neuroectodermal default pathway. Development Biol., 275, 403-421.

Vallier, L., Alexander, M. & Pedersen, R. A. 2005. Activin/Nodal and FGF pathways cooperate to maintain pluripotency of human embryonic stem cells. J Cell Sci., 118, 4495-4509.

Vallier, L., Mendjan, S., Brown, S., Chng, Z., Teo, A., Smithers, L. E., Trotter, M. W. B., Cho, C. H.-H., Martinez, A., Rugg-Gunn, P., Brons, G. & Pedersen, R. A. 2009. Activin/Nodal signalling maintains pluripotency by controlling Nanog expression. Development, 136, 1339-1349.

Vander Ark, A., Cao, J. & Li, X. 2018. TGF-β receptors: In and beyond TGF-β signaling. Cell Signal., 52, 112-120.

Varelas, X., Sakuma, R., Samavarchi-Tehrani, P., Peerani, R., Rao, B. M., Dembowy, J., Yaffe, M. B., Zandstra, P. W. & Wrana, J. L. 2008. Taz controls Smad nucleocytoplasmic shuttling and regulates human embryonic stem-cell self-renewal. Nat Cell Biol., 10, 837-848.

Varshavsky, A. 2011, The N-end rule pathway and regulation by proteolysis. Protein Sci., 20, 1298-1345.

Velasco, S., Alvarez-Muñoz, P., Pericacho, M., Dijke, P. T., Bernabéu, C., López-Novoa, J. M. & Rodríguez-Barbero, A. 2008. L- and S-endoglin differentially modulate TGFβ1 signaling mediated by ALK1 and ALK5 in L6E9 myoblasts. J Cell Sci, 121, 913-919.

Venkatesha, S., Toporsian, M., Lam, C., Hanai, J.-I., Mammoto, T., Kim, Y. M., Bdolah, Y., Lim, K.-H., Yuan, H.-T., Libermann, T. A., Stillman, I. E., Roberts, D., D'amore, P. A., Epstein, F. H., Sellke, F. W., Romero, R., Sukhatme, V. P., Letarte, M. & Karumanchi, S. A. 2006. Soluble endoglin contributes to the pathogenesis of preeclampsia. Nat Med., 12, 642-649.

Vincent, S.D., Dunn, N.R., Hayashi, S., Norris, D.P. and Robertson, E.J. 2003. Cell fate decisions within the mouse organizer are governed by graded Nodal signals. Genes Dev.., 17, 13, 1646–1662.

Walton, K. L., Johnson, K. E. & Harrison, C. A. 2017. Targeting TGF-β Mediated SMAD Signaling for the Prevention of Fibrosis. Front. of Pharmac., 8.

Wan, Y., Liu, X. & Kirschner, M. W. 2001. The Anaphase-Promoting Complex Mediates TGF-β Signaling by Targeting SnoN for Destruction. Mol Cell, 8, 1027-1039.

Wang, C., Li, Y., Zhang, H., Liu, F., Cheng, Z., Wang, D., Wang, G., Xu, H., Zhao, Y., Cao, L. & Li, F. 2014. Oncogenic PAK4 regulates Smad2/3 axis involving gastric tumorigenesis. Oncogene, 33, 3473-3484.

Wang G, Matsuura I, He D, Liu F. 2009. Transforming growth factor-b-inducible phosphorylation of Smad3. J Biol Chem., 284, 9663–73.

Wang, R., Zhu, J., Dong, X., Shi, M., Lu, C. & Springer, T. A. 2012. GARP regulates the bioavailability and activation of TGFβ. Mol Bio Cell, 23, 1129-1139.

Wang, T., Li, B.-Y., Danielson, P. D., Shah, P. C., Rockwell, S., Lechleider, R. J., Martin, J., Manganaro, T. & Donahoe, P. K. 1996. The Immunophilin FKBP12 Functions as a Common Inhibitor of the TGFβ Family Type I Receptors. Cell, 86, 435-444.

Wiater, E., Harrison, C. A., Lewis, K. A., Gray, P. C. & Vale, W. W. 2006. Identification of Distinct Inhibin and Transforming Growth Factor β-binding Sites on Betaglycan: Functional Separation of Betaglycan Co-Receptor Actions. J Biol Chem., 281, 17011-17022.

Wicks, S. J., Lui, S., Abdel-Wahab, N., Mason, R. M. & Chantry, A. 2000. Inactivation of Smad-Transforming Growth Factor-β signaling by calcium-calmodulin-dependent protein kinase II. Mol and Cell Biol., 20, 8103-8111.

Wrana, J. L., Attisano, L., Wieser, R., Ventura, F. & Massagué, J. 1994. Mechanism of activation of the TGF-β receptor. Nature, 370, 341-347.

Wrighton, K. H., Willis, D., Long, J., Liu, F., Lin, X. & Feng, X. H. 2006. Small C-terminal domain phosphatases dephosphorylate the regulatory linker regions of Smad2 and Smad3 to enhance Transforming Growth Factor-Beta signalling. J Biol Chem., 281, 38365-75.

Wu, J.-W., Krawitz, A. R., Chai, J., Li, W., Zhang, F., Luo, K. & Shi, Y. 2002. Structural Mechanism of Smad4 Recognition by the Nuclear Oncoprotein Ski: Insights on Ski-Mediated Repression of TGF-β Signaling. Cell, 111, 357-367.

Wu, L. & Derynck, R. 2009. Essential Role of TGF-β Signaling in Glucose-Induced Cell Hypertrophy. Development Cell, 17, 35-48.

Xi, Q., He, W., Zhang, X. H. F., Le, H.-V. & Massagué, J. 2008. Genome-wide Impact of the BRG1 SWI/SNF Chromatin Remodeler on the Transforming Growth Factor β Transcriptional Program. J Biol Chem., 283, 1146-1155.

Xiao, Z., Latek, R. & Lodish, H. F. 2003. An extended bipartite nuclear localisation signal in Smad4 is required for its nuclear import and transcriptional activity. Oncogene, 22, 1057-1069.

Xiao, Z., Liu, X., Henis, Y. I. & Lodish, H. F. 2000a. A distinct nuclear localisation signal in the N terminus of Smad 3 determines its ligand-induced nuclear translocation. Proc Natl Acad Sci U S A, 97, 7853.

Xiao, Z., Liu, X. & Lodish, H. F. 2000b. Importin β Mediates Nuclear Translocation of Smad 3. J Biol Chem., 275, 23425-23428.

Xin, H., Xu, X., Li, L., Ning, H., Rong, Y., Shang, Y., Wang, Y., Fu, X.-Y. & Chang, Z. 2005. CHIP Controls the Sensitivity of Transforming Growth Factor-β Signaling by Modulating the Basal Level of Smad3 through Ubiquitin-mediated Degradation. J Biol Chem., 280, 20842-20850.

Xu, L., Alarcon, C., Col, S. & Massagué, J. 2003. Distinct domain utilization by Smad3 and Smad4 for nucleoporin interaction and nuclear import. J Biol Chem., 278, 42569-77.

Xu, L., Kang, Y., Col, S. & Massague, J. 2002. Smad2 nucleocytoplasmic shuttling by nucleoporins Can/Nup214 and Nup153 feeds TGF-β signalling complexes in the cytoplasm and nucleus. Mol Cell, 10, 271-82.

Xu, L., Yao, X., Chen, X., Lu, P., Zhang, B. & Ip, Y. T. 2007. Msk is required for nuclear import of TGF-β/BMP-activated Smads. J Cell Biol., 178, 981-994.

Xu, P., Lin, X. & Feng, X.-H. 2016. Posttranslational regulation of Smads. Cold Spring Harb Perspect Biol., 8, A022087.

Yagi, K., Goto, D., Hamamoto, T., Takenoshita, S., Kato, M. & Miyazono, K. 1999. Alternatively Spliced Variant of Smad2 Lacking Exon 3: Comparison with Wild-Type Smad2 and Smad3. J Biol Chem., 274, 703-709.

Yakymovych, I., Yakymovych, M., Zang, G., Mu, Y., Bergh, A., Landström, M. & Heldin, C.-H. 2015. CIN85 modulates TGFβ signaling by promoting the presentation of TGFβ receptors on the cell surface. J Cell Biol., 210, 319-332.

Yamashita, M., Fatyol, K., Jin, C., Wang, X., Liu, Z. & Zhang, Y. E. 2008. TRAF6 Mediates Smad-Independent Activation of JNK and p38 by TGF-β. Mol Cell, 31, 918-924.

Yan, X., Lin, Z., Chen, F., Zhao, X., Chen, H., Ning, Y. & Chen, Y.-G. 2009. Human BAMBI Cooperates with Smad7 to Inhibit Transforming Growth Factor-β Signaling. J Biol Chem., 284, 30097-30104.

Yan, X., Xiong, X. & Chen, Y.-G. 2017. Feedback regulation of TGF-β signaling. Acta Biochim. Biophys. Sin., 50, 37-50.

Yan, X., Zhang, J., Pan, L., Wang, P., Xue, H., Zhang, L., Gao, X., Zhao, X., Ning, Y. & Chen, Y.-G. 2011. TSC-22 Promotes Transforming Growth Factor beta-Mediated Cardiac Myofibroblast Differentiation by Antagonizing Smad7 Activity. Mol Cell Biol., 31, 3700-3709.

Yan, Y.-T., Liu, J.-J., Luo, Y., Chaosu, E., Haltiwanger Robert, S., Abate-Shen, C. & Shen Michael, M. 2002. Dual Roles of Cripto as a Ligand and Coreceptor in the Nodal Signaling Pathway. Mol Cell Biol., 22, 4439-4449.

Yang, T., Grafe, I., Bae, Y., Chen, S., Chen, Y., Bertin, T. K., Jiang, M.-M., Ambrose, C. G. & Lee, B. 2013. E-selectin ligand 1 regulates bone remodeling by limiting bioactive TGF-β in the bone microenvironment. Proc Natl Acad Sci U S A, 110, 7336-7341.

Yilmaz, A. & Benvenisty, N. 2019. Defining Human Pluripotency. Cell Stem Cell, 25, 9-22.

Yin, T, Lallena, M. J., Kreklau, E. L., Fales, K. R., Carballares, S., Torrres, R., Wishart, G. N., Ajamie, R. J., Cronier, D. M., Iversen, P. W., Meier, T. I., Foreman, R. T., Zeckner, D., Sissons, S. E., Halstead, B. W., Lin, A. B., Donoho, G. P., Qian, Y., Li, S., Wu, S., Aggarwal, A., Ye, X. S., Starling, J. J., Gaynor, R. B., Dios, A. De., And Du, J. 2014. A novel CDK9 inhibitor shows potent antitumor efficacy in preclinical hematologic tumor models. Mol Cancer Ther., 13, 6, 1442-1456.

Yoshida, K., Matsuzaki, K., Murata, M., Yamaguchi, T., Suwa, K., Okazaki, K. 2018. Clinico-Pathological Importance of TGF-β/Phospho-Smad Signaling during Human Hepatic Fibrocarcinogenesis. Cancers (Basel), 5, 10, 6, 183.

Yoshida, K., Matsuzaki, K., Mori, S., Tahashi, Y., Yamagata, H., Furukawa, F., Seki, T., Nishizawa, M., Fujisawa, J. & Okazaki, K. 2005. Transforming Growth Factor-β and Platelet-Derived Growth Factor signal via c-Jun N-terminal kinase-dependent Smad2/3 phosphorylation in rat hepatic stellate cells after acute liver injury. Am J Pathol., 166, 1029-1039.

Yu, J., Pan, L., Qin, X., Chen, H., Xu, Y., Chen, Y. & Tang, H. 2010. MTMR4 attenuates transforming growth factor beta (TGFbeta) signaling by dephosphorylating R-Smads in endosomes. J Biol Chem., 285, 8454-62.

Yu, J. S., Ramasamy, T. S., Murphy, N., Holt, M. K., Czapiewski, R., Wei, S. K. & Cui, W. 2015. PI3K/mTORC2 regulates TGF-beta/Activin signalling by modulating Smad2/3 activity via linker phosphorylation. Nat Commun., 6, 7212.

Yu, Y. & Feng, X.-H. 2019. TGF-β signaling in cell fate control and cancer. Curr. Opin. Cell Biol., 61, 56-63.

Yuan, J.-H., Yang, F., Wang, F., Ma, J.-Z., Guo, Y.-J., Tao, Q.-F., Liu, F., Pan, W., Wang, T.-T., Zhou, C.-C., Wang, S.-B., Wang, Y.-Z., Yang, Y., Yang, N., Zhou, W.-P., Yang, G.-S. & Sun, S.-H. 2014. A Long Noncoding RNA Activated by TGF-β Promotes the Invasion-Metastasis Cascade in Hepatocellular Carcinoma. Cancer Cell, 25, 666-681.

Yumoto, K., Thomas, P. S., Lane, J., Matsuzaki, K., Inagaki, M., Ninomiya-Tsuji, J., Scott, G. J., Ray, M. K., Ishii, M., Maxson, R., Mishina, Y., and Kaartinen, V. 2013. TGF-β-activated Kinase 1 (Tak1) Mediates Agonist-induced Smad Activation and Linker Region Phosphorylation in Embryonic Craniofacial Neural Crest-derived Cells. J Biol Chem., 288, 19, 13467-13480.

Zawel, L., Le Dai, J., Buckhaults, P., Zhou, S., Kinzler, K. W., Vogelstein, B. & Kern, S. E. 1998. Human Smad3 and Smad4 Are Sequence-Specific Transcription Activators. Mol Cell, 1, 611-617.

Zhang, Y., Chang, C., Gehling, D. J., Brivanlou, A. H., Derynck, R. 2001. Regulation of Smad degradation and activity by Smurf2, an E3 ubiquitin ligase. Proc Natl Acad Sci U S A, 98, 3, 974-979.

Zhang, S., Fei, T., Zhang, L., Zhang, R., Chen, F., Ning, Y., Han, Y., Feng, X.-H., Meng, A. & Chen, Y.-G. 2007. Smad7 Antagonizes Transforming Growth Factor β Signaling in the Nucleus by Interfering with Functional Smad-DNA Complex Formation. Mol Cell Biol., 27, 4488-4499.

Zorn, A. M. and Wells, J. M. 2009. Annu. Rev. Cell Development Biol., 25, 1, 221-251.

Zoumaro-Djayoon, A.D., Ding, V., Foong, L.-Y., Choo, A., Heck, A.J.R. and Muñoz, J. 2011, Investigating the role of FGF-2 in stem cell maintenance by global phosphoproteomics profiling. Proteomics, 11, 3962-3971.

Zhu, S., Wang, W., Clarke, D. C. & Liu, X. 2007. Activation of Mps1 Promotes Transforming Growth Factor-β-independent Smad Signaling. J Biol Chem., 282, 18327-18338.

Appendix

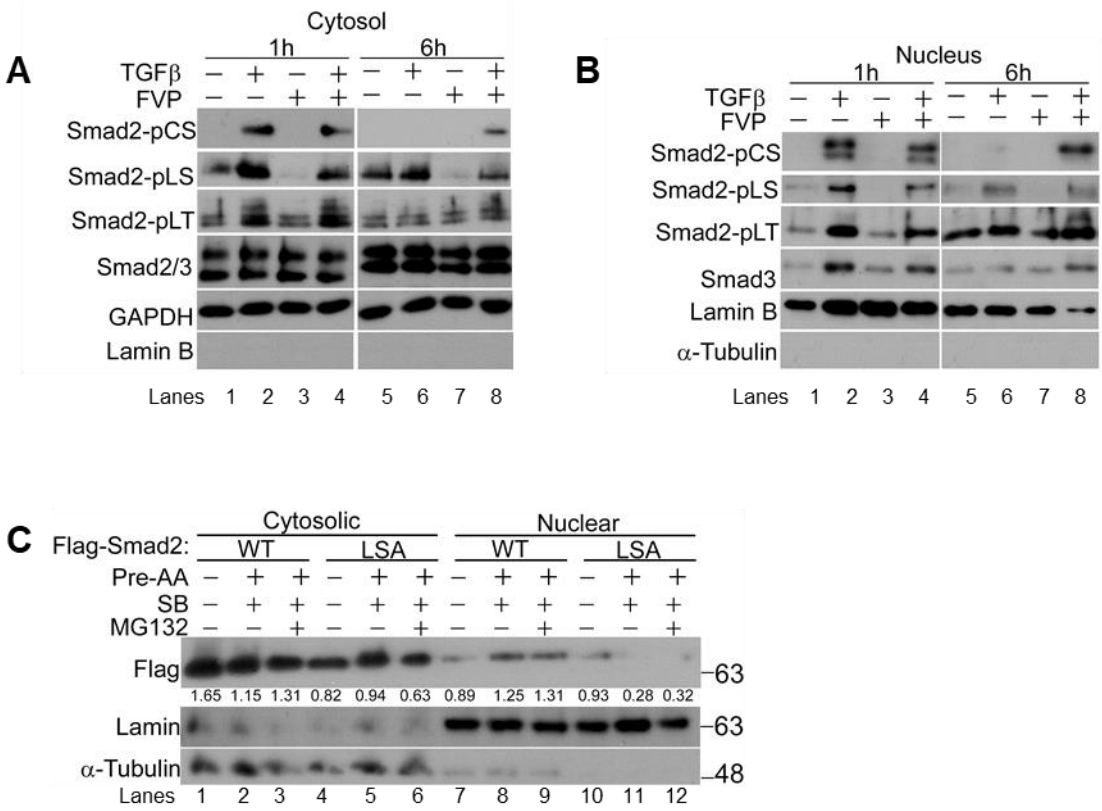

Fig A-I: Subcellular localisation of activated Smad2 upon flavopiridol treatment or absence of Smad2-pLS

Representative immunoblot of **A)** cytoplasmic and **B)** nuclear fractions of serum-starved PC3 cells treated with TGF-β and flavopiridol for 1 and 6 hours as indicated and analysed by western blotting with the indicated antibodies (n=3). **C)** Immunoblot analysis of Flag in Smad2-null HEK293T cells after transfection with Flag-Smad2-WT and –LSA cultured in 1% serum medium overnight and treated as indicated (n=2).

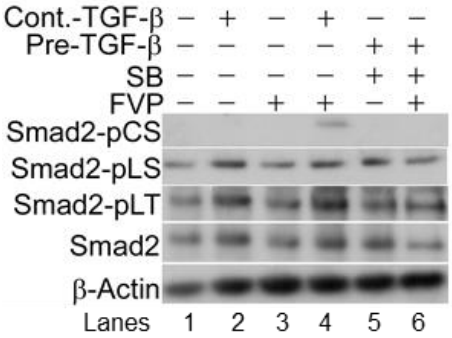

Fig A-II: Effect of flavopiridol on activated Smad2 and Smad2-pLS in HEK293T cells

Representative immunoblot of HEK293T cells treated as shown with TGF-β, SB431542, and flavopiridol for 6 hours, and western blotting done with the indicated antibodies.

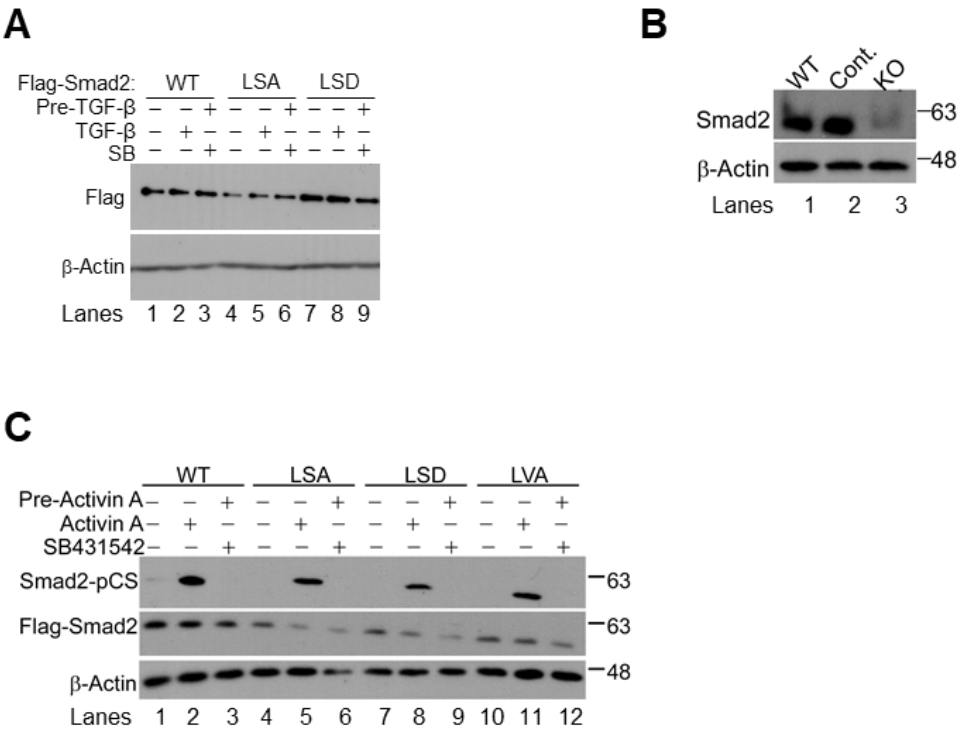

Fig A-III: Effect of pLS on Smad2 activation and stability

Representative immunoblots in Fig 5.4B and 5.4E were prepared from the same blot. The entire blot is shown here. **A)** Whole blot of Fig 5.4B- Immunoblot analysis of Flag in PC3 cells after transfection with Flag-Smad2-WT, -LSA, and -LSD in serum-free culture and treated as shown with SB431542 and either transiently or continuously with TGF-β. **B)** Immunoblot analysis of Smad2 expression in WT, KO control, and Smad2-null HEK293T cells. **C)** Whole blot of Fig 5.4E- Immunoblot analysis of Flag in Smad2-null HEK293T cells after transfection with Flag-Smad2-WT, -LSA, -LSD, and -LVA cultured in 1% serum medium overnight and treated as indicated.